Hans-Klaus Roth, Klaus Heinemann (Ed.)

5th International Symposium
Technologies for Polymer Electronics - TPE 12 -

Special Thanks go to Mrs. BIANCA KÄMMER.
She helped us again most conscientiously to cope with the wealth of Abstracts
and showed also remarkable patience in preparing this proceedings of TPE 12.

Proceedings

5th International Symposium Technologies for Polymer Electronics - TPE 12 -

Thuringian Institute of Textile and
Plastics Research, Rudolstadt
and
Ilmenau University of Technology

22. - 24. May 2012, Rudolstadt/Germany

ed. by
Hans-Klaus Roth, Klaus Heinemann

Universitätsverlag Ilmenau
2012

Impressum

Bibliografische Information der Deutschen Nationalbibliothek
Die Deutsche Nationalbibliothek verzeichnet diese Publikation in der Deutschen Nationalbibliografie; detaillierte bibliografische Angaben sind im Internet über http://dnb.d-nb.de abrufbar.

Version notice:
There are minor differences between the printed and online version.

Technische Universität Ilmenau/Universitätsbibliothek
Universitätsverlag Ilmenau
Postfach 10 05 65
98684 Ilmenau
www.tu-ilmenau.de/universitaetsverlag

Herstellung und Auslieferung
Thüringisches Institut für Textil- und Kunststoff-Forschung e.V.
Breitscheidstr. 97
07407 Rudolstadt
www.titk.de

ISBN 978-3-86360-022-8 (Druckausgabe)
urn:nbn:de:gbv:ilm1-2012100098

P r e f a c e

The previous TPE Symposia in Rudolstadt took place in 2004, 2006, 2008 and 2010. On each occasion, more than 100 participants from over 20 countries attended, giving many excellent lectures and poster contributions that are still available on CD.

TPE 12 aims at bringing together researchers and developers who area active in the area of organic electronics, with manufacturers, future users, and other interested parties. A special focus will be placed on technology approaches for the large scale fabrication of polymer electronic products, on recent material developments, and on emerging applications of plastic electronics including Organic Photovoltaics (OPV).

The scientific programme is subdivided into the following sections:

I	Introductions
II	Materials and technologies 1
III	OFETs, Sensors and related
IV	OLEDs and ECDs
V	Materials and technologies 2
VI	Solar cells / OPV 1
VII	Materials and technologies 3
VIII	Solar cells / OPV 2
IX	Materials and technologies 4
X	Posters

The Symposium is organised by both the technology oriented polymer research institute TITK Rudolstadt and the Ilmenau University of Technology (TU Ilmenau). The research institute TITK is a self-supporting research institute at the TU Ilmenau. This University has a long tradition of outstanding education in the technological sectors of electrical and mechanical engineering, nanoelectronics, information science, all fields of modern optoelectronics and others.

Regarding TPE 12 the abbreviation TITK stands for

T	**Trends** in R & D of polymer electronics and solar cells
I	**Innovations** in fabrication of organic or polymer solar cells (OPV), OLEDs, OFETs, IPCs and polymer
T	**Technologies** for production of organic or plastic electronics
K	**Know-how** exchange and transfer

The symposium will be a forum of scientific discussion about corresponding actual results of research and development as well as on application fields.

Hans-Klaus Roth
Symposium Chair

Symposium Board

International Advisory Committee

Prof. Dr. G. v. Assche (VU Brüssel, B)
Prof. Dr. R. Baumann (TU Chemnitz, D)
Prof. Dr. Ch. Brabec (Uni Erlangen, D)
Prof. Dr. V. Dyakonow (Uni Würzburg, D)
Prof. Dr. D. Fichou (UPMC Paris, F)
Prof. Dr. G. Gobsch (TU Ilmenau, D)
Prof. Dr. E. v. Hauff (Uni Freiburg, D)
Prof. Dr. G. Horowitz (Polytechnique, Palaiseau, F)
Prof. Dr. O. Inganäs (Uni Linköping, S)
Prof. Dr. G. E. Jabbour (Adv. PV. C., Uni Arizona, USA)
Prof. Dr. R. Janssen (TU Eindhoven, NL)
Dr. S. Kirchmeyer (Heraeus, Leverkusen, D)
Dr. Th. Kugler (CDT, Cambridge,UK)
Prof. Dr. D. Lupo (TU Tampere, FIN)
Dr. A. Lux (Novaled AG, Dresden, D)
Prof. Dr. N. Martin (Uni Madrid, E)
Dr. D. Müller (Merck, Darmstadt, D)
Prof. Dr. J.-M. Nunzi (Queen´s Uni, Ontario, CDN)
Prof. Dr. V. F. Razumov (ICP Chernogolovka, RUS)
Prof. Dr. H.-K. Roth (TITK, Rudolstadt, D)
Prof. Dr. N. S. Sariciftci (Uni Linz, A)
Prof. Dr. U. S. Schubert (Uni Jena, D)
Dr. M. Shkunov (Uni Surrey, UK)
Prof. Dr. H. Sirringhaus (Plastic Logic, Cambridge, UK)
Dr. B. Stadlober (Joanneum Research, Weiz, A)
Prof. Dr. L. Torsi (Uni Bari, I)
Prof. Dr. D. Vanderzande (Uni Hasselt, B)

Local Conference Committee

Dr. R.-U. Bauer (TITK, Rudolstadt)
Prof. Dr. G. Gobsch (TU Ilmenau)
Prof. Dr. K. Heinemann (TITK, Rudolstadt)
Dr. H. Hoppe (TU Ilmenau)
Mrs. B. Kämmer (TITK, Rudolstadt)
Prof. Dr. H.-K. Roth (TITK, Rudolstadt)
Prof. Dr. P. Scharff (TU Ilmenau)
Dr. S. Scheinert (TU Ilmenau)
Dr. M. Schrödner (TITK, Rudolstadt)
Dr. S. Sensfuss (TITK, Rudolstadt)

CONTENTS

Introductions

Materials and technologies 1

OFET´s, Sensors and related

OLEDs and ECDs

Materials and technologies 2

Solar cells / OPV 1

Materials and technologies 3

Solar cells / OPV 2

Materials and technologies 4

Posters

Part I: Introductions

Theoretical and experimental pathways to a new efficiency regime for molecular solar cells

L.J.A. Koster[1], S. Shaheen[2], W. Zou[3], M. Pshenichnikov[1], and J.C.Hummelen[1,3]*

1. Molecular Electronics, Zernike Institute for Advanced Materials, Nijenborgh 4, 9747 AG Groningen, The Netherlands.

2. Dept. of Physics and Astronomy, University of Denver, 2112 E. Wesley Ave., Denver, CO 80208-6900, USA

3. Stratingh Institute for Chemistry, University of Groningen, Nijenborgh 4, 9747 AG Groningen, The Netherlands. E-mail: j.c.hummelen@.rug.nl

In the first part, we present three different theoretical approaches to identify pathways to organic solar cells with power conversion efficiencies in excess of 20%. We take off after reasoning why the Shockley-Queisser limit is applicable to OPV. A radiation limit for organic solar cells is introduced that elucidates the role of charge-transfer (CT) state absorption. Provided this CT action is either sufficiently weak or present in its maximized form throughout the active layer material, organic solar cells can be as efficient as their inorganic counterparts.

Next, a model based on Marcus theory of electronic transfer that also considers exciton generation by both the electron donor and electron acceptor is used to show how reduction of the reorganization energies can lead to substantial efficiency gains.

Third, we introduce the dielectric constant as a central parameter for efficient solar cells. We analyze how the dielectric constant influences every fundamental step in OPV. We analyze and model the case of the 2009 world record PTB7:[70]PCBM cell of 7.4%, using a drift-diffusion model. Based on the model and based on the fact that the exciton binding energy diminishes with increasing dielectric constant of the medium, we find that efficiencies of more than 20% are within reach upon increasing the dielectric constant ε_r of the material to 10 (Figure 1).

(*Adv. Energy Mater. 2012,* in print)

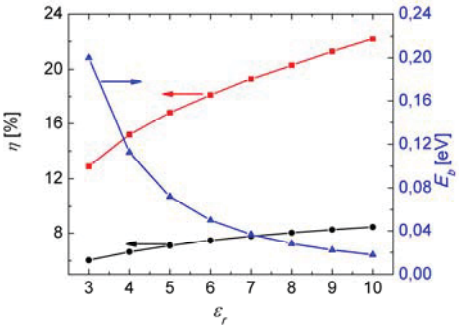

Fig1: (black line) $\eta_{(PTB7:[70]PCBM)}$ as function of ε; (blue line) exciton binding energy E_b as function of ;(red line) η of OPV with E_b optimized for each value of ε.

A completely different approach towards high efficiency PV is based on photon management. We report on our recent discovery of efficient broadband near-IR light up-conversion. Photon upconversion of the (near)infrared (NIR) photons is a promising way to overpass the Shockley-Queisser limit that sets up the maximal efficiency of 32% to a single junction solar cell. However, the practical applicability of the most efficient upconversion materials known to date at moderate light intensities (i.e. below 1000 Suns) is limited by the extremely weak and narrow-band (N)IR absorption. Here we, inspired by a natural design of photosynthetic complexes, introduce a novel concept of an upconversion material in which an organic (N)IR dye is used as an antenna for β-NaYF4:Yb,Er nanoparticles (NPs) where the upconversion occurs. The overall upconversion efficiency of the dye-sensitized NPs is dramatically enhanced (by a factor of ~3300; see Fig. 2) as a result of increased absorptivity and overall broadening of the absorption spectrum of the upconverter. The proposed concept can be readily extended to cover any desired part of the solar spectrum by applying a set of dye molecules with overlapping absorption spectra acting as an extremely broadband antenna system, connected to a suitable upconverter.

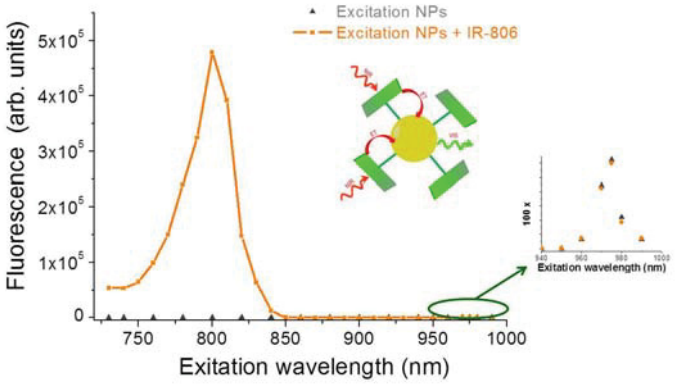

Fig 2. Upconversion action spectrum of IR-806-coated β-NaYF4:Yb,Er NPs (orange line). Insets: cartoon of dye-coated NPs and amplified action spectrum showing the original NP upconversion.

BIOGRAPHIC DATA OF PROFESSOR KEES HUMMELEN

Kees (J.C.) Hummelen was born in Groningen, The Netherlands. He received his MSc in Chemistry and a *cum laude* doctorate degree in Science under the mentorship of Hans Wynberg at the University of Groningen in 1979 and 1985, respectively. After four years of playing jazz (piano) and art video production, he spent two years as a post-doctoral fellow with Fred Wudl at UCSB. He was appointed full Professor in Chemistry in 2000 in Groningen. At present, he is the Scientific Director of the Stratingh Institute for Chemistry at the University of Groningen. The last 15 years, his main research activities were in fullerene chemistry and the development of organic photovoltaics. Other research topics are materials for molecular field effect transistors and single-molecule electronics. The Web of Science presently reports 173 papers of him with an average of 105 citations per paper.

In 2011, he was ranked as the #7 scientist in materials science worldwide by Thomson Reuters.

ORGANIC AND PRINTED ELECTRONICS: STATUS, OPPORTUNITIES AND CHALLENGES

S. Kirchmeyer*, Heraeus Precious Metals GmbH & Co. KG, Conductive Polymers Division, Chempark, Building B 202, 51368 Leverkusen, Germany

Abstract

The technology of plastic electronics is believed to open a field of low-cost electronics with new areas of application. Studies have predicted a multibillion dollar market which has generated a significant attention in research and industry. Few commercial applications have been realized, the largest sales are currently organic luminescent diodes with approximately 2 bn. US$ sales. Every technology passes through a cycle with a phase of initial high expectation followed by a phase of disillusion until finally a state of productivity is reached. At this point there is still belief that printed electronics have a high technological potential but many voices emphasize the need to convert this technology into significant business.

When technology limitations become visible, the phase of disillusion is the most critical phase of any emerging technology. The OE-A is an association which acts as a global strategic platform to build a bridge between science, technology and applications in order to grow an industry of printed electronics. Being aware of the so called hype cycles the OE-A strives to facilitate the transformation of technology into a worldwide business. In this regard the OE-A offers various tools among the most efficient being its roadmap and its demonstrator activities.

Every two years the OE-A compiles into one document a technology roadmap with input from its almost 200 members that compiles the technology status, requirements and the “Red Brick Walls” of printed electronics for each main application. The OE-A roadmap has been proved to be highly useful to guide for R+D activities and has worldwide a high reputation. “Red Brick Walls” listed in the road map are defined as “basic limitations to enter mass markets” and resemble technology challenges to be overcome for commercialization. Basic challenges comprise the circuit design and system integration, the resolution, registration and process stability of structuring processes and current limitations in of materials such as semiconductors, conductors and barrier materials.

A totally different challenge is the question how potential end users can be attracted to apply this technology. Potential end users such as companies in the retail, pharmaceutical or packaging business without a background in electronics will need a clear and realistic explanation of potentials and limits of printed electronics. On the other hand the development of printed electronic devices is currently dominated by pushing this technology rather than by a demand from the various potential markets. Demonstrators, meaning full working devices, demonstrate function and capability of printed electronics to potential end users, generate an understanding of potential and limitations, and facilitate a dialogue between the developers and the users which may finally result in new realistic applications. On the other hand the design and production of demonstrators require many partners along the value chain to cooperate and therefore helps to build a technology network.

Among the numerous “give-away” demonstrators OE-A members have built are the solar powered printed torch, a book with electronic function, solar power model airplanes, medical and packaging devices - the latter originating from its student competition.

Some examples of a successful product commercialization will be discussed which reveal that even very simple devices generate a number of technology challenges although they to be appear quite unattractive as object for scientific studies. From these examples it can be predicted that one of the next applications for printed electronics are touch screens made from materials like conductive polymers that replace indium tin oxide in their function as a transparent conductor.

BIOGRAPHIC DATA OF DR STEPHAN KIRCHMEYER

Stephan Kirchmeyer was born in 1957 in Empelde near Hannover, Germany. From 1978 to 1984 he studied chemistry at the University of Hamburg and at the University of Southern California in Los Angeles. After his thesis he went to San Jose/USA for a postdoctoral fellowship with IBM.

He joined Bayer's Central R&D 1988 and Bayer's silicone division in 1996. 1997 he transferred to the electronic chemicals group to develop the conductive polymer PEDOT.

In 2002 the business was transferred to H.C. Starck GmbH, at that time an affiliate company of Bayer. For H.C. Starck he worked subsequently as R&D manager, plant site manager, global business manager and as a director for production and technology. In 2010 the business of conductive polymers was sold to Heraeus. In Heraeus he is currently the Head of the Business Unit Functional Coatings. In June 2011 he was elected as the chair of the board of the Organic Electronics Association (OE-A).

ENHANCED ORGANIC LIGHT EMITTING DIODE AND SOLAR CELL PERFORMANCES BY SILVER NANOPARTICLES

F. LIU [1]; J.M. NUNZI* [1, 2]

[1]Department of Chemistry, Queen's University, Kingston, ON

[2]Department of Physics, Queen's University, Kingston, ON

Surface plasmons are known as collective oscillations of the conduction electrons at a metallic interface. The phenomenon has been extensively studied in the fields of surface enhanced Raman spectroscopy, metal enhanced fluorescence, and non-linear optics.[1-2] However, only limited research has been dedicated to its application in organic light emitting diode (OLED). Here we have fabricated a plasmonic OLED by incorporating silica coated silver nanoparticles (NPs) into the emitting layer of a phosphorescent organic light emitting diode (PHOLED), as shown in the schematic diagram Fig. 1. As a result, the luminescence efficiency of the PHOLED is significantly improved under low charge carrier injection level due to surface plasmon enhanced exciton formation probability. In contrast, the incorporation of uncoated bare silver NPs greatly suppresses luminescence of the PHOLED due to metal NPs induced luminescence quenching. A silica shell with thickness 13 nm or above coated on Ag NPs surface can avoid the luminescence quenching of the emitting molecules caused by Ag NPs.

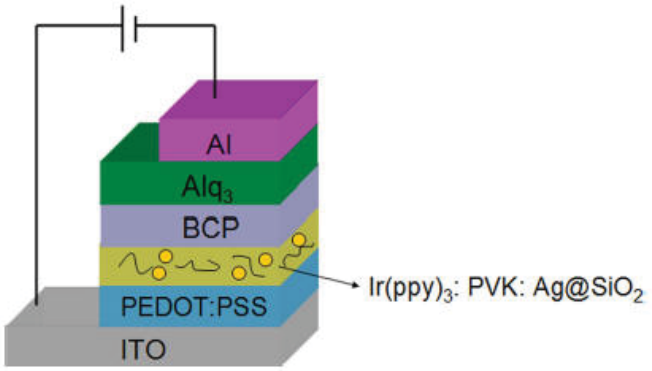

Fig. 1. Configuration of a PHOLED doped with silica coated Ag NPs

So far metal nanoparticles (NPs) have been used in thin film silicon solar cell research successfully as the substitute of traditional inverted pyramid surface texture for light trapping.

However, the application of metal NPs in organic solar cell research is not as successful as that in silicon solar cell. Although many works have been dedicated to organic solar cells incorporating NPs, none explicitly isolates the optical function of NP from its electronic function in organic solar cells due to the multiple roles played.

We designed a polymer solar cell with configuration shown in Fig. 2 from which we can investigate solely the optical functions of metal NPs in the solar cell. The incorporation of NPs underneath the active layer results in degraded performance due to massive light loss caused by Ag NPs scattering and absorption. In contrast, the incorporation of Ag NPs above active layers can harvest more sun light due to the fact that the surface plasmon of Ag NPs enhances the extinction coefficient of the active polymer layer and the back-scattering from Ag NPs improves the optical absorption path length in the active layer, thus solar cell power conversion efficiency (PCE) is improved. However, a direct contact of Ag NPs with active polymer results in exciton quenching, which compromises its enhancement effect on PCE. The best position to incorporate Ag NPs into the solar cell appears to be above the active layer, with a spacer layer, which is PEDOT in our prototype.

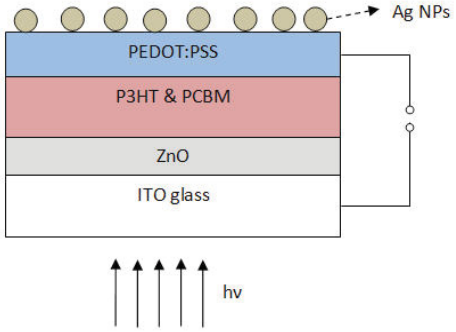

Fig. 2. Schematic diagram of an inverted plasmonic solar cell.

References

1. F. Liu, G. Aldea, and J. M. Nunzi, J. Lumin. **130**, 56 (2010).
2. J. M. Nunzi and D. Ricard, Appl. Phys. B **35**, 209 (1984).

BIOGRAPHIC DATA OF PROFESSOR JEAN-MICHEL NUNZI

Jean-Michel Nunzi is a Tier 1 Canada Research Chair, cross-appointed with the department of Physics and the department of Chemistry at Queen's University since 2006. He spent his early carrier at the Atomic Energy Commission in Saclay (France) where he has been the head of the Organic Devices Group during which he was the PI of the 1st European Project on Organic Solar Cells in 1996. He joined the University of Angers in 2000, where he built a Technical Research Team on plastic solar cells co-supported by the Ministry of Education and Research and Total (France). He is the author of above 200 research papers and 11 patents. He is a member of the French network NANORGASOL and the Photovoltaic Innovation Network in Canada.

Part II: Materials and technologies 1

ALTERNATING COPOLYMERS, ALTERNATIVE DEVICE GEOMETRIES, AND PROCESSING FOR POLYMER PHOTOVOLTAICS

Olle Inganäs
Biomolecular and organic electronics,
Center of Organic Electronics,
IFM, Linköpings Universitet

Routes towards high speed printing of photovoltaic donor/acceptor materials on flexible supports are necessary to realize the cost advantages of polymer photovoltaics. Formation of desired nanostructure from blends in solutions drying onto electrodes is necessary for optimal photocurrents. Correlating the photocurrent generation, nanostructure formation and processing when coating electrodes with active materials requires new tools for *in situ* monitoring and for process control. These can be imaging methods with low or high resolution, but also follow the formation of nanostructures through their emission signatures. We report on concurrent development of optical metrology, processing and module production using alternating copolymers.

POLYMER SYNTHESIS AS A KEY TOOL IN THE DEVELOPMENT OF IMPROVED (OPTO) ELECTRONIC MATERIALS

Ullrich Scherf

Bergische Universität Wuppertal, Macromolecular Chemistry Group (buwmakro) and Institut für Polymertechnologie, Gauss-Str. 20, D-42097 Wuppertal, Germany, Fax:+49-202-4393880, Tel: +49-202-4393871; E-mail: scherf@uni-wuppertal.de

The lecture presents some recent synthesis driven examples towards systematic control on morphology and (opto)electronic properties of conjugated oligomers and (co)polymers. The examples include conjugated (co)polymers for application in organic solar cells, [1,2] all-conjugated rod-rod block copolymers and their self-assembly in solvent mixtures and in the bulk, [1,3-5] as well as hyperbranched, multichromophoric conjugated polymers.[6]

References

[1] J. H. Seo, A. Gutacker, Y. Sun, H. Wu, F. Huang, Y. Cao, U. Scherf, A. J. Heeger, G. C. Bazan, *J. Am. Chem. Soc.* **2011**, *133*, 8416.

[2] P. Li, O. Fenwick, S. Yilmaz, D. Breusov, D. J. Caruana, S. Allard, U. Scherf, F. Cacialli, *Chem. Commun.* **2011**, *47*, 8820.

[3] Tu, G., Li, H., Forster, M., Heiderhoff, R., Balk, L. J., Sigel, R., Scherf, U.; *Small* **2007**, *3*, 1001.

[4] U. Scherf, A. Gutacker, N. Koenen, *Acc. Chem. Res.* **2008**, *41*, 1086.

[5] A. Gutacker, S. Adamczyk, A. Helfer, L. E. Garner, R. C. Evans, S. M. Fonseca, M. Knaapila, G. C. Bazan, H. D. Burrows, U. Scherf, *J. Mater. Chem.* **2010**, *20*, 1423.

[6] J.-M. Koenen, S. Jung, A. Patra, A. Helfer, U. Scherf, *Adv. Mater.* **2012**, *24*, 681, *special issue: International Symposium on Electronic/Optical Functional Molecules, Shanghai, 2012 (ISEOFM2012).*

CRYSTALLINE ORGANIC NANOFIBERS

F. BALZER[1*]; M. SCHIEK[1,2]; A. OSADNIK[2]; A. LÜTZEN[2]; H.-G. RUBAHN[1]

[1] NanoSYD, Mads Clausen Institute, University of Southern Denmark, Alsion 2, DK-6400 Sønderborg, Denmark

[2] Kekulé-Institute of Organic Chemistry and Biochemistry, Rheinische Friedrich-Whilhelms-University of Bonn, Gerhard-Domagk-Strasse 1, D-53121 Bonn, Germany

Organic semiconductors from small molecules such as *para*-phenylenes, thiophenes, or squaraines promise a vast application potential as the active ingredient in electric and optoelectronic devices [1]. Their self-organization into – sometimes crystalline – organic nanowires or "nanofibers" adds a peculiar attribute, making, e.g., nanolasers [2] or waveguides [3] relatively straightforward to accomplish. Functionalization of the molecules allows the customization of optical and electrical properties, allowing the easy formation of highly effective frequency-doubling nanoaggregates [4] or the design of light-harvesting devices such as photovoltaic cells.

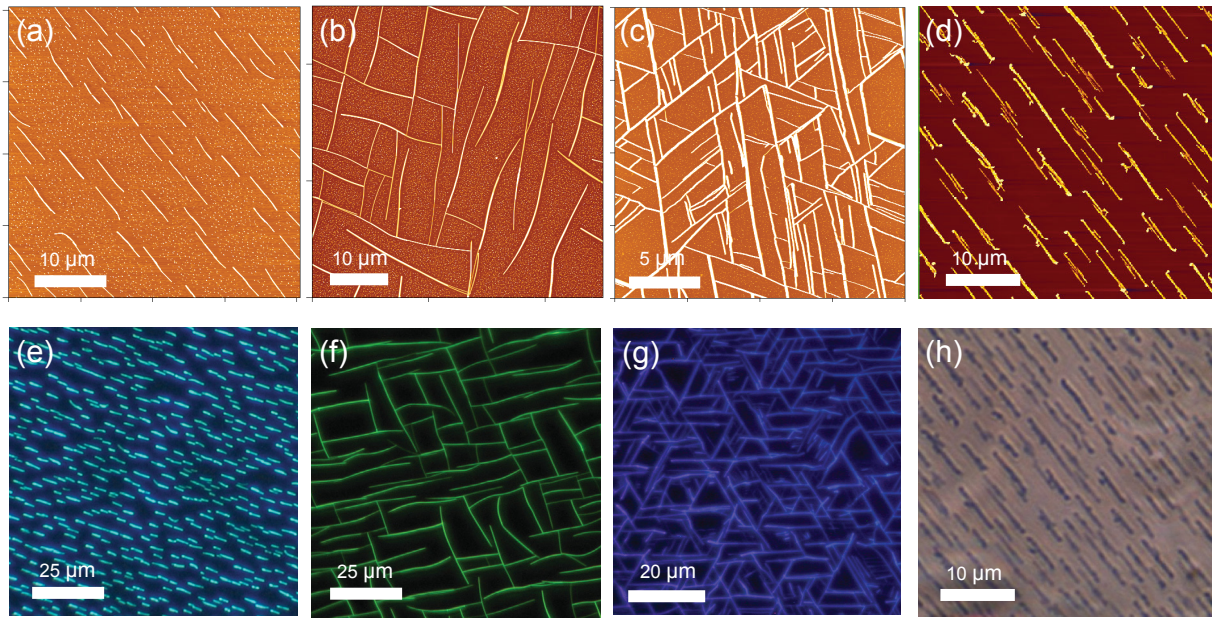

Fig. 1: AFM images, (a)-(d), and optical microscope images, (e)-(g) fluorescence microscopy and (h) optical phase contrast microscopy of PPTPP (a,e), PPTTPP (b,f), *p*-6P (c,g), and SQOH (d,h) deposited by organic molecular beam deposition of mica.

Different methods for nanowire growth have been pursued in the past such as filling of nanoporous templates, organic molecular beam deposition (OMBD) eventually leading to epitaxial growth, and precipitation from solution. In Fig. 1 examples for such nanofibers grown by OMBD are presented, both by atomic force microscopy (AFM) images, upper panel, as well as by fluorescence and phase contrast optical microscopy (lower panel).

The phenylene-thiophene co-oligomers PPTPP and PPTTPP and *para*-hexaphenylene *p*-6P form aggregates which are due to their strong fluorescence suitable for light-light generating devices, whereas the non fluorescing but broadly light-absorbing hydroxyl-squarylium SQOH is aimed to be part of a photovoltaic cell [5,6]. The different nanowire directions are determined by a combination of epitaxial growth, substrate surface symmetry, and packing of the molecules into fibers.

Molecule orientations within the nanofibers as well as with respect to substrate lattice directions are determined via polarized (fluorescence) microscopy. From this conditions for single-crystalline growth are easily identified. An example for that is shown in Fig. 2: whereas p-6P fibers on muscovite are polycrystalline due a possible twinning, the PPTPP fibers formed on KCl are single crystalline.

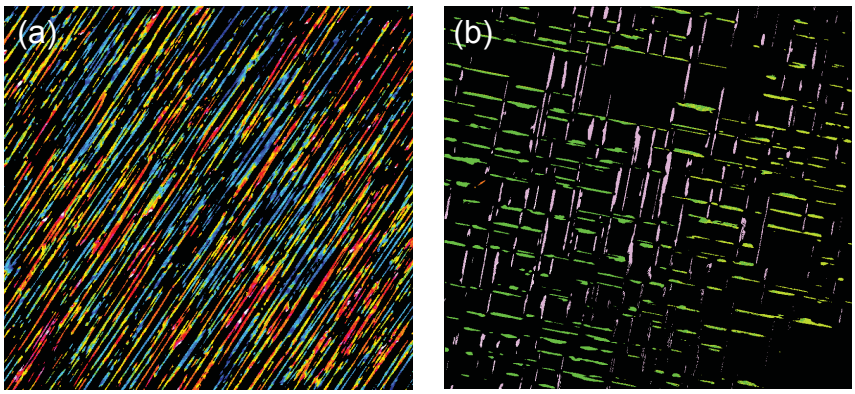

Fig. 2: Polarization microscope images of OMBD grown nanofibers from (a) *p*-6P on muscovite mica and (b) from PPTPP on KCl. The color codes the polarization direction of the emitted fluorescence after UV excitation. The *p*-6P fibers on muscovite mica are clearly polycrystalline, whereas PPTPP fibers on KCl are single crystalline.

The morphological stability of such nanowires with time, in the presence of various gases, and under thermal load is of major importance for their use in any device. Simple aging experiments under ambient conditions by atomic force microscopy already reveal substantial morphological changes by Ostwald ripening due to water vapor. Thermal annealing of nanowire samples leads to even more pronounced morphology changes, such as a strong decrease in nanowire number density, a strong increase in nanowire height, and the formation of new types of crystallites. All these experiments emphasize the need of encapsulation for any device application.

Finally, the electrostatic properties of nanofiber samples probed by Kelvin Probe Force Microscopy (KPFM) are discussed. For typical phenylene or thiophene based nanofibers the contact potential difference (CPD) is strongly related to the sample morphology.

However, for squaraine nanofibers with their high photoconductivity the CPD on the surface is much more delocalized. Illuminating the SQOH nanofibers with visible light from the microscope lamp leads to a strong increase in CPD by several hundred Millivolts, hinting to a strong photovoltage generation on the surface and being of major importance for light-harvesting devices.

[1] M. Schiek, F. Balzer, K. Al-Shamery, J. Brewer, A. Lützen, H.-G. Rubahn. Organic Molecular Technology. Small 4 (2008) 176.

[2] F. Quochi, F. Cordella, A. Mura, G. Bongiovanni, F. Balzer, H.-G. Rubahn. One Dimensional Random Lasing in a Single Organic Nanofiber. J. Phys. Chem. B 109 (2005) 21690.

[3] F. Balzer, V. Bordo, A. Simonsen, H.-G. Rubahn. Optical Waveguiding in Individual Nanometer-Scale Organic Fibers. Phys. Rev. B 67 (2003) 115408.

[4] J. Brewer, M. Schiek, H.-G. Rubahn. Nonlinear optical properties of CNHP4 nanofibers: Molecular dipole orientations and two photon cross-sections. Opt. Commun. 283 (2010) 1514.

[5] F. Balzer, M. Schiek, A. Lützen, H.-G. Rubahn. Self organized growth of organic thiophene-phenylene nanowires on silicate surfaces. Chem. Mater. 21 (2009) 4759.

[6] F. Balzer, M. Schiek, A. Osadnik, A. Lützen, H.-G. Rubahn. Organic Nanofibers from Squarylium Dyes. Proc. SPIE 8258 (2012) 82580O.

CURRICULUM VITAE DR HABIL. FRANK BALZER

born:	05.08.1966 in Biedenkopf, Germany
address:	University of Southern Denmark, Mads Clausen Institute, NanoSyd, Alsion 2, DK-6400 Sønderborg, Denmark
e-mail:	fbalzer@mci.sdu.dk

Education

01/2009	Habilitation in Experimental Physics at Humboldt-University Berlin, Germany. Topic: “Organic Nanoaggregates”
02/1998	Ph.D. in physics, University of Göttingen, Germany. Topic: “Linear and nonlinear optics at alkali island films”
02/1994	Diploma in physics, University of Göttingen, Germany. Topic: “Time resolved investigations of laser induced processes near surfaces”

Employment

Since 05/2007	Associate Professor, Mads Clausen Institute, NanoSyd, University of Southern Denmark, Sønderborg, Denmark
08/2006 – 04/2007	Fellow of the "Hanse Institute for Advanced Study", Delmenhorst, Germany
08/2001 – 08/2006	Research assistant, Physics Department, Humboldt-University Berlin, Germany
06/2000 – 07/2001	Gaesteforsker, Physics Department, University of Southern Denmark, Odense, Denmark
06/1998 – 05/2000	Postdoctoral research associate, Chemistry Department, Stanford University, Stanford, CA, USA
03/1994 – 05/1998	Research assistant, MPI für Strömungsforschung, Göttingen, Germany

Research Experience

Since 2007	self-organized growth of nanowires from organic semiconductors, (polarized) optical properties of organic nanoaggregates; scanning probe microscopy; metallic nanoparticles in food; graphene as electrode material for organic electronics
2001 – 2006	ion scattering from metallic alloys, AFM and spectroscopy on organic nanowires, Forschergruppe 463 – “Innovative pharmaceuticals and carrier systems”
2000 – 2001	organic nanowires on dielectric surfaces

1998 – 2000	molecule surface scattering, resonance enhanced multiphoton ionization, catalytic reactions on surfaces
1994 – 1998	linear and nonlinear optics of alkali clusters, laser materials treatment, photodesorption, self assembled monolayers
1988 – 1994	study of physics, University of Göttingen

Publications (h-index: 18)

47 peer-reviewed papers, 24 conference proceedings, 2 chapters in monographs, 1 book, and 2 patent applications.

ELECTRONIC TRAP STATES IN ORGANIC POLYMER-FULLERENE SOLAR CELLS

J. RAUH*[1]

[1]Experimental Physics VI, Faculty of Physics and Astronomy, Julius-Maximilians University of Würzburg, Am Hubland, 97074 Würzburg, Germany

Trap states can have a significant influence on the performance of organic solar cells, as they lower the mobility, disturb the internal field distribution and affect the recombination dynamics. We investigated the trap states in the polymer poly(3-hexylthiophene) (P3HT) as well as in fullerene derivatives commonly used as electron acceptors in organic bulk-heterojunction solar cells, namely $PC_{61}BM$ ([6,6]-phenyl C61 butyric acid methyl ester), $PC_{71}BM$ and $bisPC_{61}BM$, by thermally stimulated current measurements. This technique is based on optical trap filling at very low temperatures and subsequent heating of the sample, resulting in a thermal release of the trapped charge carriers, which is detected as a current flow. This current yields information about the activation energies and the lower limit of the trap density. Hereby, broad quasi-continuous trap distributions and trap densities in the order of 10^{16} cm^{-3} were revealed for all investigated materials (Figure 1).[1–3] Furthermore, $PC_{71}BM$ and $bisPC_{61}BM$ exhibited significantly deeper traps compared to $PC_{61}BM$.[2] This can be explained by the fact that $PC_{71}BM$ and $bisPC_{61}BM$ are isomeric mixtures, with the different isomers yielding different LUMO energies, where the lowest can act as trap states.

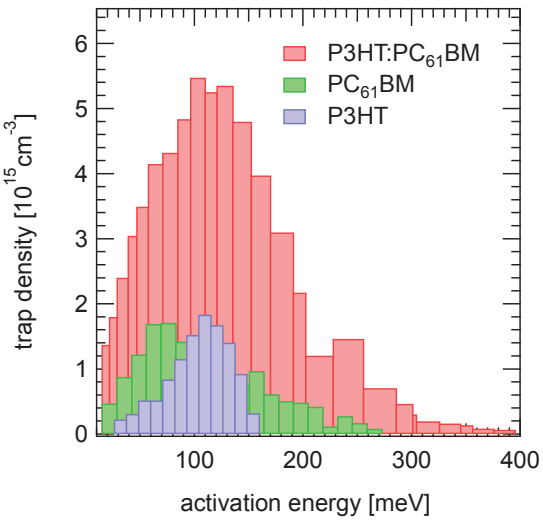

Figure 1: Trap distributions of P3HT, $PC_{61}BM$ and their blend, as obtained by thermally stimulated current measurements. All samples exhibit broad trap distributions.

In addition to the pure materials also the trap states in polymer-fullerene blends were studied, revealing that the traps in the blend are a superposition of those in the neat materials and

additional deeper trap states.[3] The ratio of these deeper traps strongly depends on the preparation conditions of the solar cells, i.e. with or without a thermal annealing step, and thus on the morphology of the solar cells.

Our investigations are complemented by current-based deep level transient spectroscopy, yielding additional information about the emission rates of the traps. These measurements reveal that even trap states with similar activation energies exhibit emission rates that can differ more than one order of magnitude. These findings are of fundamental importance to describe charge carrier dynamics, e.g. in transient experiments.

[1] J. Schafferhans, A. Baumann, C. Deibel and V. Dyakonov, *Trap distribution and the impact of oxygen-induced traps on the charge transport in poly(3-hexylthiophene)*, Appl. Phys. Lett. 93, 093303, (2008)

[2] J. Schafferhans, C. Deibel and V. Dyakonov, *Electronic Trap States in Methanofullerenes*, Adv. Energy Mater. 1, 655, (2011)

[3] J. Schafferhans, A. Baumann, A. Wagenpfahl, C. Deibel and V. Dyakonov, *Oxygen doping of P3HT:PCBM blends: Influence on trap states, charge carrier mobility and solar cell performance*, Org. Electron. 11, 1693, (2010)

BIOGRAPHIC DATA OF DR JULIA RAUH

Personal Information

Name:	**Julia Rauh**, née Schafferhans
Work Address:	Julius-Maximilians-University of Würzburg Experimental Physics VI Am Hubland, D-97074 Würzburg

Academic Education

10/2002–09/2004	Physik (Diplom): Vordiplom University of Bayreuth, Germany
10/2004–03/2005	Physik (Diplom) University of Hamburg, Germany
04/2005–11/2007	Physik (Diplom): Julius-Maximilians-University of Würzburg, Germany Thesis: *Untersuchung elektronischer Störstellen in ungeordneten organischen Halbleitern*
01/2008–06/2011	PHD in Natural Sciences (Physics) Chair of Experimental Physics VI (Energy Research), Prof. Vladimir Dyakonov Julius-Maximilians-University of Würzburg, Germany Thesis: *Investigation of defect states in organic semiconductors: Towards long term stable materials for organic photovoltaics*

Academic Career

since 07/2011	Group Leader Chair of Experimental Physics VI (Energy Research), Prof. Vladimir Dyakonov Julius-Maximilians-University of Würzburg, Germany

Scholarships/Awards

05/2008–12/2010	Postgraduate scholarship (Graduiertenstipendium nach dem Bayrischen Eliteförderungsgesetz)
12/2008	Wilhelm-Conrad-Röntgen Student Award
05/2009	Zonta Award
12/2009	Nominee: Best-Poster-Award (MRS Fall Meeting)

Part III: OFETs, Sensors and related

SMART SYSTEM INTEGRATION AND ALL-PRINTED ACTIVE MATRIX SENSORS

G. Scheipl[1], M. Zirkl[1], A. Sawatdee[2], U. Helbig[3], M. Krause[4], E. Kraker[1], P. Andersson Ersman[2], D. Nilsson[2], D. Platt[2], P. Bodö[2], S. Bauer[4], G. Domann[3], A. Mogessie[5], P. Hartmann[1], and B. Stadlober[1*]

[1]Institute of Surface Technologies and Photonics, Franz-Pichler-Strasse 30, 8160 Weiz, Austria
[2]Acreo AB, Box 787, 60117 Norrköping, Sweden
[3]Fraunhofer-Department for Silica-Research ISC, Neunerplatz 2, 97082 Würzburg, Germany
[4]Soft Matter Physics, Johannes Kepler University, Altenbergerstr. 69, 4040 Linz, Austria
[5]Department of Earth Science, Universitätsplatz 2, 8010 Graz, Austria

ABSTRACT

In organic and large-area electronics smart sensors for detection of physical forces are very promising with respect to novel user interface applications. Recently, there have been several reports on different types of active matrix sensor networks, however in most of these components the large number of process steps, substrates and materials involved make their fabrication complex, costly and hard to control, with expectedly small yield. Hence, developing an active-matrix sensor technology that is fabricated exclusively by printing and uses as few materials as possible constitutes an advance towards low-cost and large-area sensing films. Here we demonstrate the printing of a complex smart integrated sensor system using only five functional inks: the fluoropolymer P(VDF-TrFE) (Poly(vinylidene fluoride trifluoroethylene) sensor ink, the conductive polymer PEDOT:PSS (poly(3,4-ethylenedioxythiophene):poly(styrene sulfonic acid) ink, a conductive carbon paste, a polymeric electrolyte and SU8 for separation. The result is a touchless human-machine interface, including piezo- and pyroelectric sensor pixels (sensitive to pressure changes and impinging infrared light), transistors for impedance matching and signal conditioning, and an electrochromic display. Applications may not only emerge in human-machine interfaces, but also in transient temperature or pressure sensing used in safety technology, in artificial skins and in disposable sensor labels.

Keywords: HMI, P(VDF:TrFE), PEDOT:PSS, touchless, piezo- and pyroelectric sensor, organic transistors, electrochromic display (ECD)

1. INTRODUCTION

Today, printed electronics promise to radically change our means of fabricating electrical devices to the direction of low-cost, large-volume, and sustainable production on flexible or elastic substrates.[1] This increasingly allows applications of electronics "anywhere, not just everywhere".[2] Simple printed electronic devices, such as antennas,[3] printed conductive films,[4] printed memories, [5] batteries,[6] and solar cells,[7] have already been launched on the market or are close to being launched. Admittedly, a real market penetration of printed electronic products has not yet taken place mainly due to drawbacks in performance, cost, and manufacturability.

That applies in particular to more complex printed components combining different classes of devices, such as printed radio frequency identification (RFID) tags,[4] smart labels and cards,[4] smart packaging,[8] or any other type of smart integrated system. Smart sensors are very promising with respect to potential application scenarios for detection of physical forces. Recently, there have been several reports on different types of active matrix sensor networks based on, for example, an integration of pressure and thermal sensors with organic thin-film transistors (OTFTs) for an artificial skin system,[9] a combination of a fluoropolymer-based ultrasonic sensor with OTFTs,[10] large-area image sensors based on organic photodiodes and OTFTs,[10] and a strain sensor array combining OTFTs and polymer sensors. Although these devices open up new fields of applications in large-area electronics, the numerous processing steps, substrates, and materials involved make their fabrication complex, costly, and hard to control, with expectedly small yield. Hence, developing an active matrix sensor technology that is fabricated exclusively by printing as few materials as possible constitutes an advance towards low-cost and large-area sensing films.

P(VDF-TrFE) copolymers have become very attractive as functional materials for high-tech applications due to a number of excellent inherent physical properties. Apart from the usage as high-k gate dielectrics in logic gates based on miniaturized organic thin film transistors, a remnant polarization charge of more than 100 mC/m^2 qualifies these copolymers as charge storage dielectrics in non-volatile memory elements,[12] and high piezo- and pyroelectric coefficients (up to 40 $\mu C/Km^2$) [13] make them attractive for sensor- and transducer based organic devices.

The basic Ferroelectric-Active-Matrix-Sensor (FAMS) device is comprised of two components: (1) a low voltage organic thin film transistor (OTFT) or an electrochemical transistor (ECT) which is driven by (2) a temperature and/or pressure sensitive pyro- and/or piezoelectric thin film capacitor based on poly[(vinylidene fluoride-co-trifluoroethylene] (PVDF-TrFE). By locally changing the temperature or pressure on the active sensor area, an electrical charge is generated at the sensors electrodes, resulting in a voltage signal that is used to drive the gate of an OTFT or ECT, respectively. The OTFT/ECT is coupled to the sensor area by connecting one sensors electrode directly to the gate of the transistor. The temperature or pressure-dependent gate voltage is then transformed to a temperature or pressure-modulated drain current signal which is further processed by data read-out components in central electronic units. Depending on the application, such integrated sensor elements can be arranged in arrays on different flexible substrates that can easily be attached to arbitrarily curved surfaces.

2. EXPERIMENTAL

2.1 Fabrication of Lab Scale Devices

The consecutively described shadow-mask based lab scale devices have been the preliminary stage of the fully printed integrated sensor devices. The design of the lab-scale sensor is very similar to that of the fully printed ones, with a 3×6 array of circular spot forming the sensor pixels and organic thin film transistors connected to each column and row. As a substrate a PET foil with the size of 75×25 mm – thus fitting the sample holder for the shadow mask process – was used. In the first step an 80 nm film of aluminum was applied by means of electron beam (e-beam) evaporation via a shadow mask onto the PET substrate, serving as the bottom electrode of the sensor.

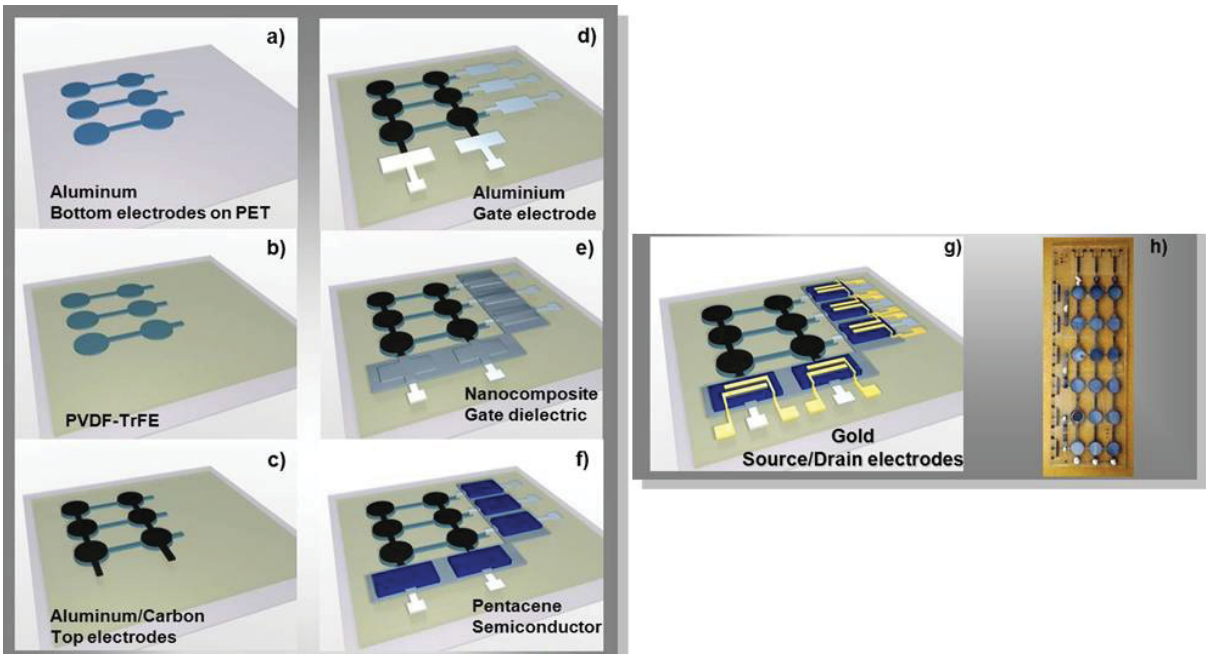

Figure 1: Process flow for the fabrication of lab-scale integrated ferroelectric polymer sensor arrays based on physical vapor-phase deposition (PVD), spin coating and patterning by shadow masks. (a) e-beam evaporation of aluminum to form the bottom electrodes of the sensor, (b) spin coating of P(VDF:TrFE) film to form the ferroelectric dielectric of the sensor, (c) e-beam evaporation of aluminum to form the top electrodes of the sensor and painting of carbon absorption layers. (d) e-beam evaporation of aluminum to form the OTFT gate electrode, (e) application of the nanocomposite gate dielectric by RF-sputtering of ZrO_2 and spin coating of Poly(vinyl cinnamate) (f) thermal evaporation of the organic semiconductor pentacene, (g) e-beam evaporation of gold to form OTFT source and drain electrodes, (h) photographic image of a flexible PVD-fabricated 3×6 sensor array with integrated OTFTs. The close-up shows the OTFT in detail, (i) AFM height image of the spin-coated P(VDF:TrFE) layer. The color map corresponds to a height scale ranging from 0-116 nm. The rms-roughness is 14.5 nm.

The next step was the deposition of an approximately 2 µm thick P(VDF-TrFE) layer (70:30 mol%) via a spin coating technique. Without any patterning this process formed the ferroelectric dielectric which was also investigated by AFM. This spin coated ferroelectric polymer film form a loose network of „spaghetti“. The roughness of the surface (rms) is relatively high (~14.5 nm) with a maximum peak of ~100 nm. The sensor was finished by shadow mask evaporation of an 80 nm aluminium top electrode on the ferroelectric material. For improved IR-absorption a graphite layer has subsequently been applied on the covering electrode.

The fabrication of the OTFTs started with e-beam evaporation of aluminium (80 nm) through a shadow mask, serving as the gate electrode being connected to the sensors top electrode. The next step was the deposition of a nanocomposite gate dielectric by RF-sputtering of ZrO_2 (40 nm) and spin coating a thin layer (20 nm) of Poly(vinyl cinnamate) (PVCI) backfilling the grainy metal oxide film and forming a seed layer for the semiconductor. This gate dielectric shows an overall capacitance of 100 – 110 nF/cm^2 and is described as high-k gate dielectric on that account.[14] Subsequently, 50 nm Pentacene are evaporated on top of the semiconductor thus forming the organic semiconductor. The OTFTs have been finalized by e-beam evaporation of Au (80 nm), forming the source- and drain electrodes. The patterning of the OTFTs was achieved by using shadow masks for all process steps mentioned afore.

2.2 Fabrication of Large Area Devices

The process flow of the screen and inkjet-printed active matrix sensor is illustrated in Figure 2. In total, six printing steps are needed to build the sensor array. A flexible 175 μm thick PET (polyethylene terephthalate) sheet is used as a substrate. First, the bottom electrodes of the pyroelectric and piezoelectric sensor capacitor (sensor pixel) are screen-printed (Figure 2a). A standard PEDOT:PSS ink was utilized, yielding smooth (root mean square (rms) roughness of 6 nm) and conductive (325 Ω per square) layers with a thickness in the range of 400–500 nm. Circular sensor spots, which are interconnected by lines, form arrays of 3x6 (see also: Figure 2g) or 3x4 pixels. In the second step, the ferroelectric polymer PVDF-TrFE is screen-printed onto the PEDOT:PSS bottom electrodes, followed by a short curing step at 110°C (Figure 2b). The curing step supports the formation of the crystalline piezo- and pyroelectric β -phase and accelerates evaporation of the solvent. With an ink containing 18 wt% fraction of the fluoropolymer, the screen-printed P(VDF-TrFE) layers have a thickness of approximately 5 μm. Atomic force microscopy (AFM) analysis of the surface morphology of the P(VDF-TrFE) film (Figure 2h) show a grainy structure with an rms roughness of 4.5 nm. The fabrication of the piezo- and pyroelectric sensor pixels is finalized by screen-printing of either 6 μm-thick carbon or 500–600 nm thick PEDOT:PSS top electrodes (Figure 2c). Both electrode materials exhibit good absorption (> 70%) in the near to mid-IR range. In contrast to the black carbon electrodes, the PEDOT:PSS electrodes appear light grey in the visible range, as shown in the photograph of the integrated sensor in Figure 1g. Since P(VDF:TrFE) is transparent in the visible range, nearly transparent sensor pixels are obtained when PEDOT:PSS is used for the top and bottom electrodes (Figure 1b). The subsequent printing steps involve the fabrication of the read-out electronics that is based on ECTs[16]. In order to minimize the number of printing steps, a lateral ECT architecture was chosen in which the gate and channel are located in the same layer [15]. Carbon-based contact lines and pads are screen-printed; this step is combined with the printing of the sensor's top electrodes (Figure 2c) (unless PEDOT:PSS is used for the top electrodes). The channel and the gate electrode, both made of PEDOT:PSS, are inkjet-printed (Figure 2d). In order to achieve a sufficient matching of the input impedance of the ECT with the high impedance of the sensor capacitance, it was necessary to significantly reduce (i) the dimensions (length and width ≈ 100 μm) and (ii) the thickness (400–500 nm for one layer) of the PEDOT:PSS transistor channel. This was achieved by inkjet printing the channel instead of screen printing thus reducing the ECTs switching current. The inkjet-printed dielectric SU-8 lacquer layer with a thickness of 6 μm separates the carbon contacts from the electrolyte (Figure 2e). The final step in the ECT production is the deposition of an electrolyte layer, which is again done by inkjet printing (Figure 2f). The whole active matrix sensor device is thus fabricated by a combination of screen and inkjet printing processes.

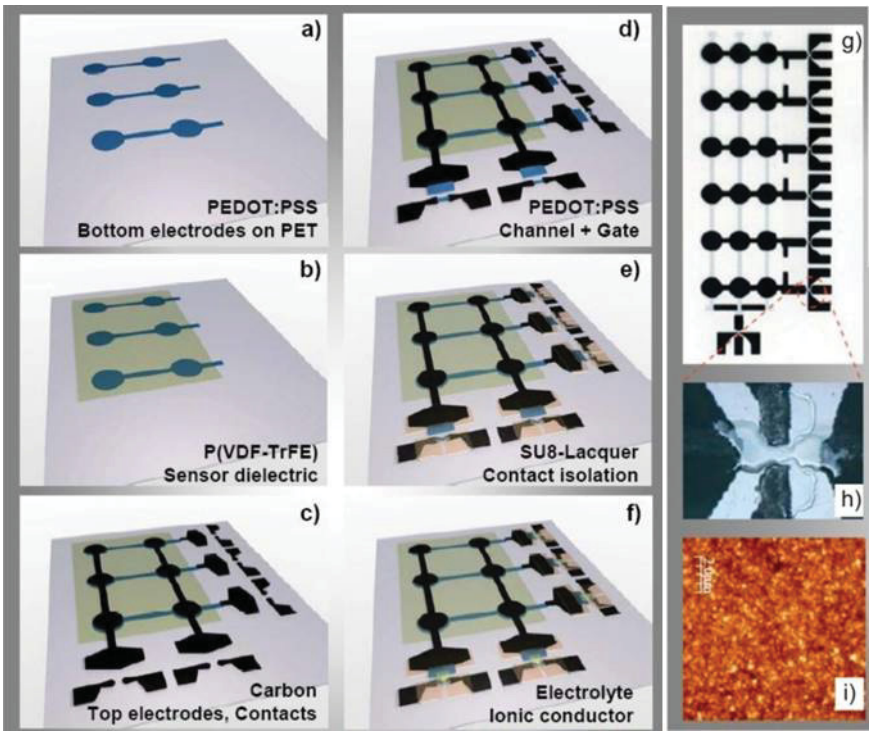

Figure 2: Process flow illustrating the fabrication of printed ferroelectric active matrix sensor arrays. a) Screen printing with PEDOT:PSS to form the bottom electrodes of the sensor pixel, b) screen printing of the ferroelectric P(VDF:TrFE) fi lm, c) screen printing of carbon to form the top electrodes of the sensor pixel, d) inkjet printing with PEDOT:PSS to form the gate and channel of the ECTs, e) inkjet printing of the SU-8 separation layer, f) inkjet printing of the ECT polymeric electrolyte, and g) photograph of an all-printed 3 x 6 sensor array with integrated ECTs. h) Close-up of the channel region of the ECT. i) AFM height image of the screen-printed P(VDF:TrFE) layer. The color map corresponds to a height scale ranging from 0–55 nm. The rms roughness of the film is 4.5 nm.[14]

2.3 Poling

For the usage as transducer material, the crystalline domains must be aligned with respect to their electrical dipoles. Therefore an electrical poling procedure must be applied for aligning the ferroelectric domains. Two different poling techniques have been used: (i) stepwise poling as described elsewhere [18][19] and (ii) hysteresis poling.

Hysteresis poling following a Sawyer-Tower circuit also enables monitoring the ferroelectric properties of the sensor by hysteresis loop measurements (Figure 3**)**. The coercive field strength required to switch the ferroelectric polarization was between 70-80 $V\mu m^{-1}$ and the resulting remnant polarization P_r (the displacement at zero electric field) was in the range of 70 mCm^{-2}. These values are close to the best values reported for ferroelectric capacitors based on spin-coated P(VDF:TrFE)[12]. To this end, hysteresis loops were recorded with electric fields in the saturation region until stable hysteresis loops were obtained. The poling process was then stopped at zero electric field. With this process, reproducible piezo- and pyroelectric characteristics were obtained in the sensor pixels.[15][21][22]

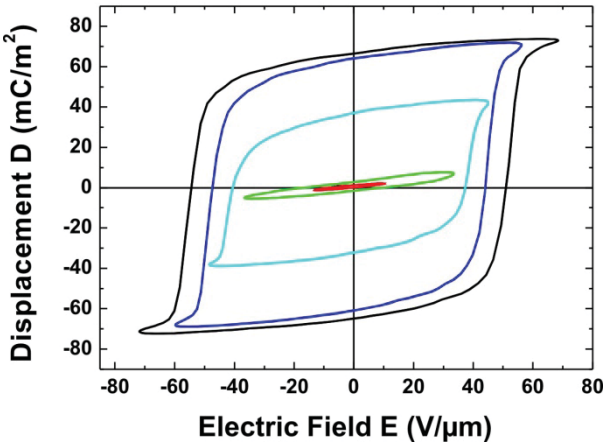

Figure 3: Hysteresis loops of a ferroelectric sensor pixel. The lines illustrate the opening of the loop with increasing electric field amplitude.

2.4 Pyroelectric Characterization

The voltage response of a sensor pixel is induced by thermal excitation with an intensity-modulated light from a laser diode emitting in the near infrared (808 nm) or with intensity-modulated mid-infrared CO_2 laser radiation at 10.5 µm. Figure 4 displays the voltage responses for excitation at 808 nm with a maximum intensity of 70 mW measured for sensors with both carbon and PEDOT:PSS top electrodes. In the frequency range from 5 to 1000 Hz the voltage response decreases monotonically, as expected for a pyroelectric detector element [22] [24] Carbon top electrodes generate a larger output voltage than PEDOT:PSS electrodes primarily owing to the somewhat higher absorption of carbon in the mid-IR.

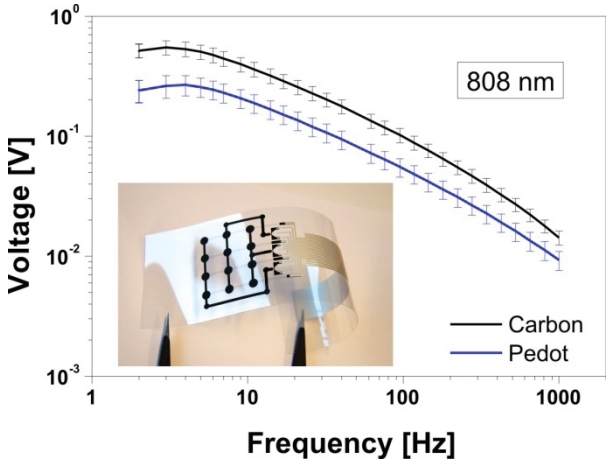

Figure 4: Frequency dependence of the pyroelectric voltage response of a sensor pixel excited by intensity-modulated light from a laser diode emitting at 808 nm for carbon and PEDOT:PSS top electrodes. The error bars illustrate the variation in the pyroelectric response across the pixels of the 3 x 4 printed sensor arrays.

The overall frequency behaviour, the influence of sensor geometry, parasitic capacitance and impedance, absorption coefficients of the top electrodes, pyroelectric sensitivity of the sensor layer and influences of fabrication processes have been evaluated and verified using mathematic modeling of the electric measurements.

3. RESULTS

In Figure 5 the frequency dependent pyroelectric current and voltage outputs of LabScale sensors with different areas are shown. Similar curves are also obtained for printed PVDF-TrFE based sensors. The impinging laser beam always excites a constant area of 3 mm^2 being much smaller than the overall area of the sensor.

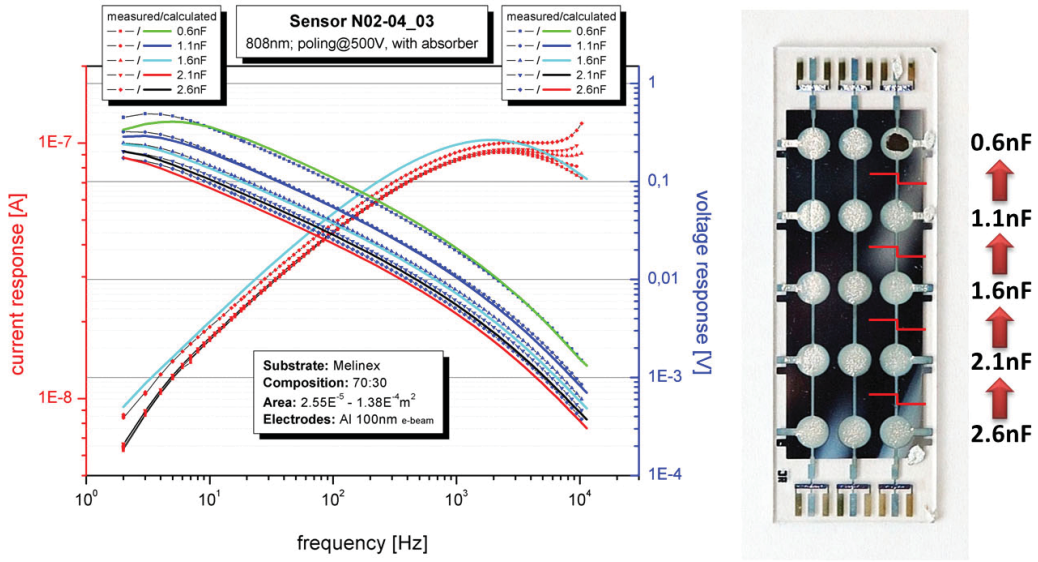

Figure 5: The influence of parasitic capacities on the pyroelectric sensor output and its mathematically assessment (solid lines) are shown *(left)*. The overall sensor area is decreased stepwise by successively cutting the connecting lines between the circular sensor fields at a constant area of excitation *(right)*. Additional explanations are given in the text.

The overall sensor area is decreased stepwise by successively cutting the connecting lines between the circular sensor fields (see Figure 5, *right)*. Accordingly the parasitic capacitance of the sensor is decreased without decreasing the excited area. As is observed in Figure 5 *(left)*, the parasitic capacities are decreasing the voltage output though are not affecting the current generated by the laser excitation. This is due to the fact that the pyroelectric current varies as

$$|V| = |I| \cdot \frac{R}{\sqrt{1+\omega^2 R^2 C^2}} \tag{3}$$

with R and C being impedance and capacitance of the equivalent circuit (thus also including capacitance and impedance of the measurement circuit). According to (3) the voltage response varies as I·R below and I/ώC above the cut-off frequency. The cut-off frequency is determined by the RC-time constant of the whole equivalent circuit. The generated pyroelectric current I can be described as

$$I = pA\,\omega\overline{T} \tag{4}$$

with p being the pyroelectric coefficient, A being the excited area and T being the average temperature of the pyroelectric layer. From (3) and (4) it becomes clear that the current response is independent of the parasitic capacitance whereas the voltage response is decreased. The resulting simulated response curves are also included in Figure 5 as continues lines. The excellent correspondence to the experimental data points fully verifies the theoretical model of the multilayer sensor and the simulation routine. As is expected the current response is not influenced by the parasitic whereas the voltage response decreases continuously with increasing parasitic capacitance.

According to the congruent results of the pyroelectric measurements and the mathematic modeling of the LabScale devices, a new design for large area and fully printed devices was developed. In this context the new design was used for an integration of the sensor device with (1) OTFTs and ECTs and (2) in a further step with an electrochromic display (ECD).

3.1 Integration of the Sensor with OTFTs and an ECD

Low leakage currents below 2 nA guarantee a very good impedance matching between the OTFT and the sensor; resulting in a complete switching of the transistor being biased by the

sensor as shown in Figure 6 (left). After the additional combination with the display, the drain current of the transistor is only marginally reduced (Figure 6 (right)). The small reduction of the drain current is caused by the current consumption of the display during the reduction / color change. The dark blue arrows are indicating the regions of the reduction according to switching the digit on and the light blue arrows are indicating the discharge of the display to its initial highly conductive "off state". The frequency of the repeated switching process was chosen to be 0,01 Hz due to the slow relaxation time of the display that is to be expected in such a simple configuration without any control electronics.

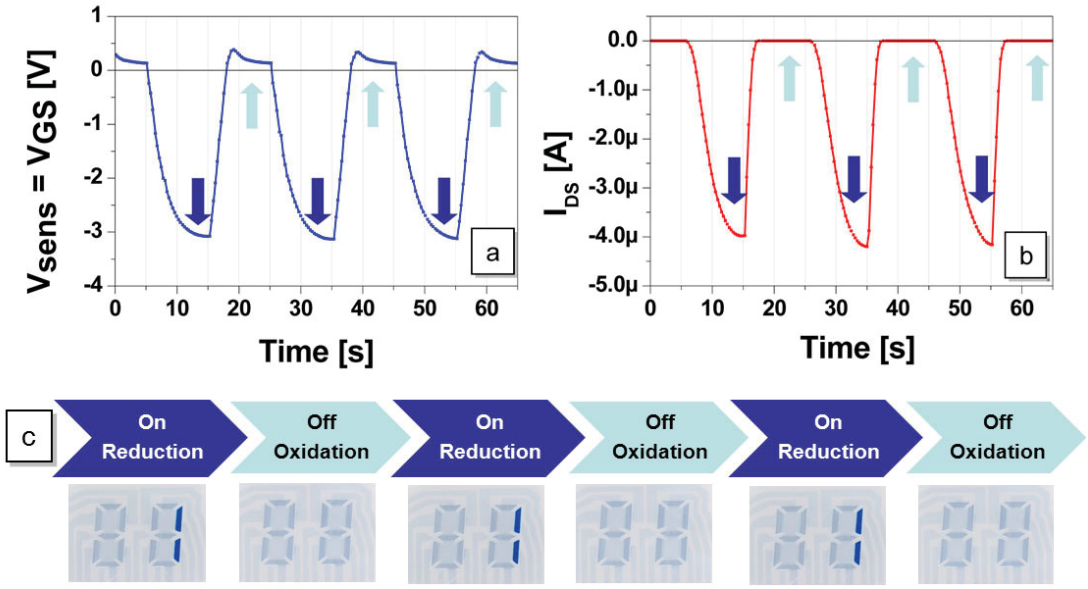

Figure 6: Sensor output (a) and drain current (b) during the color switching of the printed display. The sensor was stimulated at 0,01 Hz with a 70 mW laser diode and the drain voltage was -1 Volts. For discharging (oxidizing) the display, a 500 kΩ resistor was connected between supply voltage and ground. The arrows are indicating the color changes of the display caused by reduction/oxidation (c) of the electrolyte.

3.2 Integration of a Sensor with ECTs and an ECD

Due to the usage of ink-jet printing for the PEDOT:PSS channel in electrochemical transistors, the current consumption during the redox process of the electrolyte could be drastically reduced. Therefore the impedance matching between sensor and ECT could be adjusted and the complete switching of the transistor biased by the sensor was achieved. The maximum voltage at the carbon electrodes was about 0.7 V for an input impedance of the equivalent measurement circuit of 100 MΩ, and 0.3 V at the PEDOT:PSS top electrodes. Since the sensor is connected in parallel to the gate of the electrochemical transistor, the voltage response generated by the pyroelectric pixel is sufficient to switch the transistor current. Figure 7a displays an output characteristic of a printed ECT with a lateral electrode configuration. Since in an ECT the conductivity of the PEDOT:PSS channel is decreased by applying a positive gate voltage, these devices are normally on and can be controlled by very small voltage levels; in this case the printed ECT is switched off by applying a gate voltage of only 0.75 V (Figure 7b).

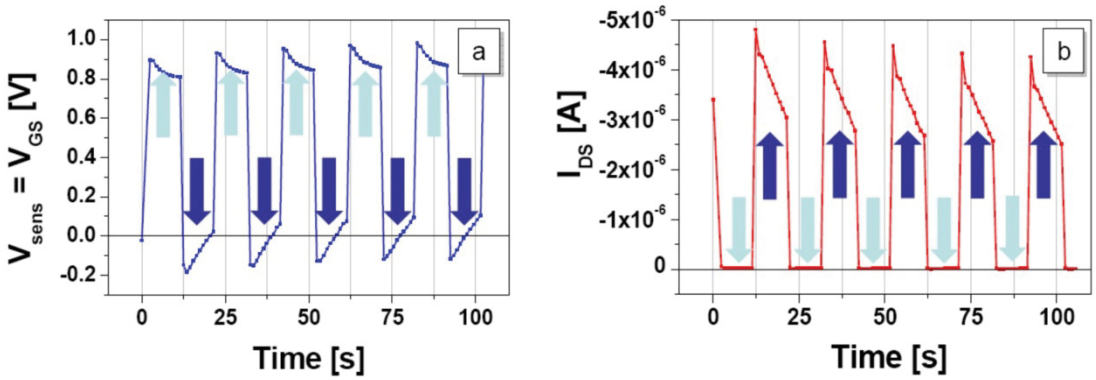

Figure 7: a) Time curve of the voltage response V_{sens} of a printed sensor pixel induced by square-wave intensity-modulated laser light (808 nm). The arrows indicate the state of the electrochromic display. b) Time curve of the ECT drain current induced by V_{sens}. Since the sensor capacitor and the transistor are connected in parallel, the ECT gate voltage corresponds to V_{sens}. The arrows indicate the state of the display.

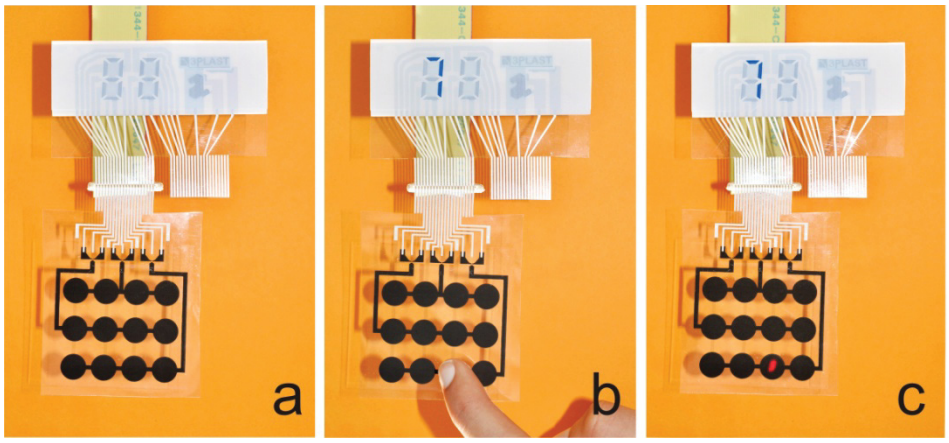

Figure 8: a) Photograph of a printed active matrix sensor consisting of a 3 x 4 array of sensor capacitors integrated with a row of electrochemical transistors connected to a printed electrochromic display. b) Activation of display segments due to infrared radiation from a human finger. c) Activation of display segments with light from a laser pointer.

REFERENCES

[1] R. Parashkov, Parashkov, R., Becker, E., Riedl, T., Johannes, H.-H., Kowalsky, W., "Large Area Electronics Using Printing Methods" Proceedings of the IEEE 93(7), 1321-1329 (2005).

[2] S. P. Lacour, in PerAda Magazine 2010 , www.perada-magazine.eu/pdf/003194/003194.pdf

[3] Schreiner, Printing the future, www.schreiner-printronics.com (2011).

[4] PolyIC homepage, PolyIC-"the chip printers", www.polyic.com (2011).

[5] ThinFilm homepage, World's first printed ferroelectric memory device, www.thinfilm.se (2011).

[6] a) Enfucell homepage, It's a paper-thin, it's a battery and it's green, www.enfucell.com (2011); b) Power Paper, Printable batteries, www.powerpaper.com (2011).

[7] Konarka homepage, Converting Light to Energy, www.konarka.com (2011).

[8] Holst Centre homepage, Smart packaging, www.holstcentre.com (2011).

[9] T. Someya, "From the Cover: Conformable, flexible, large-area networks of pressure and thermal sensors with organic transistor active matrixes," Proceedings of the National Academy of Sciences 102, 12321–12325 (2005).

[10] T. Someya, A. Dodabalapur, J. Huang, K. C. See, and H. E. Katz, "Chemical and Physical Sensing by Organic Field-Effect Transistors and Related Devices", Advanced Materials, 22(34), 3799–3811 (2010).

[11] Someya, T., Kato, Y., Shingo Iba, Noguchi, Y., Sekitani, T., Kawaguchi, H., Sakurai, T., "Integration of organic FETs with organic photodiodes for a large area, flexible, and lightweight sheet image scanners," IEEE Transactions on Electron Devices, 52(11), 2502-2511 (2005).

[12] R. C. G. Naber, C. Tanase, P. W. M. Blom, G. H. Gelinck, A. W. Marsman, F. J. Touwslager, S. Setayesh, and D. M. de Leeuw, "High-performance solution-processed polymer ferroelectric field-effect transistors," Nature Materials 4, 243–248 (2005).
[13] N. Neumann, R. Köhler, G. Hoffmann, "Application of P(VDF/TrFE) thin films in pyroelectric detectros," Ferroelectrics, vol. 118, pp. 319- 324, (1991).
[14] M. Zirkl, A. Sawatdee, U. Helbig, M. Krause, G. Scheipl, E. Kraker, P. A. Ersman, D. Nilsson, D. Platt, et al., "An All-Printed Ferroelectric Active Matrix Sensor Network Based on Only Five Functional Materials Forming a Touchless Control Interface," Advanced Materials 23, 2069–2074 (2011).
[15] M. Zirkl, A. Haase, A. Fian, H. Schön, C. Sommer, G. Jakopic, G. Leising, B. Stadlober, I. Graz, et al., "Low-Voltage Organic Thin-Film Transistors with High-k Nanocomposite Gate Dielectrics for Flexible Electronics and Optothermal Sensors," Advanced Materials 19, 2241–2245 (2007) [doi:10.1002/adma.200700831].
[16] D. Nilsson, M. Chen, T. Kugler, T. Remonen, M. Armgarth, and M. Berggren, "Bi-stable and Dynamic Current Modulation in Electrochemical Organic Transistors," Advanced Materials 14, 51–54 (2002).
[17] D. Nilsson, N. Robinson, M. Berggren, and R. Forchheimer, "Electrochemical Logic Circuits," Advanced Materials 17, 353–358 (2005) [doi:10.1002/adma.200401273].
[18] D. Setiadi, M. Sarro, and L. Regtien, "A 3x1 integrated pyroelectric sensor based on VDF/TrFE copolymer," Sensors and Actuators A: Physical 52, 103–109 (1996).
[19] M. Zirkl, B. Stadlober, and G. Leising, "Synthesis of Ferroelectric Poly(Vinylidene Fluoride) Copolymer Films and their Application in Integrated Full Organic Pyroelectric Sensors," Ferroelectrics, vol. 353, no. 1, pp. 173-185, (2007).
[20] S. Bauer, F. Bauer, [Piezoelectricity: Evolution and Future of a Technology], Springer Series in Materials Science, Berlin, Ch. 6, pp.157 (2008).
[21] J. Groten, M. Zirkl, G. Jakopic, A. Leitner, and B. Stadlober, "Pyroelectric scanning probe microscopy: A method for local measurement of the pyroelectric effect in ferroelectric thin films," Physical Review B 82, 1–11 (2010) [doi:10.1103/PhysRevB.82.054112].
[22] I. Graz, M. Krause, S. Bauer-Gogonea, S. Bauer, S. P. Lacour, B. Ploss, M. Zirkl, B. Stadlober, and S. Wagner, "Flexible active-matrix cells with selectively poled bifunctional polymer-ceramic nanocomposite for pressure and temperature sensing skin," Journal of Applied Physics 106, 034503 (2009) [doi:10.1063/1.3191677].
[23] T. Furukawa, J. X. Wen, K. Suzuki, Y. Takashina, M. Date, "Piezoelectricity and pyroelectricity in vinylidene fluoride/trifluoroethylene copolymers" J. Appl. Physics, 56, 829, (1984).
[24] P. Muralt, "Micromachined infrared detectors based on pyroelectric thin films" Rep. Prog. Phys., 64(10), 1339, (2001).

BIOGRAPHIC DATA OF DR BARBARA STADLOBER

Full Name	Barbara Stadlober	
Position	Head of Research Group	
Affiliation	Institute of Surface Technologies and Photonics, JOANNEUM RESEARCH, Franz-Pichlerstrasse 30, A-8160 Weiz	
Title of talk	Smart system integration and all-printed active matrix sensors	
Abstract	In organic and large-area electronics smart sensors for detection of physical forces are very promising with respect to novel user interface applications. Recently, there have been several reports on different types of active matrix sensor networks, however in most of these components the large number of process steps, substrates and materials involved make their fabrication complex, costly and hard to control, with expectedly small yield. Hence, developing an active-matrix sensor technology that is fabricated exclusively by printing and uses as few materials as possible constitutes an advance towards low-cost and large-area sensing films. Here we demonstrate the printing of a complex smart integrated sensor system using only five functional inks: the fluoropolymer P(VDF-TrFE) (Poly(vinylidene fluoride trifluoroethylene) sensor ink, the conductive polymer PEDOT:PSS (poly(3,4-ethylenedioxythiophene): poly(styrene sulfonic acid) ink, a conductive carbon paste, a polymeric electrolyte and SU8 for separation. The result is a touchless human-machine interface, including piezo- and pyroelectric sensor pixels (sensitive to pressure changes and impinging infrared light), transistors for impedance matching and signal conditioning, and an electrochromic display. Applications may not only emerge in human-machine interfaces, but also in transient temperature or pressure sensing used in safety technology, in artificial skins and in disposable sensor labels.	
A brief biography	Dr. Barbara Stadlober has studied solid state physics at the Karl-Franzens-University in Graz. After finishing her PhD at the Technical University in Garching (Germany) on High Temperature Superconductors she worked six years as a technology development engineer for power silicon chips at Infineon Technologies AG in Villach (Austria). Starting from 2002 she established the Organic Electronics group at the Institute of Nanostructured Materials and Photonics of JOANNEUM RESEARCH in Weiz (Austria). Since 2010 she is head of the research unit “Micro- and Nansotructuring” at the – intermediately enlarged - Institute of Surface Technologies and Photonics of JOANNEUM RESEARCH. Her main interests are organic electronics and optoelectronics, process development, novel nanostructuring methods and organic sensor technologies.	

Organic biosensors based on biocompatible solution-processable materials

PD Dr.-Ing. Giuseppe Scarpa
Institute for Nanoelectronics, Technische Universität München, Germany

Simple, low-cost portable devices, which can perform reliable fast diagnostic procedures and can be used as disposables in life science, cover a wide range of sensing applications, i.e., food and environmental monitoring or detection of biological hazardous material. Field-effect transistors based on organic materials [organic thin-film transistor (OTFTs)] can provide a promising answer in the aforementioned field of applications. Besides low-cost large-area substrate-independent fabrication capability, organic materials offer a unique opportunity when used in sensing application, in which the semiconducting material acts both as active transport layer and sensing component. Here, we report on OTFTs-based sensing devices using a biofunctionalized, biocompatible solution-processable organic semiconducting polymer, which can be operated in complex biological media in direct contact with living cells, opening up the possibility of developing easy to handle, inexpensive test stripes for reliable, and fast biological assays.

Bio-Bibliography: PD Dr.-Ing. Giuseppe Scarpa is Staff Lecturer & Team Leader at the Institute for Nanoelectronics, Technische Universität München, Germany. He graduated in electrical engineering at the University of Rome "Tor Vergata", Italy, in 1998. In 1999 he joined the Walter Schottky Institute of the Technical University of Munich (TUM), Germany, where he received his PhD degree working on design and fabrication of quantum cascade lasers (2003). He is currently staff lecturer at the electrical engineering department and staff scientist at the Institute for Nanoelectronics of TUM. His research focuses on the fabrication of a variety of nanostructures (such organic devices and nanomagnets) and on the development of various nanofabrication technologies based on nanoimprint lithography as well as on biosensors and biochips based on organic materials.

POLYMER SCHOTTKY BARRIER TRANSISTORS

S. Georgakopoulos[1], D. Sparrowe[2], F. Meyer[2], M. Shkunov[1]

1 Advanced Technology Institute, University of Surrey, Guildford GU2 7XH, UK

2 Merck Chemicals, Chilworth Technical Centre, University Parkway, Southampton SO16 7QD, UK

Organic Field-Effect Transistors perform well with ohmic source and drain contacts. However, long term operational stability is typically achieved with high ionisation potential (IP) semiconductors with IP values more than 5.3eV.[1,2] Due to high IP ohmic injection it is becoming problematic, and transistors suffer from injection problems due to the formation of Schottky contacts.

In this work we demonstrate new approach for organic transistors where high IP indenofluorene copolymers with IP values as high as 5.4eV and 5.8eV are used as the semiconducting layers. We deliberately utilise Schottky barriers and special transistor geometry to manipulate charge depletion under the source electrode.[3] As a result we obtain two significant outcomes:

i) we can successfully use high IP polymers with excellent environmental stability,

ii) we achieve excellent I-V curves with saturated voltage as low as 2V for transistors with a channel length of 2.5μm and thick insulating layer of ~1 μm.

The main feature of these transistor devices is the reverse-biased source Schottky barrier which depletes the semiconductor of charge in the vicinity of the source electrode. This depletion extends to the semiconductor/insulator interface and pinches off the channel, leading to a low saturation voltage, which is preserved without down-scaling the insulator thickness as required for typical Field-Effect Transistors. Additionally, for sufficiently strong barriers the output current of the transistor does not scale with channel length. These properties come at the cost of reduced current due to the highly resistant depletion region, and other peculiarities.

In summary, we anticipate that organic transistor fabrication technology could benefit from this new approach by allowing low-cost deposition of thick insulators instead of specialised ultra-thin insulators for low saturation voltages.

Moreover, due to transistor current insensitivity to the channel length, low-resolution channel patterning and printing techniques can be utilised for this type of transistors.

References:

1. I. McCullough, M. Heeney, M.L. Chabinyc, D. DeLongchamp, R.J. Kline, M. Colle, W. Duffy, D. Fischer, D. Gundlach, B. Hamadani, R. Hamilton, L. Richter, A. Salleo, M. Shkunov, D. Sparrowe, S. Tierney, W. Zhang. Adv. Mater. 21, 1091 (2009)

2. S. Georgakopoulos, D. Sparrowe, F. Meyer, M. Shkunov. Appl. Phys. Lett. 97, 243507 (2010)

3. J.M. Shannon, F. Balon. Solid-State Electronics 52, 449 (2008)

CUTOFF FREQUENCY OF ORGANIC FIELD EFFECT TRANSISTORS: A SIMULATION STUDY

S. SCHEINERT*, I. HÖRSELMANN

Ilmenau Technical University, Institute of Micro- and Nanoelectronics and Center of Micro- and Nanotechnologies, PF 100565, D-98684 Ilmenau, Germany

Cutoff frequency is a crucial parameter for many applications of the OFET in organic electronic circuitry. For an ideal transistor this frequency is independent on the insulator thickness and scales with μ/L^2 so that both increasing the mobility μ and reducing the channel length L result in higher values. However, the behavior of the real OFET is strongly influenced by high S/D contact barriers, increased contact resistance and traps. We have carried out 2D simulations of the BOC (S/D bottom contact) and TOC (S/D top contact) OFETs to describe the influence of these effects on the cutoff frequency. As already described in the literature for the BOC OFET [1], series resistance and large overlap capacitances reduce the expected increase of the cutoff frequency reducing the channel length. However our comparison shows this effect is stronger in the TOC structure. The same tendency is valid for the influence of the insulator thickness. Whereas the BOC OFET shows the expected behavior, the cutoff frequency of the TOC one is reduced with reduced thickness. In contrast, for higher S/D contact barriers the cutoff frequency is stronger reduced in BOC OFETs.

Two dimensional simulations have been carried out with the program Sentaurus [2]. The program solves the poisson and continuity equations. For the small signal analysis the complex (small signal) admittance $\underline{Y}$ matrix is computed giving the current response at a given node to a small voltage signal at another node $j = \underline{Y}\, u = A\, u + i\, \omega\, C\, u$. The small signal current gain can be calculated by:

$$h_{21} = \frac{i_d}{i_g} = \frac{A_{dg} + i\omega C_{dg}}{A_{gg} + i\omega C_{gg}} \qquad (1)$$

and the cut-off frequency follows from $|h_{21}|=1$. The simulated device structures are shown in Fig. 1. The used material parameters for the 50nm thick P3HT layer are the following: mobility $\mu=0.02cm^2V^{-1}s^{-1}$, affinity χ =3.0eV, gap E_g=2.0eV, doping level $N_A=5\times10^{16}$ cm^{-3}, density of states in the valence and conduction band $N_V=N_C=10^{21}cm^{-3}$. The oxide thickness is 50nm.

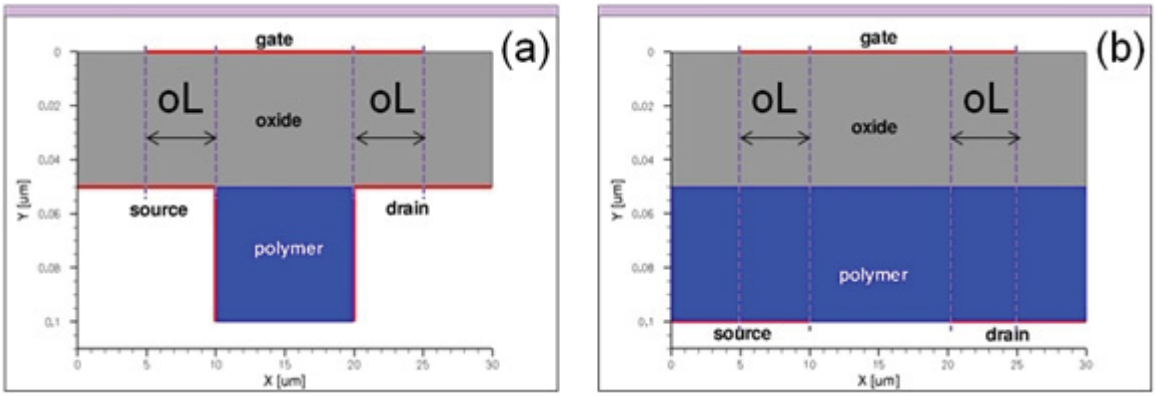

Fig.1. Simulated device structure of the BOC (a) and TOC (b) OFET.

In Fig. 2a simulated cut-off frequencies for different overlap length between the S/D- and gate contacts are shown. Without overlap the simple equation for f_t describes well the BOC transistor behavior. In the TOC OFET the parasitic resistance between the S/D contacts and the channel at the oxide interface are the reason for the reduced cut-off frequency for shorter channels. Contact resistance reduce frequency limit for shorter channels. This effect is more pronounced in the BOC structure as visible from fig.2b. However, also in this case the analytical equation for f_t including series resistance describes well the simulated values.

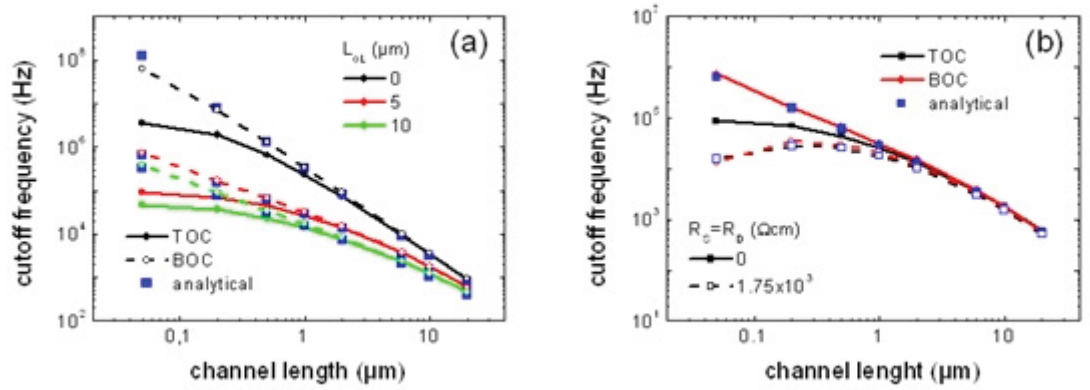

Fig.2 Cut-off frequency of the TOC and BOC OFET vs. channel length for V_{GS}=-6V, V_{DS}=-1V and different overlap length (a) and contact resistance (b).

High contact barriers at source and drain reduce the efficient injection of carriers. Consequently, their influence on the frequency was investigated and the results are shown in fig. 3.

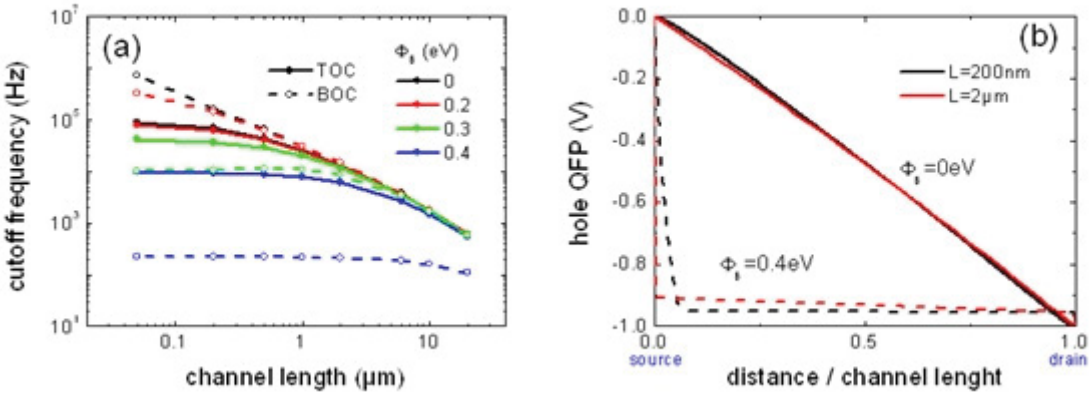

Fig.3 Cut-off frequency of the TOC and BOC OFET vs. channel length for V_{GS}=-6V, V_{DS}=-1V and different S/ work functions (a) and the quasi Fermi potential along the channel near the oxide interface (b).

The cut-off frequency is strongly reduced for higher barriers and again this effect is stronger pronounced in the BOC OFET than in the TOC one. Furthermore, comparing the results with that one of the additional series resistance the constant value despite reduced channel length is visible. The reason for this can be explained with fig. 3b. In the case of contact resistance the channel length determines strongly the potential drop over the series resistance reducing the cut-off frequency with reduced channel length. Contrary, for high contact barriers the potential drop near the contacts does not depend on the channel length resulting in a constant value of f_t.

Traps can also have an influence on the frequency limit. But their effect depends strongly on the trap parameters. Furthermore, in TOC OFETs bulk traps modify the parasitic resistance between the S/D contacts and the channel at the oxide interface.

References

[1] A. Hoppe, D. Knipp, B. Gburek, A. Benor, M. Marinkovic, V. Wagner, Organic Electronics **11**, 626 (2010).

[2] Sentaurus Device User Guide, Version E-2010.12, December 2010, Synopsys

BIOGRAPHIC DATA OF DR SUSANNE SCHEINERT

Degrees

- Diploma in Electrical Engineering in 1975
- Dr.-Ing. in 1992 in the field of SOI electronics
- Dr.-Ing. habil. in 2006 in the field of organic electronics

At present she works in the field of organic electronics with the main focus on organic field effect devices.

THE INFLUENCE OF HOLE INJECTION BARRIERS ON ORGANIC FIELD-EFFECT TRANSISTORS: CONNECTION WITH PHOTOEMISSION DATA [a]

G. PAASCH[*1], S. SCHEINERT[2], M. GROBOSCH[1], I. HÖRSELMANN[2], M. KNUPFER[1], and J. BARTSCH[2]

[1] Institute for Solid State and Materials Research IFW Dresden, PF 270116, D-01171 Dresden, Germany

[2] Ilmenau Technical University, Institute of Micro- and Nanoelectronics and Center of Micro- and Nanotechnologies, PF 100565, D-98684 Ilmenau, Germany

The operation of organic devices as organic field-effect transistors (OFET) depends critically on the contact between the organic layer and the material for source/drain electrodes. Small barriers for carrier injection are required for efficient operation. In order to support the understanding of organic devices, photoemission spectroscopy has been used to determine the properties of metal/organic interfaces. Values for the hole injection barrier determined in the last decade by different groups are frequently of the order of 0.5...1eV. It is not clear whether barrier lowering due to the image charge is sufficient to make contacts with such barriers efficiently for carrier injection. Indeed, no results have been reported where the preparation of the samples for the photoemission study and for the devices is the same.

Here we discuss results of such an investigation for OFETs with P3HT as active layer and with gold source/drain contacts [1]. The measured hole barrier at the gold contact of 0.6eV results from the Au work function of 4.6eV. Taking into account the dependencies of the mobility on the carrier concentration and on the field for the Gaussian density of states (DOS) of disordered organics, measured OFET current characteristics cannot be described well with such contacts but rather for work functions of 4.7eV or larger. Considering the method to determine the barrier from photoemission data and the Gaussian DOS of the hopping transport states, we present a quantitative connection [1] between the barrier as determined from photoemission and the barrier as used in the device simulation. Then we show however, that the definition of the band edge for a Gaussian DOS is problematical.

[*] Corresponding Author: g.paasch@ifw-dresden.de

In photoemission experiments the hole barrier is extracted by linear extrapolation of the upper part of the measured intensity as demonstrated in Fig.1. There the Fermi energy is at binding energy zero and therefore a barrier of 0.6eV is obtained. A fit of the upper part of the spectrum by a Gaussian can be analytically extrapolated and gives the same value. It is clearly seen in Fig.1 that towards the Fermi energy the spectrum shows a tail. It arises from the measurement and does not reflect energy states present there. Here a first problem emerges: From UPS intensities one obtains information in the region down to about 1 to 5 % of the maximum DOS. On the other hand, OFETs operate in accumulation at concentrations of about 10^{18} cm^{-3}, which is slightly more than 10^{-3} of the total density. Therefore, the tail measurable with UPS lies far above the DOS values determining the OFET operation.

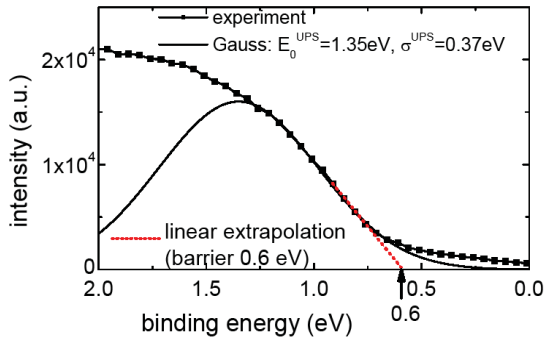

Fig.1. Measured UPS intensity, linear extrapolation for barrier determination, Gaussian fit of the upper part of the spectrum.

Moreover, the Gaussian curve approximating the upper part of the spectrum is rather broad with a variance of 370meV. But in order to describe the measured current characteristics one has to assume a Gaussian DOS

$$D(E) = \frac{1}{\sqrt{2\pi}\sigma}\exp\left(-\frac{(E-E_0)^2}{2\sigma^2}\right) \qquad (1)$$

(Maximum at E_0 and variance σ, determining the mobility) which is much narrower with a variance much less than 100meV. Such variance is in accordance with values reported for other devices. We suppose therefore that the narrow Gaussian DOS determining the hopping transport represents the tail region of the broader Gaussian measured by photoemission. This is demonstrated in Fig.2 showing from the narrow transport DOS only the tail. The continuous transition from the broad photoemission Gaussian to the narrow Gaussian transport DOS is possible for different rations m of their maxima. In Fig.2 the values m=10, 20, 30 are chosen. Smaller values are unrealistic since the transition must occur clearly below the measured UPS intensity.

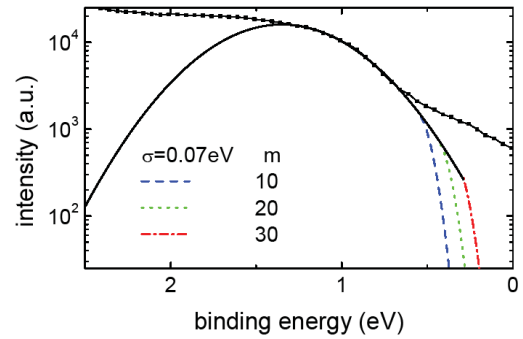

Fig.2. The tail of the Gaussian fit is replaced by a steeper tail of the narrower Gaussian DOS.

Values larger than m= 30…50 can also be excluded, since transport at densities characteristic for accumulation must take place in the narrow tail. In this way, the position of the narrow transport DOS is fixed relative to the photoemission data with an unknown parameter m in the region indicated in Fig. 2. There remains the question on the position of the band edge relative to the narrow transport DOS.

For this purpose we show in Fig.3 the hole density as function of the Femi energy (relative to the maximum E_0 of the narrow transport DOS). The curves with symbols are calculated numerically. The non-degenerate approximation (dashed) is given by [2]

$$\frac{p}{N_0} = \exp\left(-\frac{E_F - (E_0 + \sigma^2/2kT)}{kT}\right). \qquad (2)$$

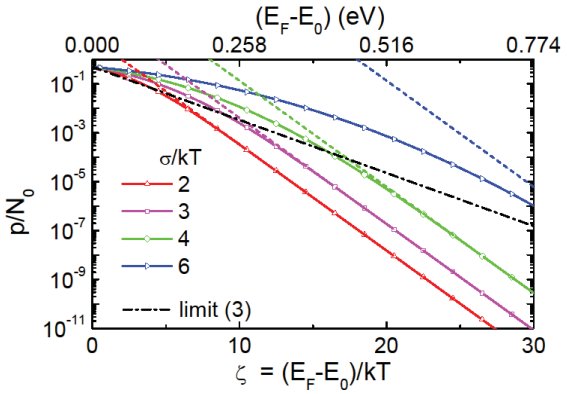

Fig.3. Hole density for the system with a Gaussian DOS: Numerical values with symbols, dashed the non-degenerate approximation (2). Dash-dotted the limit (3) for the transition from non-degeneration to degeneration.

In Fig.3 there is shown also the limit for the transition from low density non-degeneration to degeneration (dash-dotted line) which occurs at

$$E_F - E_0 = \sigma^2/kT. \qquad (3)$$

It is clearly seen in Fig.3 that for smaller variance the non-degenerate approximation works well for concentrations occurring in OFET accumulation layers. This approximation was used in the simulations presented in Ref. [1].

Comparing Eq. (2) with the conventional expression for the hole density one can argue that the valence band edge is situated at $E_V = E_0 + \sigma^2/2kT$. Using this value and the transition from the photoemission intensities to the Gaussian transport DOS, one can establish a relation between the barrier as determined by photoemission and that one needed in device simulation. This was done in Ref. [1]. However, the assumption, that the band edge is situated relative to the maximum of the Gaussian DOS as $E_V = E_0 + \sigma^2/2kT$ is unfortunately not unique. There are different imaginable possibilities. Thus, one can also assume that the band edge is situated at the position (3) where the transition from non-degeneration to degeneration takes place. One can also arbitrarily suppose that the band edge is situated at a position where the density is decreased to n% (e.g.1%) of its maximum value or that the DOS is decreased to n% (e.g.1%) of its maximum value.

Thus, at present, it is hard to establish a well-defined connection between the barrier as determined from photoemission and the position of the band edge needed in device simulation. At first, the position of the transport DOS relative to the measured photoemission date is not well defined (the factor m given above) and secondly, there is no unique definition of the position of the band edge relative to the maximum of the transport DOS.

Highly desired are experimental methods for determination of the transport DOS in the concentration region where the transport takes place.

References

[1] S. Scheinert, M. Grobosch, G. Paasch, I. Hörselmann, M. Knupfer, J. Bartsch: Contact characterization by photoemission and device performance in P3HT based organic transistors, J. Appl. Phys., in press.

[2] G. Paasch and S. Scheinert: Charge carrier density of organics with Gaussian density of states: Analytical approximation for the Gauss–Fermi integral, J. Appl. Phys. **107**, 104501 (2010)

[a] Extended Abstract, 5th International Symposium **Technologies for Polymer Electronics** TPE12, 22-24 May 2012 Rudolstadt / Germany

BIOGRAPHIC DATA OF PROFESSOR GERNOT PAASCH

- Diplom-Physiker (1967, Technical University Dresden)
- Dr. rer. nat. (1970,Technical University Dresden)
- Dr. sc. nat. (1976; converted into Dr. rer. nat. habil. 1991, Technical University Dresden)

- Technical University Dresden (1967-1977)
- Lomonossov Moscow State University and Institute of Physical Problems Moscow (Postdoc with Prof. M.I. Kaganov, Group of I.M.Lifshiz, 1974-1975)
- Martin- Luther- University Halle- Wittenberg, Dozent (1977-1979)
- Technical University Ilmenau, full Professor for Theoretical Physics (1979-1987)
- Institute of Solid State and Materials Research (since 1988) (formerly Zentralinstitut für Festkörper- und Werkstofforschung), senior scientist, with research Groups Conducting Polymers, Electrochemistry and Conducting Polymers, Group for Theoretical Solid State Physics
- Technical University Ilmenau, Guest Professor for Nanoelectronics 1996-1998
- Retired 2007, part time employed, guest scientist

PRINTED DIODES: PHYSICS AND APPLICATIONS

Donald Lupo, Kaisa Lilja, Petri Heljo, Sampo Tuukkanen, Miao Li

Department of Electronics, Tampere University of Technology,
Korkeakoulunkatu 3, PO Box 692, FI-33101 Tampere

Printed rectifying diodes, while not as heavily studied as printed TFTs, play an important role in electronic circuitry, e.g. in RF rectification or as an alternative display back plane structure. Printed organic diodes place less severe demands on charge carrier mobility or lateral resolution than conventional organic TFTs, but bring their own challenges. In this talk work done in our group on gravure printed Schottky diodes will be presented, with discussion of how the printing process can affect interfaces and device physics. The integration of printed Schottky diodes into circuits such as rectifiers, charge pumps and display backplanes is then demonstrated.

The development of printed electronic components and circuits offers a novel way to produce flexible and lightweight electronics using additive roll-to-roll processes on low-cost substrates. Though there is a wealth of information on organic LEDs (OLEDs), organic photovoltaics (OPV) and organic thin film transistors (OTFTs), much less has been written about rectifying diodes. Diodes have a number of applications in electronics, including rectification of radio frequency signals [1,2] for signal demodulation and for providing DC power to RFID chips and distributed sensor networks, as well as in display backplanes [3]. We have been working in the Organic Electronics Group at TUT for some years on mass production compatible, air stable gravure printed organic Schottky diodes, focussing on the air stable, amorphous organic semiconductor poly(triarylamine) (PTAA).

Interfaces and diode performance

We have fabricated with high (up to 100,000) rectification ratios using very simple, mass manufacturing compatible processes: screen printing + wet etching to pattern Cu on PET and gravure printing to deposit PTAA, anode material (silver flake ink) and, in the case of circuits, dielectrics for crossovers. However, it has been important to study the devices and interfaces carefully to understand and optimise the diodes, as the printing process can significantly affect the materials and interfaces and thus device properties. Current-voltage curves demonstrate high rectification in a device for which Cu is the cathode and Ag is the anode, which does not fit to a simplistic energy level diagram.

In addition, we observed that the diodes behaved differently depending on whether the Cu had been deposited by evaporation or sputtering; diodes with sputtered Cu cathodes showed a higher rectification ratio but also a higher onset of space charge limited current (SCLC) [4,5]. Kelvin probe measurements indicated a nominal work function of the Ag flake ink of 5.2 eV, corresponding to Ag_2O, which could explain good hole injection. The measured values for Cu (4.8 and 5.0 eV) could not explain the fact that Cu acts as a "good" cathode, or the difference between the two Cu electrodes.

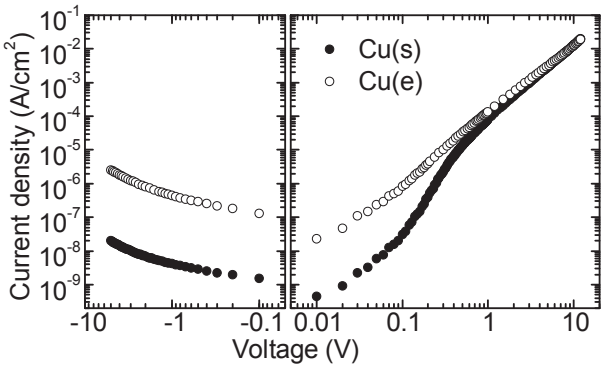

Figure 1. Log J- log V -performance of diodes with evaporated [Cu(e)] and sputtered [Cu (s)] copper cathodes. Source: Ref. 4.

The combination of impedance spectroscopy and XPS depth profiles gave more insight into the phenomenon. The impedance spectra recorded over a range of voltages indicated at least one additional interlayer, which appeared to be at the semiconductor/cathode interface (Fig. 2). The XPS data show that the interfacial layer in the diodes with sputtered copper cathodes consists of a thin layer of Cu_2O and an organic layer with a combined thickness of 5 - 6 nm. In contrast, the interfacial layer in diodes with evaporated copper cathodes is thinner, only 4 nm. Based on these data we can explain the effect based on changes in Fermi level pinning [Lilja2], which changes the effective barrier between Cu and semiconductor and depends on the interlayers. Due to the increase in Schottky barrier with increasing interlayer, fewer charge carriers are able to flow from the cathode to the semiconductor under reverse bias and the reverse current is lower. However, in forward bias the field is still high enough to assist tunnelling through the barrier.

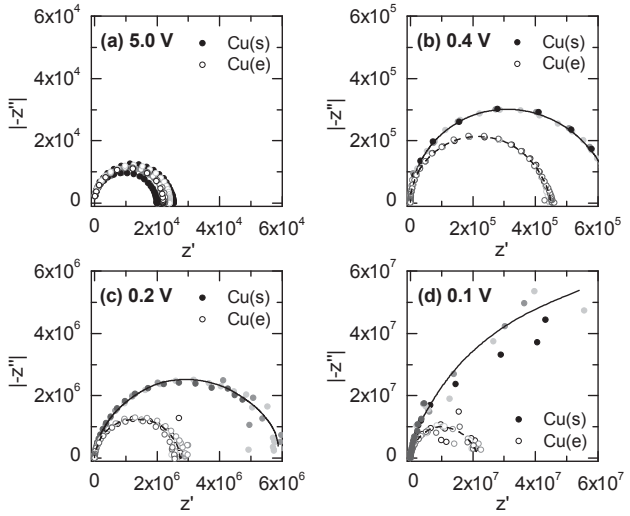

Figure 2. Cole-cole plots of the diode impedance with evaporated (open circle) and sputtered (closed circle) cathode contacts at forward bias voltages of 0.1 V, 0.2 V, 0.4 V and 5 V. The frequency increases from right to left from 10 Hz to 1 MHz. Source: Ref. 5

Printed Diode Backplanes

As displays become more complex, connecting a lead to each pixel is no longer an option, and matrix addressing is necessary, in which the display is divided into rows and columns and addressed a row at a time. Many display media, for example common "electronic paper" media, require an electronic circuit for each pixel, a so-called active matrix (AM) architecture. Most commonly, these switching elements are thin film transistors (TFTs), but earlier displays also used thin film diodes (TFDs) as switching elements. Recently, organic semiconductors have been used to develop TFT AM display driving circuits [Gel04, Hui02]. However, there are challenges associated with fabricating organic TFT backplanes; fine patterning is required to define a short channel, and high charge carrier mobility is needed to get sufficient on current. Diodes, on the other hand, require no fine lateral patterning as current flows vertically through a thin film, significant currents can be achieved with quite low mobilities. Therefore it may be useful to return to the TFD concept using organic diodes, as reported by Nilsson et al. [3], especially for applications where very high resolution and fast switching are not needed.

We developed a novel backplane architecture which allowed fabrication of a TFD backplane for a bistable front plane medium with unpatterned front electrode, and implemented this architecture using the gravure printed diodes described above. Using this architecture, we were able to demonstrate matrix driving of a simple 4 x 4 prototype based on E Ink Vizplex^{TM} front plane [6], as shown in Figure 3.

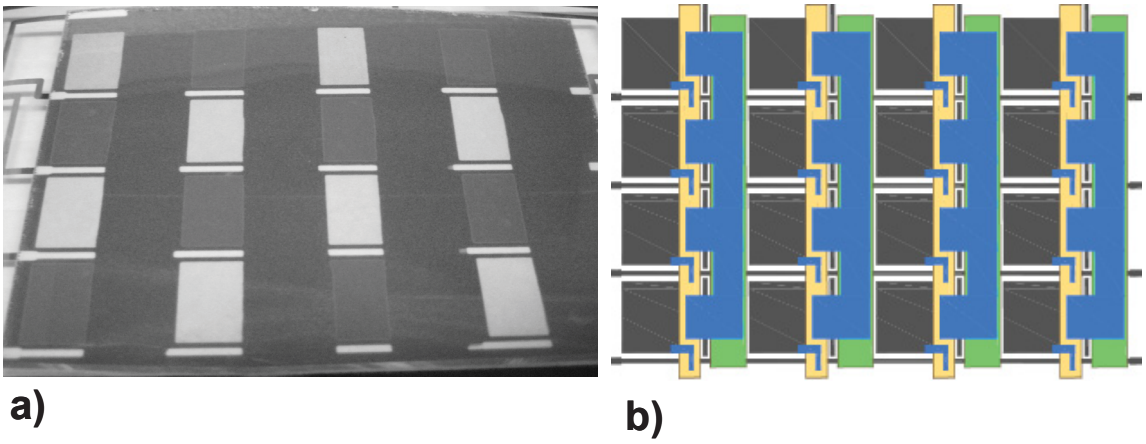

Figure 3. Diode backplane laminated to Vizplex™; a) an image of a functional display with 7V driving voltage, b) a schematic presentation of the printed diode backplane. Source: Ref. 6.

RF Rectification

As mentioned above, an important application of rectifying diodes is the rectification of radio frequency signals. Organic semiconductor rectifier diodes were reported previously [7,8] but these studies either used evaporated semiconductors and shadow mask evaporation or photolithographic patterning of electrodes or showed poor high frequency performance Spin casting has also been used to deposit organic layers but it can not be considered a high throughput process, and RF performance was poor. High throughput processes, such as coating and printing technologies, need to be demonstrated if there is to be hope of manufacturing organic rectifier diodes on a scale that can be of industrial interest.

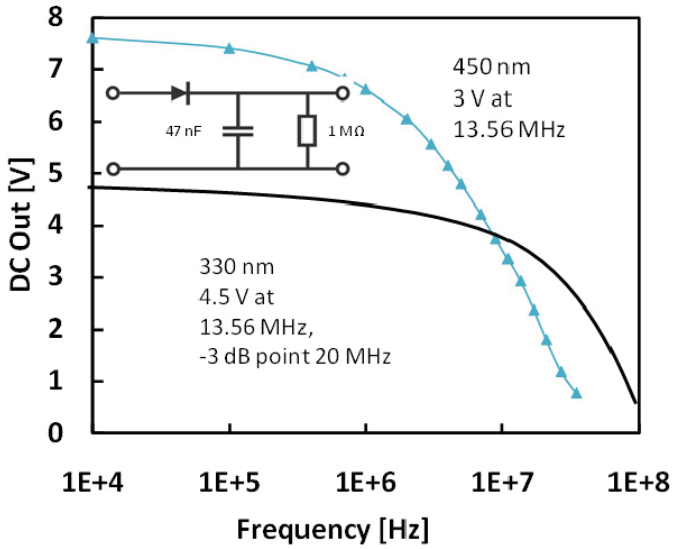

Figure 4. Frequency dependence of rectification from a printed diode half-wave rectifier for two different active layer thicknesses. Source: Ref. 9.

We found that the Cu/PTAA/Ag architecture described above not only shows high rectification ratios in dc measurement, but also surprisingly good RF performance. In reference [2] we reported a half-wave rectifier based on a printed diode that demonstrated rectification up to 10 MHz. In later work [9] we showed that by optimising the diode parameters including layer thickness it was possible to rectify significantly higher frequencies, with a 3 dB point as high as 20 MHz (Figure 4).

For a number of applications, a supply voltage higher than the voltage directly obtainable from the RF signal is needed, e.g. to drive the logic elements in a chip, especially if organic transistors are used. Therefore a means of voltage multiplication is needed. For this reason we have begun looking at printed charge pump circuits based on multiple printed diodes and capacitors for rectification and amplification of RF input signals. Recently we demonstrated printed charge pump circuits based on gravure printed Schottky diodes and ink jet printed capacitors [10]. When the diodes and capacitors were fabricated on the same substrate

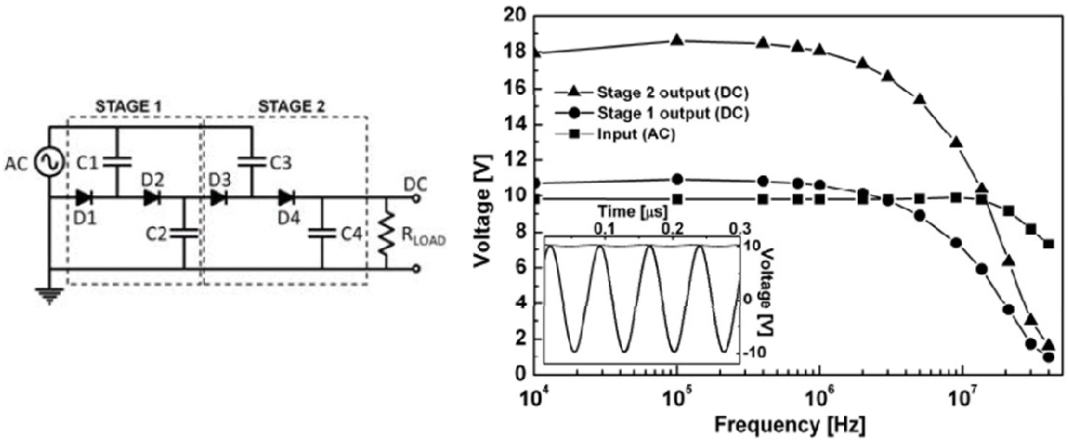

Figure 5. Diagram of printed charge pump circuit and output characteristics. Source: Ref. 10.

(monolithic integration) some amplification of an input signal could be seen but performance was modest due to degradation of the diode contact as a result of the high temperature sintering of the nano-silver ink used for the capacitors. When the capacitors and diodes were fabricated on separate substrates to avoid this issue, performance was improved, with 19 V from 2 stages at 100 kHz for a 10V input sine wave and an output of 10.4 V at 13.56 MHz, which is over twice the output of a half-wave rectifier. With further optimisation of the diodes and capacitors as well as additional stages we expect to achieve further voltage amplification, and work is ongoing in this area. In particular, we are investigating the use of RF energy harvesting in energy harvesting circuits for distributed sensors.

In summary, we have shown that it is possible to use mass production, high throughput compatible fabrication methods and air stable materials to fabricate diodes with excellent rectification behaviour, even at radio frequencies, and to use these diodes to fabricate circuits for applications in RF rectification and display backplanes.

Acknowledgement

The authors thanks T. Joutsenoja, R. Österbacka, H. Majumdar, K. Lahtonen and M. Valden (co-authors on work cited herein) for their cooperation. This work was supported by the UPM Kymmene Corporation and by the Academy of Finland.

References

[1] S. Steudel, K. Myny, V. Arkhipov, C. Deibel, S. de Vusser, J. Genoe and P. Heremans. *Nat. Mater.* **4** (2005) 597

[2] K. E. Lilja, T. G. Bäcklund, D. Lupo, T. Hassinen and T. Joutsenoja, *Organic Electronics*, **10** (2009) 1011-1014.

[3] B. J. L. Nilsson, *U.S. Patent No. 7405775*, 29 Jul. 2008

[4] K. E. Lilja, H. S. Majumdar, F. S. Pettersson, R. Österbacka and T. Joutsenoja, *ACS Applied Materials & Interfaces*, **3** (2011) 7-10

[5] K. E. Lilja, H. S. Majumdar, K. Lahtonen, P. Heljo, S. Tuukkanen, T. Joutsenoja, M. Valden, R. Österbacka and D. Lupo, *Journal of Physics D: Applied Physics*, **44** (2011) 295301

[6] K. E. Lilja, T. G. Bäcklund, D. Lupo, J. Virtanen, E. Hämäläinen and T. Joutsenoja, *Thin Solid Films*, **518** (2010) 4385-4389

[7] L. S. Roman, M. Berggren, and O. Inganäs. *Appl. Phys. Lett.* **75** (1999) 3557

[8] A. Yuming, S. Gowrisanker, H. Jia, I. Trachtenberg, E. Vogel, R. M. Wallace, B. E. Gnade, R. Barnett, H. Stiegler, and H. Edwards. *Appl. Phys. Lett.* **90** (2007) 262105

[9] K. Lilja, *PRODI* workshop, Munich, 2010

[10] P. Heljo, K.E. Lilja, S. Tuukkanen, D. Lupo, *Proc. LOPE-C* 2011

BIOGRAPHIC DATA OF PROFESSOR DONALD LUPO

Donald Lupo studied chemistry at Davidson College in North Carolina, USA and gained his Ph.D. in physical chemistry at Indiana University, Bloomington, IN , USA under the supervision of Prof. George Ewing. Subsequently he worked as a post-doctoral fellow in the Laboratory for Physical Chemistrat the ETH in Zürich, Switzerland on IR laser photochemistry in the group of Prof. Martin Quack. He reinvented himself as a materials scientist after taking up a position in central research at Hoechst AG in Frankfurt am Main, Germany in 1986, where he worked in nonlinear optics based on Langmuir-Blodgett films, polymer OLEDs and solid state dye sensitised solar cells (DSSC) based on amorphous organic semiconductors. At Sony International (Europe) GmbH he built up the Materials Science Laboratory in Fellbach, Germany and continued his work on polymer OLEDs and organic solar cells. At NTera Ltd. in Dublin, Ireland he was head of display R&D for paper-like displays based on electrochromic nanomaterials. He then spent 8 years as a technology consultant working on pass printed electronics, roll to roll printable displays and dye solar cells with companies such as UPM Kymmene, Merck and G24 Innovations. In 2010 he accepted a call to a professorship in electronic materials in the Department of Electronics at Tampere University of Technology and joined the faculty in August 2010. There he is responsible for activities in electronics materials and manufacturing, with interests in printed diodes, transistors and solar cells and in the effect of printing processes on materials, interfaces and devices.

CURVED AND FLAT AROMATICS: MULTITASK COMPONENTS IN MOLECULAR MACHINES AND ELECTRONIC MATERIALS

Mateo-Alonso, A.

Dr. Aurelio Mateo-Alonso, [1]Freiburg Institute for Advanced Studies, Albertstr. 19 and Institut für Organische Chemie und Biochemie, Albertstr. 21, 79104 Freiburg, Germany

amateo@frias.uni-freiburg.de

The design and synthesis of organic molecular and supramolecular materials based on curved and flat aromatics will be discussed focusing on different applications such as; (i) the design of fullerene-based molecular machines as models for artificial photosynthetic reaction centers and property-switchable materials; (ii) the synthesis of oligo- and polyazaacenes for electronic applications, their self-assembly into nanohybrids (with colloidal particles), and their use as surfactants for carbon nanotubes.

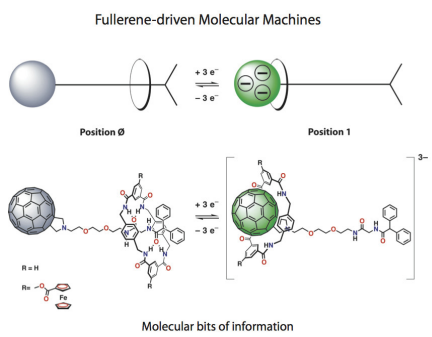

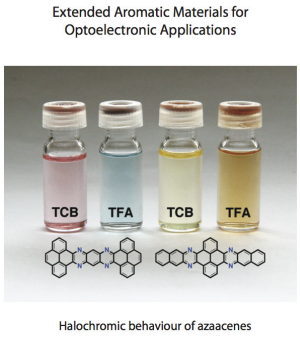

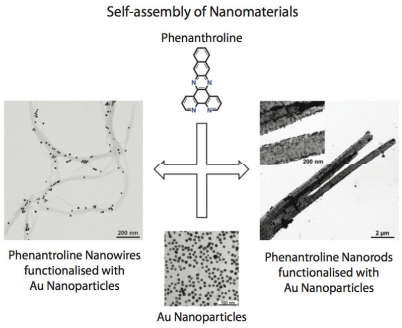

References:

Molecular Machines and Applications: [1] **Chem. Comm.** 2010, 46, 9089-9099. [2] **J. Am. Chem. Soc.**, 2008, 130, 14938-14940. [3] **J. Am. Chem. Soc.** 2008, 130, 1534-1535. [4] **Angew. Chem. Int. Ed.**, 2007, 46, 8120-8126. [5] **Chem. Comm.**, 2007, 1945-1947 [6] **Angew. Chem. Int. Ed.**, 2007, 46(19), 3521-3525. [7] **Chem. Comm.**, 2007, 1412-1414. [8] **Org. Lett.**, 2006, 8(22), 5173-5176.

Oligo-, Polyazaacenes and Nanocarbons: [1] **Chem. Comm.** 2011, 47, 514-516. [2] **Chem. Comm.** 2010, 46, 9122-9124. [3] **Chem. Asian J.** 2010, 5, 482-485. [4] **Nature Chemistry,** 2009, 1, 243-249. [5] **J. Mater. Chem.,** 2009, 19, 4329-4324. [6] **Chem. Eur. J.,** 2008, 14, 8837-8846. [7] **J. Am. Chem. Soc.,** 2008, 130, 8733-8740. [8] **J. Phys. Chem. A,** 2007, 111, 12669-12673.

Curriculum Vitae – Prof. Aurelio Mateo-Alonso

Freiburg Institute for Advanced Studies
Universität Freiburg
Albertstr. 19
Freiburg 79104, Germany

E-mail: amateo@frias.uni-freiburg.de
Date of birth: 15/05/1976

Qualifications and Relevant Experience

2009-Present **Group Leader** (Freiburg Institute for Advanced Studies, FRIAS, Freiburg, Germany). I have been granted with an equivalent status to a **Habilitation** holder by the Albert-Ludwigs-Universität Freiburg.

2008-2009 **NANOCARB Research Associate** in the group of Prof. Maurizio Prato (Università degli Studi di Trieste, Italy). Funded by the European Union.

2006-2008: **INSTM Research Associate** in the group of Prof. Maurizio Prato (Università degli Studi di Trieste, Italy). Funded by INSTM (Italian Interuniversity Consortium on Materials Science and Technology).

09/2007: **Visiting Scientist** in the group of Prof. Dirk M. Guldi (Universität Erlangen-Nürnberg, Germany).

2004-2006: **Marie Curie RTN Fellow** in the group of Prof. Maurizio Prato (Università degli Studi di Trieste, Italy). Funded by the European Union through the Research Training Network (RTN) EMMMA (Exploiting Mechanical Motion of Molecular Architectures).

2000-2004: **Ph.D. in Chemistry**. "Radical-anions of 1,6-dialkoxyphenazine macrocycles as chiral electrogenerated bases"Supervised by Prof. J.H.P. Utley and Dr. P.B. Wyatt (Queen Mary, University of London, U.K.). Project studentship funded by EPSRC (UK's Engineering and Physical Sciences Research Council).

2000-2002: **Teaching Assistant**. Queen Mary, University of London, U.K.

1999-/2000: **M.Sc. in Organic Chemistry**. "Transformations of sulphinyl-, sulphenyl- and ethoxycarbonyl derivatives of 1-methyl-2-cyclohexenol". Supervised by Dr. M.C. Maestro Rubio and Prof. J. L. García Ruano (Universidad Autónoma de Madrid, Spain).

1994-1999: **B.Sc. in Organic Chemistry** at Universidad Autónoma de Madrid, Spain.

Languages

- **Spanish:** Mother language.
- **English**: Fluent (**spoken and written**). Supported by different certificates (TOEFL 553, First Certificate).
- **Italian:** Fluent (**spoken and written**).
- **German:** Beginners level A1.2.

Funding

- 2012: ERA-Chemistry. **Principal Investigator**.
- 2012: Deutsche Forschungsgemeinschaft (DFG ref. AU373/1-1). **Principal Investigator**.
- 2011: Deutscher Akademischer Austausch Dienst (DAAD Italy Fellowships). **Principal Investigator**.
- 2011: Deutscher Akademischer Austausch Dienst (DAAD India Fellowships). **Principal Investigator**.
- 2011: Freiburg Institute for Advanced Studies. Joint project with Prof. Maria Anita Rampi (Universita di Ferrara, Italy). **Principal Investigator**.
- 2010: Verband der Chemischen Industrie (Bu/SK 185/13). **Principal Investigator**.
- 2010: Deutscher Akademischer Austausch Dienst (DAAD PPP Vigoni ref. 507281163). **Principal Investigator**.
- 2009: Freiburg Institute for Advanced Studies. **Principal Investigator**.
- 2007: Università di Trieste (Young Researchers Program). **Principal Investigator**.
- 2006: Ministero dell'Università e della Ricerca (Principal Investigator: Maurizio Prato, prot. 2006034372). **Co-Principal Investigator**.
- 2006: Italian Interuniversity Consortium on Materials Science and Technology (INSTM Fellowship). **Principal Investigator**.

Awards

- 2012: **Young Investigator Award** of the Fullerenes, Nanotubes and Carbon Nanostructures Division of the Electrochemical Society (USA).
- 2011: **RSEQ-Sigma-Aldrich Young Investigator Prize** awarded by the Spanish Royal Chemical Society (RSEQ).
- 2010: Finalist of the European Young Investigator Award (EUCHEMS). Special Mention of the Jury.
- 2009: **Eugen-Graetz Prize** awarded by the University of Freiburg.
- 2007: **Young Researchers Prize** awarded by Università di Trieste.
- 2003: **Prize** awarded for on-time PhD completion. Department of Chemistry, Queen Mary, University of London.

Scholarships and Allowances

- 2008: **Travel Allowance** for attending the VII Spanish-Italian Symposium in Organic Chemistry (SISOC VII). Oviedo, Spain (7–10 September 2008).
- 2004: **Travel Allowance** for attending the Euresco Conference on "Chemistry and Physics of Multifunctional Materials", Tomar, Portugal (11–16 September 2004).
- 2003: **Travel Allowance** for attending the Royal Society of Chemistry, Reaction Mechanisms Group Conference, (19 September, 2003), Avecia, Huddersfield, UK.
- 1997: **Scholarship** awarded for distinction in Classical Mechanics, Universidad Autónoma de Madrid.

Refereeing Experience

I have been invited to act as referee for Organic Letters; the Journal of Organic Chemistry; Chemical Society Reviews; Energy and Environmental Science; Chemical Communications; Chemical Sciences; Journal of Materials Chemistry; Organic & Biomolecular Chemistry; Physical Chemistry Chemical Physics; Chemistry an Asian Journal; Fullerenes, Carbon Nanotubes and Carbon Nanostructures; Tetrahedron; Nanotechnology; Aust. J. Chem.; Nanoscale.

Editorial Experience

- Journal of Materials Chemistry, guest editor, special issue to be issued in 2013.
- Journal of Materials Chemistry/Soft Matter joint web-theme issue "FRIAS – Black Forest Focus on Soft Matter". Link

Reviewing of Research Grant Applications

- Italian National Research Council (Consiglio Nazionale delle Ricerche CNR, Italy).
- Spanish Evaluation National Agency (Agencia Nacional de Evaluación y Prospectiva ANEP, Spain).
- Flanders Research Foundation (Fonds Wetenschappelijk Onderzoek Vlaanderen FWO, Belgium).

Participation on External Selection Committees

- 2011: MCF position (Assistant Professorship) in Physical Chemistry at the University of Strasbourg, France.

Participation on MSc and PhD Committees

- Pascal Ellerbrock, Diploma thesis 2011, Universität Freiburg.
- Konrad Lehr, Diploma thesis 2010, Universität Freiburg.
- Ippei Usui, PhD Thesis 2010, Universität Freiburg.

Conference Organisation

- Co-organiser of the **4th Black Forest Focus on Soft Matter** conference, Titisee, 20-23 July 2010.
- Co-organiser of the **8th Black Forest Focus on Soft Matter** conference, to be held in 2012.

Mentoring & Teaching Experience

✔ Undergraduate Courses: I have worked as a part-time teaching assistant/laboratory demonstrator in Queen Mary College in different courses, in which I was responsible of presenting, assisting, and facilitating laboratory exercises. Courses included: Foundation, Chemistry of Polyfunctional Organic Compounds, Advanced Experimental Chemistry, Last year Miniprojects

✔ I have been granted with a status equivalent to a **Habilitation** holder by the Albert-Ludwigs-Universität Freiburg, thus I possess the right to promote PhD, Master, Diploma and Bachelor Students.

✔ **Scientists supervised**:

- PhD. Cinzia Spinato, Universität Freiburg/POLYMAT Fundazioa (2012-).
- PhD. David Boschert, Universität Freiburg (2012-).
- MSc. Cinzia Spinato, Università di Venezia/Universität Freiburg (2011-).
- PhD. Sudhakar Gaikwad, Universität Freiburg/ POLYMAT Fundazioa (2011-).
- Postdoc Rajesh S. Bhosale, Universität Freiburg/ POLYMAT Fundazioa (2011-).
- Bachelor Student, Mads Grüninger, Universität Freiburg (2011).
- Bachelor Student, Burkhardt Pösel, Universität Freiburg (2011).
- Diploma Student, David Boschert, Universität Freiburg (2010-).
- Postdoc Niksa Kulisic, Universität Freiburg (2010-).
- PhD. Francesco Scarel, Universität Freiburg (2009-).
- PhD. Sunil Choudhary, Universität Freiburg (2009-).
- PhD. Sandeep More, Universität Freiburg (2009-).
- MSc. Francesco Scarel, Università di Trieste (2008-2009).
- PhD. Niksa Kulisic, Università di Trieste (2007-2010)

39 publications. 29 articles in refereed journals (**14** as **corresponding author**, 21 as first author), 8 book chapters and 2 conference proceeding. (1 × Nature Chemistry; 1 × Acc. Chem. Res.; 2 × Angew. Chem. Int. Ed.; 3 × J. Am. Chem. Soc.; 6 × Chem. Comm.). **H-Index 13**. Citations 427. Researcher ID A-8600-2010.

a) Peer-reviewed publications

[29] N. Kulisic, S. More, and **A. Mateo-Alonso*** "A tetraalkylated pyrene building block for the synthesis of pyrene-fused azaacenes with enhanced solubility" **Chem. Comm.** 2011, 47, 514-516.

[28] P. Aloukos, K. Iliopoulos, S. Couris* D.M. Guldi* C. Sooambar, **A. Mateo-Alonso**, D. Bonifazi* and M. Prato* "Photophysics and Transient Nonlinear Optical Response of Donor– [60]fullerene Hybrids" **J. Mater. Chem.** 2011, 21, 2524-2534.

[27] A. Montellano-Lopez, **A. Mateo-Alonso** and M. Prato* "Materials Chemistry of Fullerene C_{60} Derivatives" **J. Mater. Chem.** 2011, 21, 1305-1318.

[26] **A. Mateo-Alonso*** "Mechanically interlocked molecular architectures functionalised with fullerenes" **Chem. Comm.** 2010, 46, 9089-9099.

[25] M. Grzelczak, N. Kulisic, M. Prato and **A. Mateo-Alonso*** "Multimode assembly of phenanthroline nanowires decorated with gold nanoparticles" **Chem. Comm.** 2010, 46, 9122-9124.

[24] **A. Mateo-Alonso*** and M. Prato* "Synthesis of fullerene-stoppered rotaxanes bearing ferrocene groups on the macrocycle" **Eur. J. Org. Chem.** 2010, 1324-1332.

[23] **A. Mateo-Alonso,*** N. Kulisic, G. Valenti, M. Marcaccio, F. Paolucci* and M. Prato,* "Facile synthesis of highly stable tetraazaheptacene and tetraazaoctacene dyes" **Chem. Asian J.** 2010, 5, 482-485.

[22] P. Bodis, M.R. Panman, B.H. Bakker, **A. Mateo-Alonso**, M. Prato, W.J. Buma, A.M. Brouwer, E.R. Kay, D.A. Leigh, and S. Woutersen. "Two-dimensional vibrational spectroscopy of rotaxane-based molecular machines" **Acc. Chem. Res.** 2009, 42, 1462-1469.

[21] C. Ehli, C. Oelsner, D.M. Guldi,* **A. Mateo-Alonso**, M. Prato, C. Schmidt, C. Baches, F. Hauke, A. Hirsch, "Manipulating SWNT – chemical doping with perylene dyes", **Nature Chemistry**, 2009, 1, 243-249.

[20] V. Sgobba, A. Troeger, R. Cagnoli, **A. Mateo-Alonso**, M. Prato,* F. Parenti, A. Mucci, L. Schenetti* and D.M. Guldi* "Electrostatic layer by layer construction and characterization for photoelectrochemical solar cells based on water soluble polythiophenes and carbon nanotubes" **J. Mater. Chem.**, 2009, 19, 4329-4324.

[19] **A. Mateo-Alonso**,* C. Ehli, D.M. Guldi,* and M. Prato* "Charge transfer reactions along a supramolecular gradient" **J. Am. Chem. Soc.**, 2008, 130, 14938-14940.

[18] G.M.A. Rahman, D.M. Guldi,* N. Jux, M. Tchoul, W.T. Ford, **A. Mateo-Alonso** and M. Prato,* "Interactions in Functionalized Single-Walled Carbon Nanotubes-Polymer / Porphyrin Donor Acceptor Nanohybrids" **Chem. Eur. J.**, 2008, 14, 8837-8846. **Selected as Very Important Paper**.

[17] V. Georgakilas, A. Bourlinos, D. Gournis, C. Trapalis, M. Melle Franco, **A. Mateo-Alonso**, M. Prato. "Multi-Purpose Organically Modified Carbon Nanotubes" **J. Am. Chem. Soc.**, 2008, 130, 8733-8740.

[16] S. M. Mendoza, J. Berná, E. M. Pérez, E. R. Kay, **A. Mateo-Alonso**, C. De Nadaï, S. Zhang, J. Baggerman, P.G. Wiering, D. A. Leigh, M. Prato, A. M. Brouwer, P. Rudolf* "Core level photoemission of rotaxanes: a summary on binding energies", **J. Electron. Spectrosc. Relat. Phenom.** 2008, 165, 42-45.

[15] **A. Mateo-Alonso**,* K. Iliopulos, S. Couris,* and M. Prato.* "Efficient modulation of the nonlinear properties of fullerene derivatives" **J. Am. Chem. Soc.** 2008, 130, 1534-1535.

[14] **A. Mateo-Alonso**,* C. Ehli, K.H. Chen, D.M. Guldi,* and M. Prato,* "Dispersion of single-walled carbon nanotubes with an extended diazapentacene derivative" **J. Phys. Chem. A**, 2007, 111, 12669-12673.

[13] **A. Mateo-Alonso**,* D.M. Guldi,* F. Paolucci* and M. Prato,* "Fullerenes: Multitask components in molecular machinery" **Angew. Chem. Int. Ed.**, 2007, 46, 8120-8126.

[12] **A. Mateo-Alonso,*** G. Fioravanti, M. Marcaccio, F. Paolucci,* G.M.A. Rahman, C. Ehli, D.M. Guldi* and M. Prato,*. "An electrochemically driven molecular shuttle controlled and monitored by C_{60}" **Chem. Comm.**, 2007, 1945-1947

[11] E. Xenogiannopoulou, M. Medved, K. Iliopoulos, S. Couris,* M.G. Papadopoulos D. Bonifazi,* C. Sooambar, **A. Mateo-Alonso**, and M. Prato,* "Nonlinear optical properties of ferrocene- and porphyrin-[60]fullerene dyads" **ChemPhysChem.**, 2007, 8, 1056-1064.

[10] **A. Mateo-Alonso**,* C. Ehli, G.M.A. Rahman, D.M. Guldi,* G. Fioravanti, M. Marcaccio, F. Paolucci* and M. Prato,* "Tuning electron transfer through translational motion in molecular shuttles" **Angew. Chem. Int. Ed.**, 2007, 46(19), 3521-3525.

[9] **A. Mateo-Alonso**,* P. Brough and M. Prato,* "Stabilization of fulleropyrrolidine N-oxides through intrarotaxane hydrogen bonding" **Chem. Comm.**, 2007, 1412-1414.

[8] **A. Mateo-Alonso,*** G.M.A. Rahman, C. Ehli, D.M. Guldi, G. Fioravanti, M. Marcaccio, F. Paolucci and M. Prato, "Photophysical and electrochemical properties of a fullerene-stoppered rotaxane" **Photochem. Photobiol. Chem.**, 2006, 5, 1173-1176.

[7] **A. Mateo-Alonso,*** G. Fioravanti, M. Marcaccio, F. Paolucci,* D.C. Jagesar, A. M. Brouwer, and M. Prato.* "Reverse shuttling in a fullerene-stoppered rotaxane" **Org. Lett.**, 2006, 8(22), 5173-5176.

[6] **A. Mateo-Alonso**, C. Sooambar, M. Prato,* "Fullerene photoactive dyads assembled by axial coordination with metals" **C. R. Chimie**, 2006, 9, 944-951.

[5] **A. Mateo-Alonso**, C. Sooambar, M. Prato,* "Synthesis and applications of amphiphilic fulleropyrrolidine derivatives" **Org. Biomol. Chem.**, 2006, 4, 1629-1637.

[4] **A. Mateo-Alonso**, M. Prato,* "Synthesis of a soluble fullerene-rotaxane incorporating a furamide template" **Tetrahedron**, 2006, 62(9), 2003-2007.

[3] **A. Mateo Alonso**, R. Horcajada, M. Motevalli, J.H.P. Utley,* P.B. Wyatt,* "The reactivity, as electrogenerated bases, of chiral and achiral phenazine radical-anions, including application in asymmetric deprotonation" **Org. Biomol. Chem.** 2005, 3(15), 2842-2847.

[2] **A. Mateo Alonso**, R. Horcajada, R. Chudasama, H. Groombridge, M. Motevalli, J.H.P. Utley,* P.B. Wyatt.* "Synthesis of phenazine derivatives for use as precursors to electrochemically generated bases" **Org. Biomol. Chem.** 2005, 3(15), 2832-2841.

[1] **A. Mateo Alonso**, R. Horcajada, R. Mandalia, H. Groombridge, M. Motevalli, J.H.P. Utley,* P.B. Wyatt,* "Generation of strong, homochiral bases by electrochemical reduction of phenazine derivatives" **Chem. Comm.** 2004, 412-413.

b) Book chapters and conference proceedings

[10] F. Scarel, **A. Mateo-Alonso**, "Fullerenes and their derivatives" in Nanomaterials Handbook 2nd Edition. Ed. Y. Gogotsi, CRC Press, Boca Raton, **2012**.

[9] **A. Mateo-Alonso**, "Fullerene containing rotaxanes and catenanes" in Supramolecular Chemistry of Fullerenes and Carbon Nanotubes. Ed. N. Martin and J.F. Nierengarten. Willey, **2011**.

[8] A. Montellano-Lopez, **A. Mateo-Alonso**, M. Prato, "Applications of fullerenes in materials science" in Fullerenes: Principles and Applications 2nd Edition. Eds. F. Langa de la Puente, J.F. Nierengarten. Royal Society of Chemistry, London, **2011**.

[7] M. Wielopolski, **A. Mateo-Alonso**, D.M. Guldi, "Functionalized fullerenes: synthesis and functions" in Carbon Nanomaterials. Ed. Kadish and D'Souza. World Scientific **2011**.

[6] V. Sgobba, A. Troeger, A. Mateo-Alonso, M. Prato, F. Parenti, R. Cagnoli, A. Mucci, L. Schenetti, D.M. Guldi **Abs. Papers Am. Chem. Soc.** 2009, 238, 489.

[5] S. Campidelli, **A. Mateo-Alonso**, M. Prato, "Applications of fullerenes in materials science" in Fullerenes. Eds. F. Langa de la Puente, J.F. Nierengarten. Royal Society of Chemistry, London, **2006**.

[4] **A. Mateo-Alonso**, D. Bonifazi, M. Prato, "Functionalization chemistry of fullerenes" in Carbon Nanotechnology. Ed. L. Dai. Elservier B.V., Amsterdam, **2006**.

[3] **A. Mateo-Alonso**, N. Tagmatarchis, M. Prato, "Fullerenes and their derivatives" in Carbon Nanomaterials. Ed. Y. Gogotsi, CRC Press, Boca Raton, **2006**.

[2] **A. Mateo-Alonso**, N. Tagmatarchis, M. Prato, "Fullerenes and their derivatives" in Nanomaterials Handbook. Ed. Y. Gogotsi, CRC Press, Boca Raton, **2006**.

[1] J.H.P. Utley, H. Groombridge, R. Horcajada, **A. Mateo-Alonso**, R. Mandalia, P.B. Wyatt. **Proceedings Volumes of the Electrochemical Society**. Mechanistic and Synthetic Aspects of Organic and Biological Electrochemistry. Eds. D. G. Peters, J. Simonet, and H. Tanaka. The Electrochemical Society, **2003**.

Invited Lectures at International Conferences

[21] Technologies for Polymer Electronics (TPE12), Rudolstadt, Germany. 22-24 May 2012.
[20] Young Investigator Award Lecture, 221st ECS Meeting, Seattle, Washington, 6-10 May 2012.
[19] International Symposium on Electronic/Optic Functional Molecules (ISEOFM2012), Shanghai, China. 11-13 March 2012.
[18] Chemiedozententagung, Freiburg, Germany. 5-6 March 2012.
[17] **Plenary Lecture**. RSEQ-Sigma-Aldrich, Torremolinos, Spain. 25-28 October 2011.
[16] F-Pi-10, Beijing, China. 13-17 October 2011.
[15] ISPAC-23, Münster, Germany. 5 September 2011.
[14] Max-Planck Institute for Autonomous Systems, Stuttgart, Germany. 11 April 2011.
[13] Fullerene Silver Anniversary Symposium, Crete, Greece. 4-10 October 2010.
[12] EUCHEMS, Nuremberg, Germany. 29 August-2 September 2010.
[11] EUCHEMS Young Investigators Symposium, Nuremberg, Germany. 29 August-2 September 2010.
[10] 4th Black Forest Focus on Soft Matter Titisee, Germany. 20-23 July 2010.
[9] MolMat 2010. Montpellier, France. 5-8 July 2010.
[8] **Plenary Lecture**. Spanish-Italian Symposium in Organic Chemistry VIII. Padova, Italy. 3-6 July 2010.
[7] Young chemists at Friuli Venezia-Giulia meeting. Udine, Italy. 30 September 2008.
[6] VII Spanish-Italian Symposium in Organic Chemistry VII. Oviedo, Spain. 9 September 2008.
[5] Italian National Congress on Supramolecular Chemistry. Trieste, Italy. 19-22 Sep 2007.
[4] Electrochemical Society Meeting. Chicago. U.S.A. 6-10 May 2007.
[3] Slonano Conference Lubiana, Slovenia. 20-21 September 2006.
[2] NanoItaly Conference. Trieste, Italy. 22-24 May 2006.
[1] RSC Reaction Mechanisms Conference, 19 September 2003, Avecia, Huddersfield, UK.

Invited Seminars

[16] University of Sussex, UK. 2 November 2011.
[15] University of Birmingham, Birmingham, UK. 20-21 October 2011.
[14] University of Fribourg, Fribourg, Switzerland. 6 July 2011.
[13] University of Linz, Linz, Austria. 16 June 2011.
[12] University of Liverpool, UK. 9 March 2011.
[11] University of East Anglia, Norwich, UK, 21 February 2011.
[10] Northwestern University, Evanston, U.S.A., 28 October 2010.
[9] Institut Català d'Investigació Química, Tarragona, Spain. 14 Sep. 2010.
[8] Institut de Ciència de Materials de Barcelona, Spain. 13 Sep. 2010.
[7] Leibniz Institute for Polymer Research. Dresden, Germany. 8 June 2010.
[6] Dep. Quim. Organica. Universidad Autonoma de Madrid, Spain. 13 May 2010.
[5] Département de Chimie, Facultés Universitaires Notre-Dame de la Paix, Namur, Belgium. 14 October 2009.
[4] Zernike Institute for Advanced Materials. Groningen, The Netherlands. 3 November 2008.
[3] Freiburg Institute for Advanced Studies. Germany. 21 October 2008.
[2] Dep. Chemistry & Pharmacy. Universität Erlangen. 27 June 2008.
[1] Institute of Chemical Sciences and Engineering, Ecole Polytechnique Fédérale de Lausanne. Lausanne, Switzerland. 6 February 2008.

Part IV: OLEDs and ECDs

HIGHLY EFFICIENT ORGANIC LIGHT EMITTING DIODES FOR LIGHTING APPLICATIONS

Björn Lüssem

Starting from a lab-curiosity, organic light emitting diodes have matured into a promising technology that is beginning to enter commercial markets. OLED displays can be found in a growing number of appliances such as mobile phones, mp3-players and TV-sets. For lighting applications several companies are planning to launch first products in the near future.

For both applications, OLED displays and OLED lighting, a high efficiency is essential. The external quantum efficiency η_q, defined as the ratio of the number of photons emitted from the OLED to the number of electron/hole pairs injected into the device is given by [1]

$$\eta_q = \gamma\chi\eta_{PL}\xi = \eta_{\text{int}}\xi \qquad \text{(Eq. 1)}$$

With γ the charge carrier balance, χ the singlet/triplet ratio, η_{PL} the efficiency of radiative decay of excitons, and finally ξ the outcoupling efficiency. The first three factors are often combined to the so called internal quantum efficiency η_{int}, which describes how efficiently photons are generated inside the device. In state-of- the-art OLEDs, the internal quantum efficiency can be optimized by using highly efficient phosphorescent emitters and charge carrier blocking layers, and internal quantum efficiencies close to 100% are possible. However, most photons are trapped inside the OLED cavity, resulting in an outcoupling efficiency ξ as low as 20%. Thus, to increase the efficiency of OLEDs further, improvements in the outcoupling efficiency are mandatory.

1. Increasing the Outcoupling Efficiency of Monochrome OLEDs

The low outcoupling efficiency is due to the different refractive index of the organic layers, the glass substrate, and air. Light generated inside the OLED is reflected at the interface between the organic layers (including ITO) and the glass substrate, feeding so called waveguided modes, and at the interface between glass substrate and air, feeding so called substrate modes. Furthermore, the molecule can excite plasmons travelling along the metallic electrode.

The strength of the different optical loss channels can be quantified by advanced optical simulations [2]. The molecular emitter is modeled as emitting dipole which couples to the different modes in the OLED cavity. Fig. 1 shows the distribution of loss channels for a red OLED with varying thickness of the electron transport layer (ETL) [2]. The red OLED consist of BPhen:Cs as ETL with varying thickness, BAlq as hole blocking layer, NPB:Ir(MDQ)$_2$

as red emission layer, Spiro-TAD as electron blocking layer, and MeO-TPD as hole transport layer (Fig. 1a). The simulation results are compared to the experimentally determined external quantum efficiency, shown by black dots (Fig. 1b). The EQE agrees exceptionally well with the simulation results (outcoupled photons, blue area). It shows an oscillation with the ETL thickness, which can be explained by the resonance conditions of the OLED cavity – at 70nm the OLED shows a first resonance and at 250nm a second one.

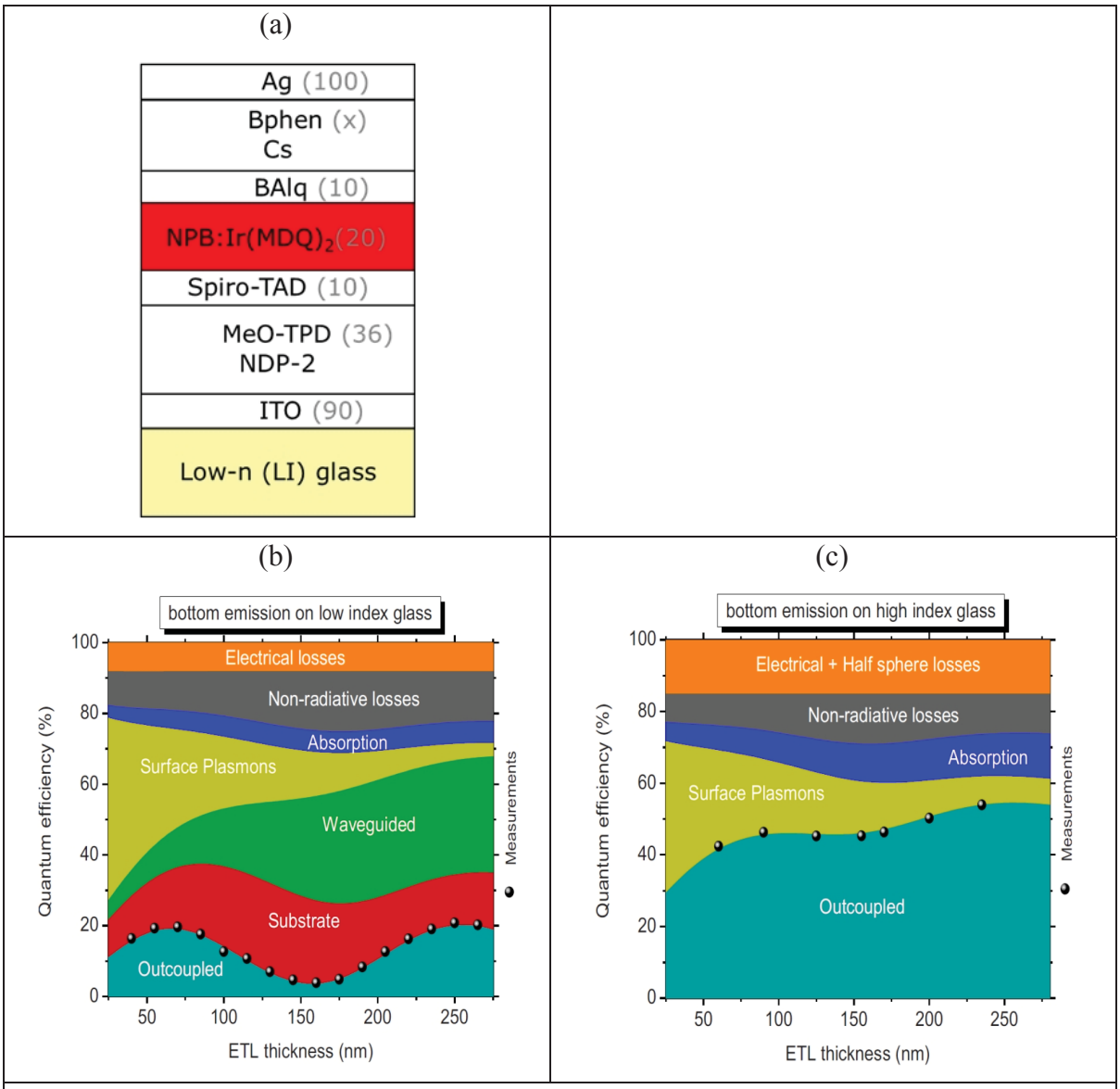

Fig. 1: Different loss channels for a red OLED with varying thickness of the electron transport layer on low index glass (a) and on high index glass (b) measured with an outcoupling lense [2]

From Fig. 1b) it can be concluded that at low ETL thickness losses due to coupling to plasmonic modes are most pronounced. As coupling to plasmons is a near field interaction, it decreases with increasing distance of the emitter from the cathode, i.e. with increasing ETL thickness. However, increasing the ETL thickness increases losses due to waveguided modes. Thus, additional means of avoiding waveguided modes have to be applied to increase the

EQE significantly.

In Fig. 1c) one possibility to avoid waveguided modes is shown. The OLED is built on a substrate with an increased refractive index, which is matched to the organic layers. Thus, reflections at the glass substrate are avoided. To further increase the efficiency, an outcoupling lense is applied to the glass substrate to avoid reflections at the glass/air interface. As can be seen in Fig. 2c) the waveguided and substrate modes are fully avoided and the device reaches an efficiency of beyond 50%.

2. *Design of Highly Efficient White OLEDs with Increased Outcoupling Efficiency*

The concepts shown in Fig. 1 have to be applied to white OLEDs. To obtain a well-balanced, high quality white emission, the emission of a red, green and blue emitter has to be mixed. To reach highest efficiency, all emitters should be phosphorescent emitters utilizing the singlet as well as the triplet state.
In Fig. 2 the design of a highly efficient white OLED utilizing phosphorescent red, green and blue emitters is shown [3].

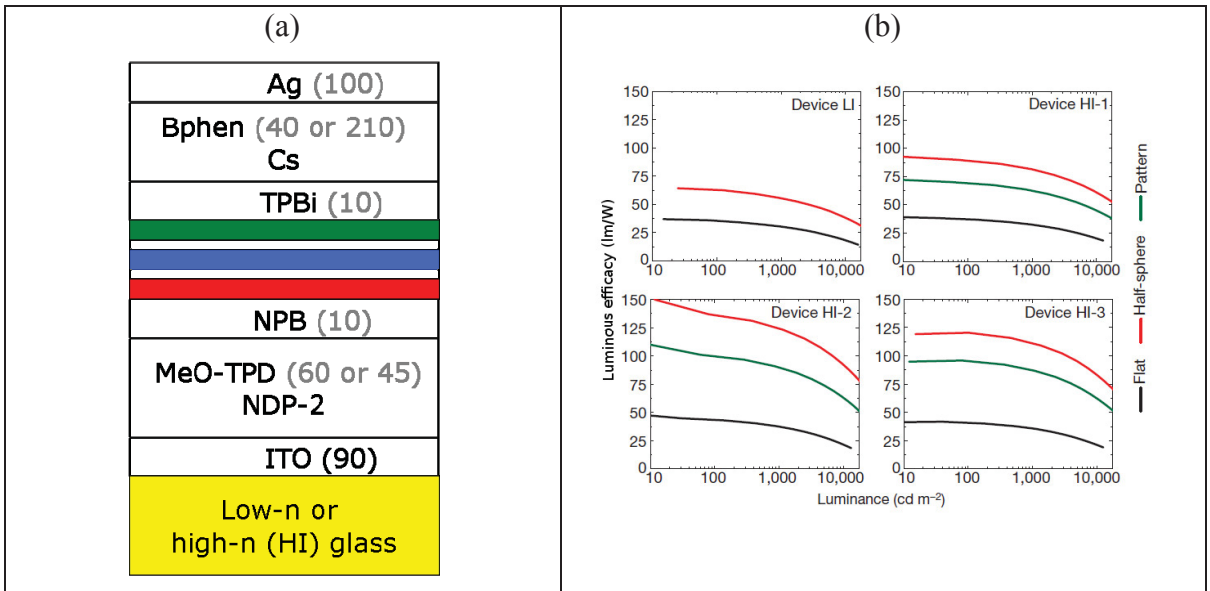

Fig. 2: Design of a highly efficient white OLED (a). The luminous efficacy of devices built on low index glass (LI), built on high index glass in the first resonance condition (HI-1), and on high index glass in the second resonance condition (HI-2) is shown in (b) [3].

The device consists of an ETL (BPhen:Cs) with two different thickness (corresponding to the first and second resonance), a hole blocking layer (TPBi), emission layers, an electron blocking layer (NPB) and a hole transport layer (MeO-TPD:NDP2). To increase the efficiency of the OLED, it is built on low index and on high index glass (Device LI and devices HI). On

high index glass, the OLED is built with a small ETL thickness (corresponding to the first resonance condition, device HI-1) and with a larger ETL thickness (devices HI-2 and HI-3).

The luminous efficacy or power efficiency is measured without any additional outcoupling structure applied to the substrate (flat device), with a large outcoupling lense applied to the substrate (half-sphere) and with a high index outcoupling structure consisting of small pyramids cut into the glass attached to the substrate (pattern).
The efficiency of these OLEDs is shown in Fig. 2b. As expected, the highest efficiency is reached for the OLED on high index glass with thicker ETL. Using a large outcoupling lens, more than 120 lm/W are obtained. Using a scalable outcoupling structure 90lm/W are reached.
However, in this so-called all-phosphorescent approach the phosphorescent blue emitter is prone to degradation and the devices have a lifetime of 1-2h only. An alternative to the all-phosphorescent approach is the triplet-harvesting approach, in which the phosphorescent blue emitter is replaced by a fluorescent emitter without losing efficiency.

3. White OLEDs using Fluorescent Blue Emitters: The Triplet Harvesting Approach

As discussed above, white OLEDs using phosphorescent blue emitters show highest efficiency but exhibit a low lifetime. The lifetime of fluorescent emitters is higher, but fluorescent emitters only emit from their singlet state and all excitons formed in the triplet state are lost, which significantly limits device performance.
A solution to this problem is the triplet harvesting approach. A fluorescent blue emitter with a high lying triplet state is used. The triplet state exceeds the triplet state of the phosphorescent red emitter, so that triplets formed on the blue emitter are transferred to the phosphorescent emitter and are harvested there. Thus, in principle all excitons formed in the device are utilized and an internal quantum efficiency of 100% is possible.

(a)

material	thickness
ITO	90
MeO-TPD:NDP2	40: 2wt%
Spiro-TAD	10
4P-NPD: $Ir(MDQ)_2acac$	5: 5 wt%
4P-NPD	5
BPhen	10
BPhen:Cs	90
Al	0.5
MeO-TPD:NDP2	65: 2wt%
Spiro-TAD	10
TCTA: $Ir(ppy)_3$: $Ir(dhfpy)_2acac$	10: 8 wt% 1 wt%
TPBi	10
BPhen:Cs	75
Al	100

(b)

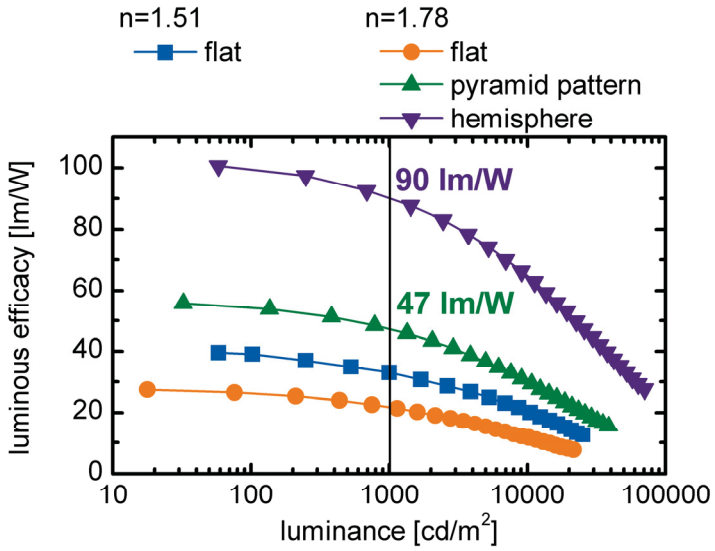

Fig. 3: Stacked white triplet-harvesting OLEDs (TCTA: 4,4',4'' tris(N-carbazolyl)-triphenylamine, TPBi: 2,2'2''-(1,3,5-benzenetriyl)-tris[1-phenyl-1H-benzimidazole], Ir(dhfpy)2acac: bis(2-(9,9-dihexylfluorenyl)-1-pyridine) (acetylacetonate). Two OLEDs – a yellow one and a blue/red triplet harvesting OLED – are stacked (a), so that a white spectrum is reached (b). On high-index glass, 90lm/W are reached with a large outcoupling lense [4].

The triplet harvesting OLED is shown in Fig. 3a [4]. The OLED is a stacked OLED consisting of a red/blue OLED (4P-NPD and 4P-NPD:$Ir(MDQ)_2(acac)$) and a yellow OLED (having an emission layer consisting of TCTA:$Ir(ppy)_3$:$Ir(dhfpy)_2acac$). Triplets formed on the blue emitter 4P-NPD can be transferred to the red emitter $Ir(MDQ)_2(acac)$ and are harvested there. The efficiency of this device is shown in Fig. 3b). For the flat device on low index glass a luminous efficacy of ~30lm/W is reached. This value can be significantly increased if the device is built on high-index glass and measured with a large outcoupling lense (90lm/W). Using the same scalable outcoupling structure as for the all-phosphorescent OLED shown in Fig 2, a luminous efficacy of 47lm/W is reached.

4. Conclusion

Current OLEDs reach internal quantum efficiencies of almost 100% and are mostly limited by the low outcoupling efficiency. Therefore, to design highly efficient OLEDs, care has to be taken to avoid plasmonic losses and losses due to waveguided modes.

To realize white OLEDs, the emission of at least 3 emitters has to be combined to obtain a broad, white spectrum. Combining three phosphorescent emitters yields highest efficiency, but the phosphorescent blue emitter is prone to degradation. However, in the triplet harvesting approach the phosphorescent blue emitter can be replaced by a fluorescent one without losing efficiency. Thus, triplet-harvesting could be a possible route towards highly-efficient and stable white OLEDs.

[1] R. Meerheim, B. Lüssem, and K. Leo, Proceedings of the IEEE **97**, 1606 (2009).
[2] R. Meerheim et al., Applied Physics Letters **97**, 253305 (2010)
[3] S. Reineke, F. Lindner, G. Schwartz, N. Seidler, K. Walzer, B. Lüssem, and K. Leo, Nature **459**, 234 (2009).
[4] T. Rosenow, M. Furno, S. Reineke, S. Olthof, B. Lüssem, and K. Leo, Journal of Applied Physics **108**, 113113 (2010)

BIOGRAPHIC DATA OF DR BJÖRN LÜSSEM

Björn Lüssem studied electrical engineering at the RWTH-Aachen and the University of Bath and obtained his degree as Diplom-Ingenieur in 2003. He prepared his PhD thesis at the Research Center in Jülich, Germany in the field of molecular electronics. His thesis concentrates on Scanning-Tunnelling Microscopy of pure and mixed self-assembled monolayers and has been awarded the VDE-Promotionspreis and the Günther-Leibfried-Preis. After staying at the Materials Science Laboratory of Sony in Stuttgart from 2006-2008, he joined Prof. Leo's group at the TU Dresden, where he is now head of the Organic Light Emitting Diodes group. His main interests are new semi-conducting devices based on organic materials and their differences or similarities to inorganic semiconductors.

ROLL-TO-ROLL PROCESSING OF FLEXIBLE OLED FOR LIGHTING APPLICATIONS

C. MAY, S. MOGCK

Fraunhofer IPMS, Center for Organic Materials and Electronic Devices Dresden COMEDD, Maria-Reiche-Straße 2, 01109 Dresden, Germany

OLEDs are considered as the second solid-state-lighting technology for new flat, large-area, and efficient lighting solutions. OLED lighting on glass substrates has been successfully started the market entry. Flexible OLED will open up new degrees of freedom in design. A novel approach has been started to develop high efficient small molecule OLED stack deposition on flexible plastic webs and metal strips in a roll-to-roll vacuum process Within COMEDD such a roll-to-roll line based on vacuum deposition was successfully installed. Beside the vacuum evaporation process the paper covers further process approaches like substrate patterning, inert lamination and inspection issues. Monochrome devices processed by roll-to-roll on "endless" substrates will be presented.

1. Introduction

With growing maturity and performance of OLED technology, the applications will range from less demanding such as e.g. signage and decorative lighting up to large area flexible illumination, automotive applications and general lighting with higher requirements in terms of efficiency and reliability. At the moment first OLED prototypes for lighting attract a lot of attention. In case of small molecules devices application of phosphorescent dopants and the use of the p-i-n design resulted in a white OLED demonstration with efficiency over 90 lm/W [1]. For significant penetration into the general lighting market, OLED technology will have to meet or exceed the high standards with respect to energy efficiency, long lifetime and low production costs that have been set by fluorescent and LED lighting. It is believed that the price can drop significantly by transferring the batch fabrication into high throughput inline or roll-to-roll processing (R2R) [2, 3, 4]. The higher throughput and the use of relatively cheap metal foil and plastic web as substrates can be a major cost reducing step. In the present paper, the general feasibility of the p-i-n top-emitting OLED design [4] application on flexible aluminium foil is evaluated in a roll-to-roll process. In addition to the roll-to-roll OLED vacuum deposition a substrate patterning and the OLED encapsulation process by foil lamination under protective nitrogen atmosphere will be outlined briefly.

2. Roll-to-Roll process line

R2R vacuum deposition and fabrication of small molecule OLEDs on flexible substrates are carried out in the RC 300-MB roll-to-roll vacuum coater (supplier Von Ardenne Anlagentechnik GmbH [3], figure. 1). The machine enables processing of metal or plastic substrates with a width of 300 mm and a thickness of 70 to 500 µm.

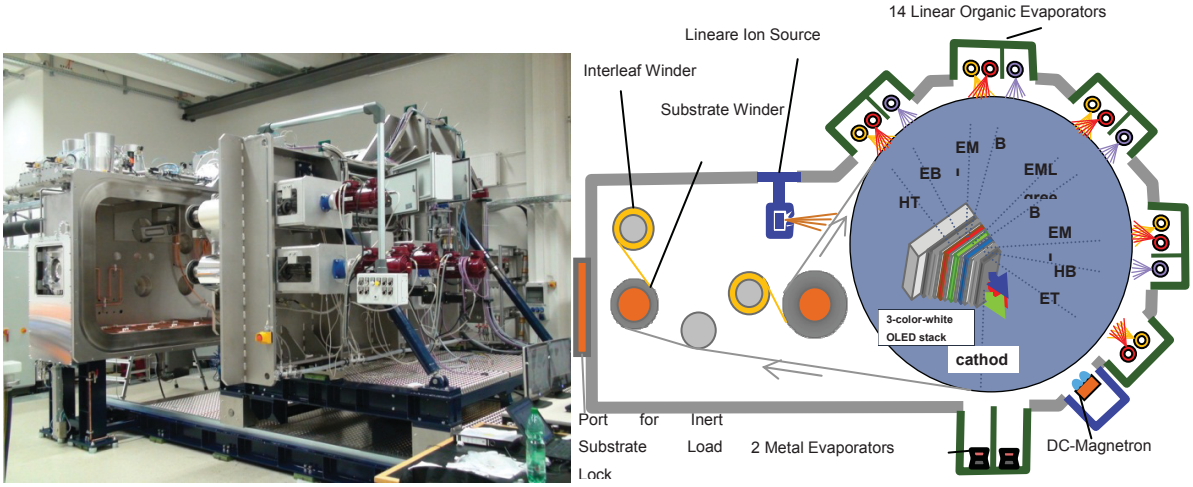

Figure 1: Photograph of the RC 300-MB roll-to-roll vacuum coater (left), schematic cross section (right).

Before the OLED vacuum deposition process can be started a nonconductive passivation layer must be printed on the aluminium band, as seen in figure 2. The substrate patterning with a passivation layer is necessary to isolate the anode (aluminium foil) from the metallization (cathode and metal contact lines) after the OLED stack deposition.

During the organic- and metal evaporation a shadowing with integrated strip masks in the deposition drum allow a proper patterning of devices. Finally, the processed OLED on aluminium foil are pre-encapsulated by reactive magnetron sputtering of Al_2O_3.

After the pre-encapsulation process, the coated coil will be transferred under inert condition to the encapsulation process performed in the coating- and lamination unit, as seen in figure 3.

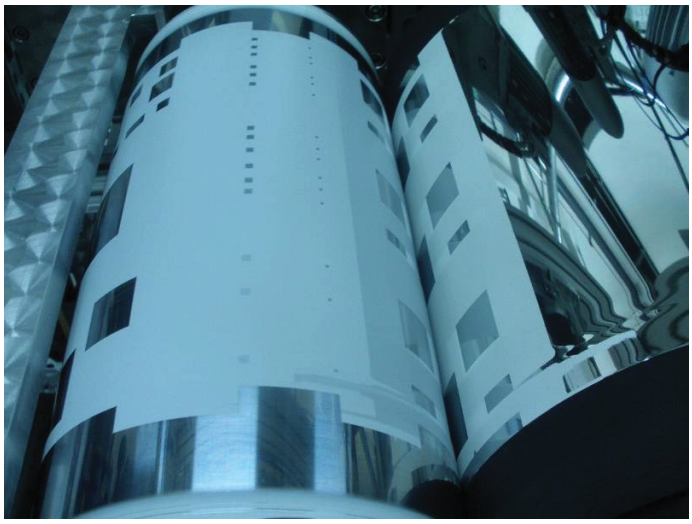

Figure 2: Photograph of the gravure printing unit for the substrate patterning with a passivation layer to separate electrically the electrodes of OLED devices.

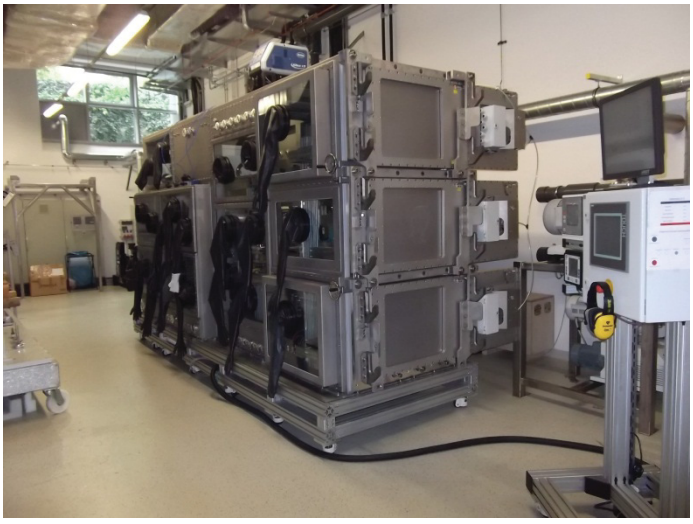

Figure 3: Photograph of the inert box with integrated substrate patterning- and foil lamination unit.

The roll-to-roll OLED fabrication process will be supported by an optical inspection system to discover yield relevant defect issues. High efficient small molecule OLED lighting systems coated in a vacuum process have a device thickness in sub-µm range. Therefore, particles with a size < 1 µm can be critical to the device performance, like efficacy and yield. For this reason a roll-to-roll optical inspection system is needed which fulfils the defect resolution requirement in a sub-µm range. A winding unit with integrated inspection system of CCD line scan cameras and a moveable optical microscope has the following inspection modes (see figure 4) were installed, enabeling:

- a 100% web inspection with CCD line scan cameras with a pixel resolution down to 14 µm.

- a defect review mode for further analysis of defects detected by the 100% inspection.
- automatic image recording on homogeneous and patterned web to determine the defect density by image processing of the recorded images to reach a defect resolution in µm range (resolution depends on the used objective).
- layout recordings to identify patterned defects.

Figure 4: A photograph of the roll-to-roll optical inspection system for metal foil and plastic films encaged in a clean room carbine of ISO6 to minimize particle contaminations during the inspection.

The goal of all inspection modes is the quantification and identification of the defect types which affects the device performance.

3. Results

Working green pin OLED devices with an active OLED area up to 60 x 60 mm² and pre-encapsulated with Al_2O_3 were realized on aluminium web as demonstrated in figure 5.

Figure 5: Electrical tests of 60 x 60 mm² green pin OLED devices on a aluminium band.

The comparison between a green p-i-n OLED with a 1st p-HTL (black curve, figure 6) and 2nd p-HTL (red and green curve, figure 6) shows one order of magnitude less leakage current.

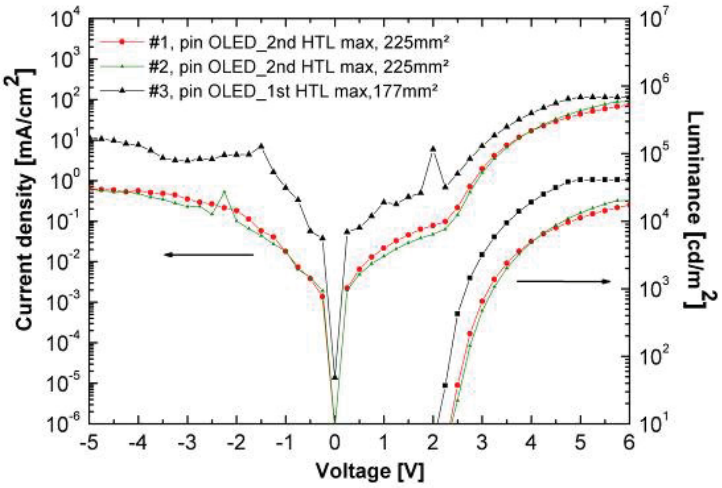

Figure 6: A diagram of electro-optical characterisation of the green pin OLED devices on aluminium foil. The 2nd maximum of the hole transport layer (HTL) allows stable OLED devices. Thicker HTL layers can further planarize rough substrate surfaces to get reproducible OLED devices (red and green curve).

4. Conclusions and Outlook

It was demonstrated that aluminium foils are suitable as substrates for fabrication of high efficient p-i-n OLEDs in the R2R vacuum processing. Homogenous light emission from OLEDs with areas on larger scale (60 x 60 mm²) and pre-encapsulated with an thin film Al_2O_3 layer deposited by reactive magnetron sputtering without significant reduction of the luminance can be obtained. The R2R patterning process with a passivation layer is suitable to fabricate 2- dimensional OLED lighting areas. R2R inspection techniques could be successfully brought into operation which will enable to control the defect levels during the process. In the future the reproducibility of the OLED R2R process needs to be further improved using the R2R inspection. The R2R vacuum coater will be equipped with up to 14 organic linear evaporators to allow fabricating high efficient white p-i-n OLEDs. In parallel, the development of bottom emitting OLEDs on plastic films is planned. The particle monitoring of the R2R process line will be integrated during the R2R OLED process to setup efficient defect prevention concept to obtain a stable yield.

5. Acknowledgements

This work was funded by the German Ministry of Education and Science within the project R2flex (Project ref. 13N11058).

6. References

[1] S. Reineke, et al., White organic light-emitting diodes with fluorescent tube efficiency, Nature, vol.459, (2009)

[2] C. May, et al., In-line deposition of organic light-emitting devices for large area applications, Thin Solid Films, vol. 516, p. 4609, (2008)

[3] C. Deus, et. al., Technology and equipment for roll-to-roll processing of small molecule OLEDs for lighting applications, 8th Int. Conf. on Coatings on Glass and Plastics, ICCG 2010. Proceedings : June 13-17, 2010, Braunschweig, 2010, ISBN 978-3-00-031387-5, p.117-122

[4] P. Freitag et al: Novel Approaches for OLED Lighting, SID 2011 Digest of Technical Papers, ISSN 0097-966X/11/4202-1067, p.1067

BIOGRAPHIC DATA OF DR CHRISTIAN MAY

Dr. Christian May, born 1967 studied Physical Metallurgy at Freiberg University of Mining and Technology. He received his PhD from same university in 1999. From 1997 he was with Von Ardenne Anlagentechnik, a supplier of high tech vacuum equipment, as project manager dealing with large area thin film deposition. Since 2003 he is with Fraunhofer Institute of Photonic Microsystems IPMS in Dresden. First he was responsible for the development of fabrication technologies for large area OLED lighting and organic solar cells. Since beginning 2009 he is acting as Head of the Business Units “Organic Materials and Systems” first and “Lighting and Photovoltaics” now. Since 2011 he is also deputy of the institute director of COMEDD – Center for Organic Materials and Electronic Devices Dresden within Fraunhofer IPMS.

REALIZING NOVEL AND FUNCTIONAL LIGHT-EMITTING ELECTROCHEMICAL CELLS

Ludvig Edman*

The Organic Photonics and Electronics Group, Department of Physics, Umeå University, 901 87 Umeå, Sweden.

**ludvig.edman@physics.umu.se*

Light-emitting electrochemical cells (LECs) offer a number of important advantages over competing emissive technologies -- notably the utilization of air-stabile electrodes and very thick active materials -- but the critical drawback has been a short operational lifetime. We have set out on a quest to resolve this problem and been able to identify a number of lifetime-limiting chemical [1] and electrochemical [2] side reactions. By following motivated and straightforward design principles to minimize the extent of these side reactions, we are now able to repeatedly realize LEC devices that emit with significant brightness (>100 cd/m^2) and good efficiency (>2 lm/W for red emission, >10 lm/W for green emission) for several months of uninterrupted operation.[3,4] The figure to the right presents the long-term operation of an optimized red-emitting LEC, and the inset shows a flexible LEC with a similar promising device performance.

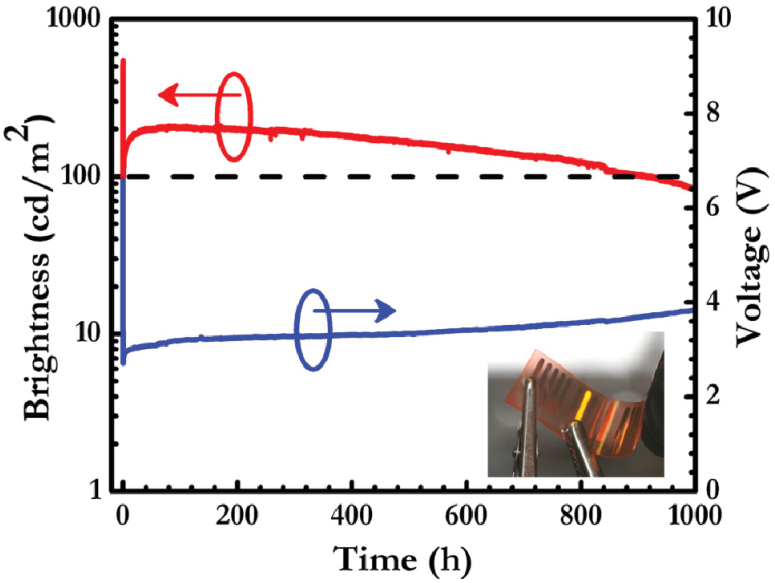

In another development, we have performed a parallel optical probing and scanning Kelvin probe microscopy study on planar LEC devices during operation, and the acquired light emission and potential profiles present irrefutable evidence for that electrochemical doping takes place *in-situ* in the active material, and that a dynamic p-n junction structure can self-assemble in an LEC during operation.[5] Finally, we have conceptualized and demonstrated a truly metal-free and "all-plastic" LEC device comprising a graphene cathode and a conducting-polymer anode.[6] Both electrodes in this device architecture are transparent and the light emission is accordingly omni-directional. Moreover, all parts of the device can be processed from solution, which -- in combination with the elimination of expensive and/or reactive metal materials -- promises to pave the way for a low-cost production of functional light-emitting devices.

References

[1] Wågberg, T., et al., Advanced Materials, 2008, 20, 1744.

[2] Fang, J., et al., Journal of the American Chemical Society, 2008, 130, 4562.

[3] Fang, J., et al. Advanced Functional Materials, 2009, 19, 2671.

[4] Sandström, et al. Appl. Phys. Lett. 2010, 96, 053303.

[5] Matyba, P., et al., Nature Materials, 2009, 8, 672.

[6] Matyba, et al., ACS Nano, 2010, 4, 637.

MULTICOLORED ELECTROCHROMIC MODULES FOR ECD APPLICATIONS

G. Nazmutdinova*[1)], H. Schache [1)], M. Schroedner [1)] and D. Raabe [2)]

[1)] TITK Institute, Department of Physical Materials Research, Breitscheidstraße 97, 07407 Rudolstadt, Germany, e-mail: Nasmutdinova@titk.de
[2)] Neustraße 4, 07774 Dornburg-Camburg

Introduction

Electrochromic materials change their optical properties in response to an electric field.

The interest in these materials has increased in the last few years due to their potential application on "smart-windows", automobile mirrors, low-refractive materials in filters and non-emissive displays. Widely used examples are tungsten oxide, viologens and conjugated polymers as derivatives of poly(thiophene), poly(pyrrole) and poly(aniline). In fact, organic electrochromic materials offer several advantages with respect to inorganics, not only in terms of flexibility, easy of processing and low cost, but also with respect to both efficiency of coloration and fine-tuning ability of the band gap (and the colour) through chemical structure modification [1]. The structure of a classical electrochromic device is a typical multilayer electrochemical cell, consisting of up to seven layers of materials, transparent to visible light. The electrochromic material is coupled to an ion conductor, solid or liquid electrolyte and an ion storage layer. These three optically transparent layers are sandwiched between two conductors, at least one of them must be transparent. The resulting five layers are protected by two transparent plastic or glass substrates. Alternatively, two electrochromic species can be present in two symmetrically arranged layers, for such a case, cathodic and anodic coloration processes are simultaneously driven.

Triphenylamine (TPA)-containing polymers have received considerable interest as electrochromic [2] and hole-transport materials for use in organic electroluminescence devices [3], because of their relatively high charge mobility and low ionization potentials [4-5]. The TPA radical cation is not stable and tends to dimerize rapidly forming tetraphenylbenzidine (TPB) by tail-to-tail coupling. The last is more easily oxidized than the starting TPA and undergoes further oxidation at the applied potential [6]. The coupling reaction could be prevented by incorporating at the para-position of the phenyl group electron-donating substituents [7-8]. So far, there had been done some attempts to introduce TPA units into the main or side chain of the polymer backbone and in this way there have been prepared new high-performance systems with novel optoelectronic functions [9-15].

Results

In this paper we report on a device based on an electrochromic non-conjugated copolymer having alternating TPD (triphenylamine dimer) and diphenylxylylene units in the backbone with good amorphous film forming properties and high glass transition temperature of T_g ~ 240°C. The synthesis of poly[(4-methylphenyl)imino-4,4'-diphenylene-(4-methylphenyl)-imino-1,4-phenylene-phenylmethylene-1,4-phenylene-phenylmethylene-1,4-phenylene] (poly-TPD (4Me)-DPX) polymer is described in [16-17]. The structural formula with the oxidation scheme is presented in the Fig.1.

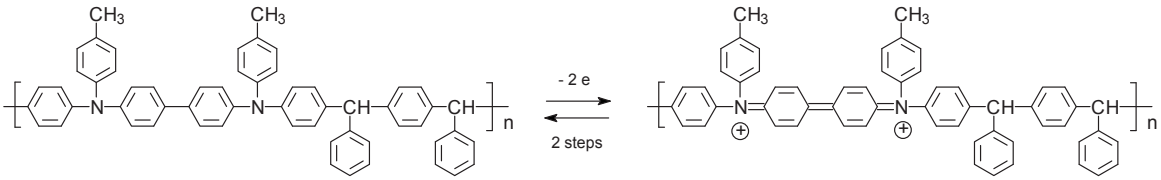

Fig.1 Electrochemical oxidation of poly-TPD(4Me)-DPX.

The oxidation is carried out in two steps with consistently oxidation of amino groups and creating radical cations and dications.

The solid-state electrochromic device was constructed using the sandwich structure FTO/ TPD(4Me)-DPX/gel-electrolyte/ion storage layer/FTO. The poly-TPD(4Me)-DPX film was spin coated from solution to a thickness of 300 nm. The gel-electrolyte, that enabled the charge transport between the electrochromic and the charge balancing counter electrode consisted of the salt lithium-bis(trifluoromethylsulfonyl)imide ($LiTf_2N$), the plasticized polymer poly(vinylidenefluoride-co-hexafluoropropylene) (PVDF-HFP) and the ionic liquid 1-ethyl-3-methyl-imidazolium bis(trifluoromethylsulfonyl)imid ($EMITf_2N$). The mixture of cerium and titanium oxides was fabricated by a sol-gel process and used as ion storage layer. The spin-coated film of the sol with subsequent annealing shows a transmission of about 70 % in the wavelength range from 500 nm up to 1100 nm. All device fabrication was performed in an inert atmosphere glove box to minimize exposure to water and oxygen.

The optical and electrochemical properties of EC-devices were investigated by UV-vis spectroscopy and cyclic voltammetry. Fig.2a shows the cyclic voltammogram of the polymer solution with two oxidation peaks because of successive forming radical cation and dication. Anodic oxidation was cycled over 50 cycles without noticeable change. In the polymer film (Fig.2b) the two peaks substantially merge together to form one broad asymmetrical peak.

a)

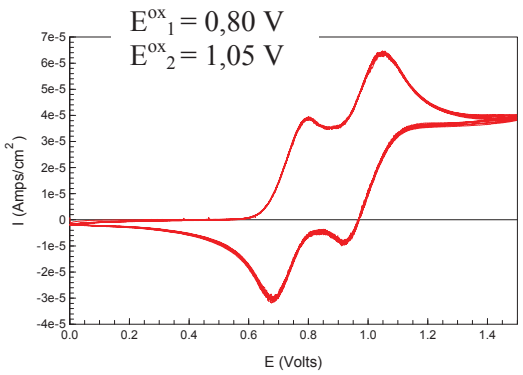

b)

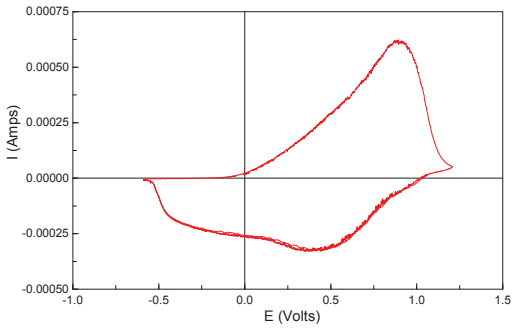

Fig.2. Cyclic voltammograms (a) of poly-TPD(4Me)-DPX in methylene chloride solution, c = 0.005 mol/l, Bu_4NPF_6, c = 0.1 mol/l, 50 cycles, CE: Pt-disc electrode and (b) of EC-device from Fig. 3, scan-rate: 15 mV/s, T: 25°C.

The EC-device shows multicolor electrochromic behaviour with color change from neutral colorless to orange and then through transient green to blue (Fig.3).

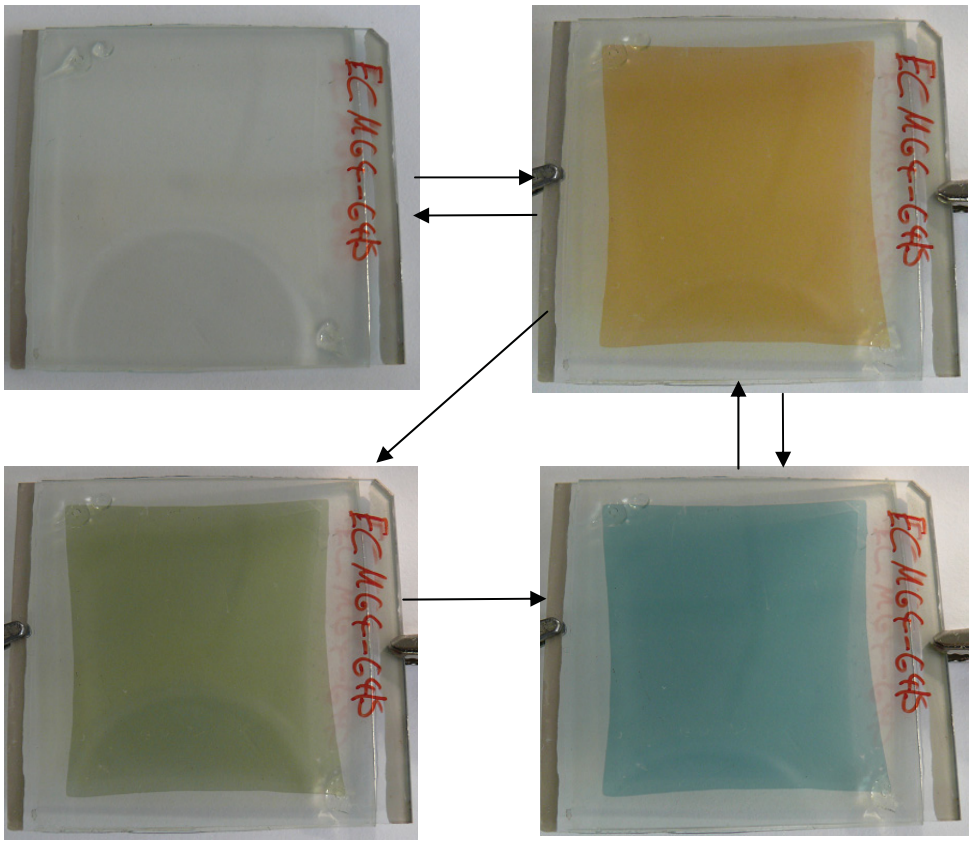

Fig. 3. Solid-state multicolor electrochromic device with poly-TPD(4Me)-DPX film, gel-electrolyte PVDF-HFP, $LiTf_2N$ in $EMITf_2N$ and a CeO_2/TiO_2 film as ion storage layer.

Electrochromism of the device was monitoried by a UV-vis spectrometer at different applied potentials. The device is ideally colorless in the whole visual optical range with a transmission of 70 %. When the applied potential increased positively from 0 to 0.45 V, the film turned into orange to give an absorption band at 475 nm.

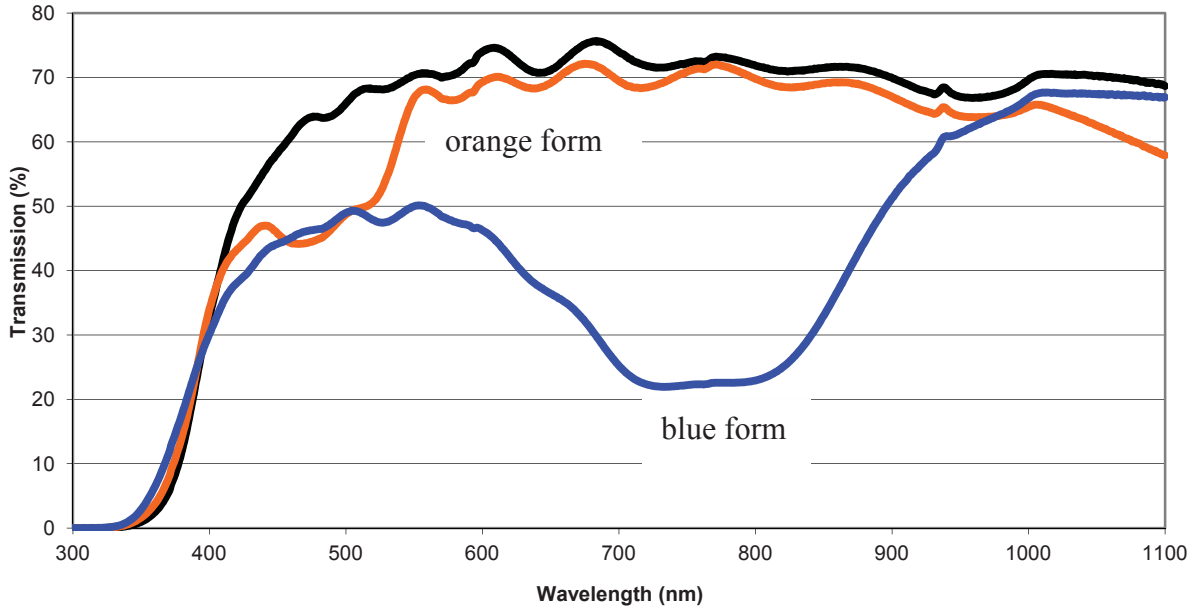

Fig.4. Transmission spectra of EC-device from Fig.3 in the neutral (black curve) and two oxidized states, correspondingly at E=0.45 V (orange curve, λ=475 nm) and at E=1.1 V (blue curve, λ=770 nm).

Further raising the voltage up to 1.1 V resulted in a colour change of the device into blue accompanying the increase of absorption around 770 nm. The electrochromic characteristics of the EC-device from Fig.3 are summarized in Table 1. For a device, with an active electrochromic area dimension of 3.8 cm x 4.2 cm (15.96 cm²) the time for switching from a clear state of 74.5 % of transmission to, for example, a blue state of 22% was measured to be 7.5 s and the reverse switching was completed within 6 s at room temperature (25°C) (Fig. 5). Colour switch was uniform along the whole surface of the device. Switching time was obtained by means of applying potential steps between +1.1 V and –0.6 V, and the switching speed was defined as the time necessary to complete 88 % of the total transmission change recorded at 770 nm. Optimal devices were reversible during 10000 switching cycles with negligible change of the coloration efficiency.

Table 1. Electrochromic behaviour of the EC-device from Fig.3

Characteristic	colorless/orange (λ=475 nm)	colorless /blue (λ=770 nm)
electrochromic contrast, **Δ%T**	21	52
optical density **OD** = log ($T_{Bleaching}/T_{Colouring}$)	0.17	0.54
Coloration efficiency (cm^2/C) **η** = log ($T_{Bleaching}/T_{Colouring}$) /Q	**387**	**340**
Switching time, T (sec)	~10	~10

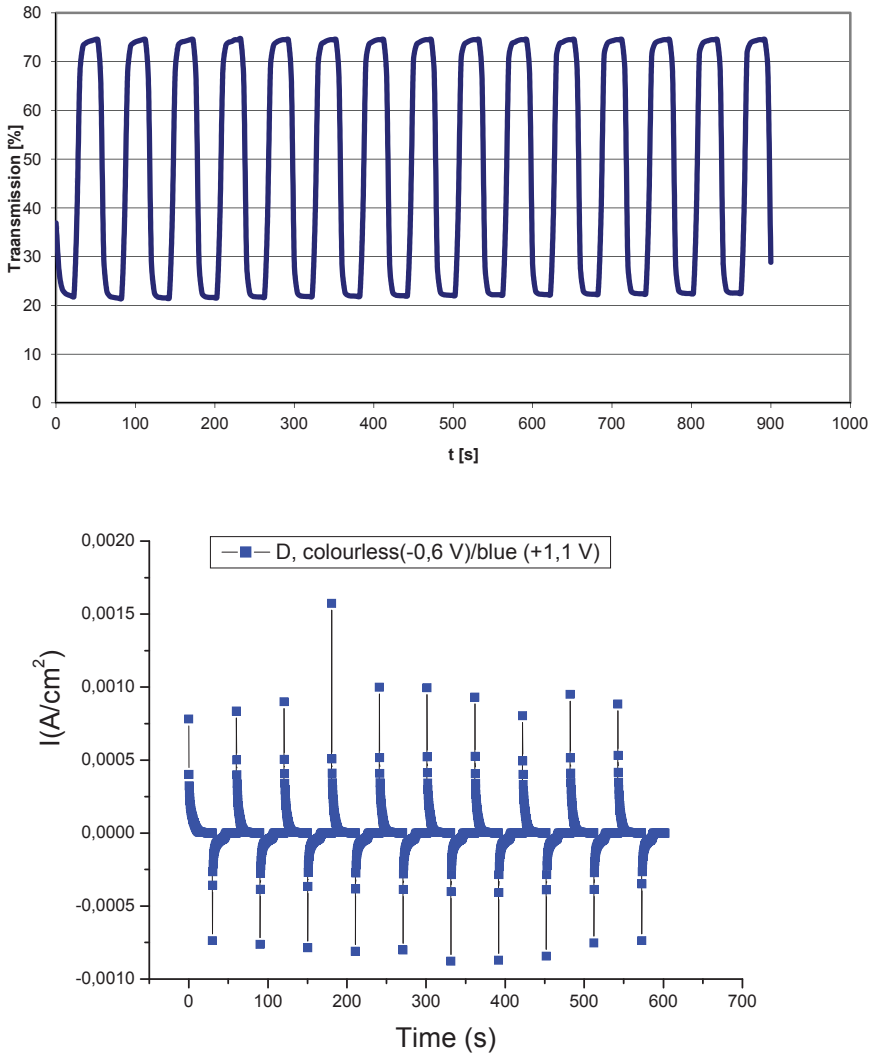

Fig. 5. Changes of optical transmission monitored at 770 nm (above) and electrode current (below) as a function of time for EC-device from Fig. 3 under application of repetitive pulse voltage of +1.1 V and –0.6 V.

Acknowledgement

Financial support from Federal Ministry for Economy and Technology BMWi (project IW071048 and MF110097) is gratefully acknowledged.

References

1. A. Argun, P.-H. Aubert, B. Thompson, I. Schwendeman, C. Gaupp, J. Hwang, N. Pinto, D. Tanner, A. MacDiarmid and J. Reynolds; Chem. Mater. 2004, 16, 4401-4412
2. G.-S. Liou, Y.-L. Yang, W.-C. Chen and Y. O. Su; J. Polym. Sci.: Part A: Polym. Chem., Vol. 45, 2007, 3292-3302
3. R. H. Mitschke, P.J. Bäuerle, J. Mater. Chem., 10, 2000, 1471
4. Y. Shirota; J. Mater. Chem., 2000, 10, 1-25
5. Y. Shirota; J. Mater. Chem., 2005, 15, 75-93
6. E. T. Seo, R.F. Nelson, J.M Fritsch, L.S- Marcoux, D.W. Leedy and R.N., Adams J. Am. Chem. Soc, 1966, 88, 3498-3503
7. A. Ito, H. Ino, K. Tanaka, K. Kanemoto und T. Kato, J. Org, Chem., 2002, 67, 491-498.
8. K.-Y. Chiu, Y. O. Su ,G.-S. Liou, S.-H. Cheng; J. Electroanal. Chem., 575, 2005, 283
9. H.-Y. Lin and G.-S. Liou, J. Polym. Sci: Part A: Polym. Chem., V. 47, 2009, 285-294
10. G.-S. Liou, C.-W. Chang, H.-M. Huang and S.-H. Hsiao; J. Polym. Sci.: Part A: Polym. Chem., Vol. 45, 2007, 2004-2014
11. G.-S. Liou and H.-Y. Lin, Macromolecules, 42, 2009, 125-134
12. C.-W. Chang, H.-J. Yen, K.-Y. Huang, J.-M. Yen and G.-S. Liou; J. Polym. Sci: Part A: Polym. Chem., V. 46, 2008, 7937-7949
13. F. Liang, Y.-J. Pu, T. Kurata, J. Kido and H. Nishide; Polymer, 46, 2005, 3767-3775
14. J. Qu, R. Kawasaki, M. Shiotsuki, F. Sanda and T. Masuda; Polymer, 47, 2006, 6551-6559
15. C.-W. Chang, G.-S. Liou and S.-H. Hsiao; J. Mater. Chem., 17, 2007, 1007-1015
16. H.-H. Hörhold, D. Raabe, M. Helbig, German patent application, DE 19832943, 1998
17. W. Holzer, A. Penzkofer, H.-H. Hörhold, D. Raabe, M. Helbig, Optical materials, 15 (2000), 225-235

BIOGRAPHIC DATA OF DR GULNARA NAZMUTDINOVA

Gulnara Nazmutdinova was born in Kazan, Russia in 1967. She studied chemistry at the Kazan State University (at present Kazan (Volga Region) Federal University).

Her Ph.D. work was performed under the supervision of Professor Alexey V. Zakharov and major research scientist Ph.D. Valery G. Shtyrlin (Kazan, Russia). From 1995-2000 she worked as scientist at the Laboratory of Coordination Compounds (Kazan State University, Russia) researching the complex formation and chemical exchange in solutions of the transition metals complexes as well as the biological activity of the metals complexes.

In 2000 she moved to the Thuringian Institute for Textile and Plastics Research (TITK, Rudolstadt, Germany) and worked as a visiting scientist. Since 2002 she is a staff scientist at TITK.

Her current research interests cover the polymer electrolytes (for dye-sensitized solar cells, electrochromic displays and Li-batteries), ion-storage layers as well as the optical and electrochemical properties of polymers, with special focus on electrochromic systems.

Part V: Materials and technologies 2

PHOTOGENERATION AND ULTRAFAST DYNAMICS OF EXCITONS AND CHARGES IN POLYMER/FULLERENE/QUANTUM DOT BLEND FILMS

Laurens D.A. Siebbeles

Optoelectronic Materials Section, Department of Chemical Engineering,
Delft University of Technology, Delft, The Netherlands
email: l.d.a.siebbeles@tudelft.nl

Summary

Photogeneration and decay of excitons and charges in the conjugated polymer poly(3-hexylthiophene) (P3HT) with PCBM or PbS quantum dots as electron acceptors were studied with ultrafast laser spectroscopy. Insights in the mechanism of charge carrier formation (via carrier multiplication) are discussed.

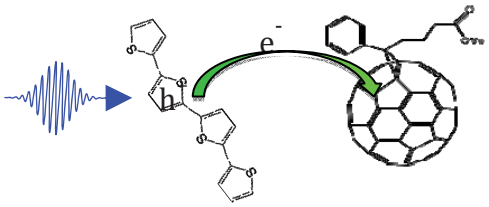

Introduction

Thin blend films of a conjugated polymer and a fullerene derivative are of interest for application in low cost photovoltaic cells. To date, some of the best efficiencies (near 5%) have been reported for devices based on a thin blend film of the conjugated polymer regioregular poly(3-hexylthiophene) (P3HT), and [6,6]-phenyl-C_{61}-butyric acid methyl ester (PCBM) as electron acceptor. However, the nature and dynamics of photoexcitations in P3HT and blend films with PCBM have been subject of debate.

The present work provides insights about the nature of primary photoexcitations in P3HT and blend films with PCBM and or PbS quantum dots (QDs). QDs are of interest for application in high efficiency solar cells in which absorption of a single photon leads to generation of multiple excitons via carrier multiplication.

The photogeneration quantum yield and dynamics of charge carriers and excitons were studied with ultrafast optical pump-probe spectroscopy and time-resolved terahertz or microwave conductivity measurements.

Discussion

In neat P3HT the quantum yield for direct photogeneration of charge carriers amounts to 0.15 per absorbed photon.[1] The remaining fraction of absorbed photons leads to formation of excitons. Recombination of charges reduces the quantum yield to about 25% of its initial value on a timescale of 100 ps followed by decay to a no longer observable yield after 1 ns. Addition of 50% PCBM by weight, leads to ultrafast (<200 fs) formation of charge pairs with a total quantum yield of 0.5. The presence of 50% PCBM causes exciton decay to be about an order of magnitude faster than in neat P3HT, which is expected to be at least in part due to interfacial exciton dissociation into charge carriers. The yield of charges in the blend has decayed to about half its initial value after 100 ps, while no further decay is observed within 1 ns. The small fraction (~1%) of excitons in neat P3HT that is probed by photoluminescence measurements has a lifetime of 660 ps, which significantly exceeds the 200 ps lifetime of

non-fluorescent excitons that are probed by transient absorption measurements. The non-fluorescent excitons have a diffusion coefficient of about 2×10^{-4} cm^2/s, which is an order of magnitude smaller than reported values for fluorescent excitons. The interaction radius for second order decay of photoexcitations is as large as 8-17 nm, in agreement with an earlier result in the literature.[2]

The quantum yield for photogeneration of charge carriers in P3HT:PCBM blends was found to be virtually temperature independent for timescales up to tens of nanoseconds after photoexcitation of P3HT.[3] This implies that a description of charge generation on basis of the Onsager-Braun model with an initial electron-hole distance of the order of nanometers is inadequate. Factors that can give rise to negligible temperature dependence include coupling of the initially hot exciton with excess vibrational energy, the high driving force for electron transfer from the polymer to PCBM, the high dielectric constant along the polymer chain direction and charge delocalization. The decay of charges due to recombination and/or trapping on longer times becomes faster at higher temperature as a result of thermally activated electron and hole mobilities.

Extraction of charges from multi-excitons in PbS quantum dots (QDs) was studied for blend films with P3HT and/or PCBM. Photoexcitation of the QDs in a blend with P3HT yielded no observable terahertz (THz) photoconductivity. However, for blends with P3HT and PCBM a significant THz photoconductivity is observed within 1 ps after photoexcitation of the QDs. The charges hardly decay on a ns timescale. Multiple-charges could be extracted from multi-excitons in the QDs. This is of great promise for development of highly efficient solar cells based on carrier multiplication.

Conclusions

Photoexcitation of P3HT leads to significant generation of free charges in addition to excitons. Exciton dissociation at an interface with PCBM leads to ultrafast charge generation with an initial yield that is virtually independent of temperature. Multi-excitons in PbS QDs can be dissociated into free charges in blend films with P3HT and PCBM.

References

[1] J. Piris, T.E. Dykstra, A.A. Bakulin, P.H.M. van Loosdrecht, W. Knulst, M.T. Trinh, J.M. Schins, L. D.A. Siebbeles, *J. Phys. Chem. C*, **113**, 14500, 2009.

[2] A. Ferguson, N. Kopidakis, S.E. Shaheen, G.J. Rumbles, *J. Phys. Chem. C,* **112**, 9865, 2008.

[3] W.J. Grzegorczyk, T.J. Savenije, T.E. Dykstra, J. Piris, J.M. Schins and L.D.A. Siebbeles, *J. Phys. Chem. C,* **114**, 5182, 2010.

BIOGRAPHIC DATA OF PROFESSOR LAURENS D. A. SIEBBELES

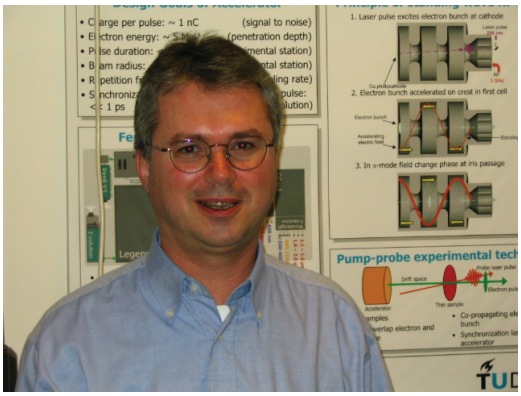

Laurens Siebbeles (1963) studied chemistry at The Free University in Amsterdam and obtained his PhD degree at the FOM-institute for Atomic and Molecular Physics in Amsterdam. He was a post-doc at the University of Paris Sud in France. Currently he is head of the opto-electronic materials section at the Delft University of Technology in The Netherlands. He studies the dynamics of charges and excitons in organic materials and semiconductor nanocrystals. Charges and excitons are produced with high-energy electron or laser pulses and probed by time-resolved optical and microwave or terahertz measurements. The experiments are supported by theory of charge and exciton dynamics.

POLYMER SOLAR CELLS BLENDED WITH SILICON NANOWIRES

S. Sensfuss[1]*; H. Schache[1], B. Eisenhawer[2], G. Andrae[2], M. Pietsch[2], S. Shokhovets[3], M. Himmerlich[4], E. Klemm[5], M. Kroll[6], T. Pertsch[6]

[1] TITK Rudolstadt, Dept. Functional Polymer Systems and Physical Research, Breitscheidstr. 97, D-07407 Rudolstadt, Germany, *e-mail: sensfuss@titk.de
[2] Institute of Photonic Technology, Dept. Photonic Silicon, Albert-Einstein-Str. 9, D-07745 Jena, Germany
[3] Technical University of Ilmenau, Institute for Physics, Weimarer Str.32, D-98684 Ilmenau, Germany
[4] Technical University of Ilmenau, Center for Micro and Nanotechnologies, Gustav-Kirchhoff-Str. 7, D-98693 Ilmenau, Germany
[5] Jenpolymer Materials Ltd. & Co. KG, Wildenbruchstr.15, D-07745 Jena, Germany
[6] Friedrich Schiller University Jena, Institute of Applied Physics, Max-Wien-Platz 1, D-07743 Jena

Solar cells based on conjugated polymers can be processed from solution or dispersion which offers a very important technological potential for low-cost fabrication using high-volume processes like reel to reel technologies. The main limitations of polymer solar cells are assigned to the absorbance only of a small part of the solar spectrum and the limited charge carrier mobility, which restricts the possible film thickness of the organic photoactive layer to below 300 nm. Hybrid inorganic-organic solar cells may be promising candidates to overcome these limitations and became a subject of increasing interests during the past few years. The combination of semiconducting polymers with inorganic nanoparticles remain the advantage of solution processing while benefiting from a broader absorption and/ or a better charge transport. The application of silicon nanowire (SiNW) structures in solar cells offer the chance to use their extraordinary light trapping capabilities resulting in an outstanding light absorption, significantly reduced reflections, superior charge carrier transport properties and a clearly increased p-n junction area.

Here we report about P3HT:[60]-PCBM polymer solar cells blended with semiconducting or highly n-doped silicon nanowires in the absorber layer. The silicon nanowires were prepared by chemical vapour deposition or silver catalyzed electroless etching into silicon wafers (Fig.1). They were removed from the initial substrate by sonication in chlorobenzene. For first hybrid solar cells different amounts of the SiNW dispersion were added to the P3HT:[60]-PCBM blend using the usual device architecture glass/ ITO/ PEDOT:PSS/ P3HT:PCBM:SiNW/ Al (Fig.2).

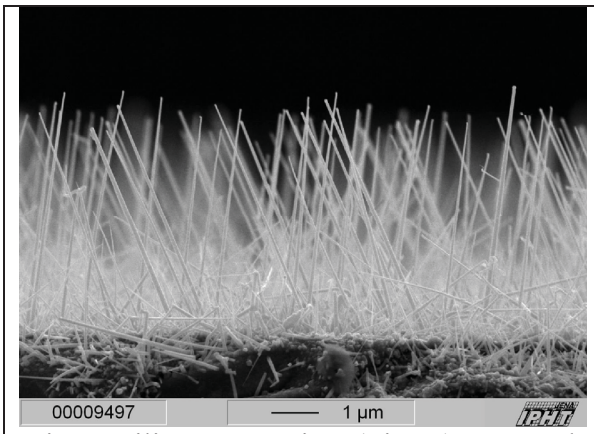

Fig.1a Silicon nanowires (SiNW) prepared by chemical vapour deposition (CVD) catalyzed by gold colloids

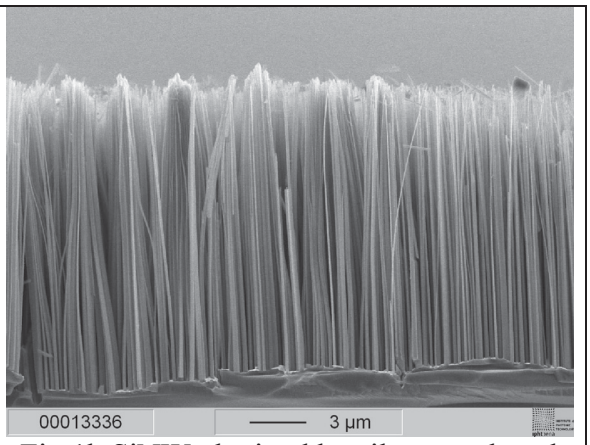

Fig.1b SiNW obtained by silver catalyzed electroless etching into silicon wafers

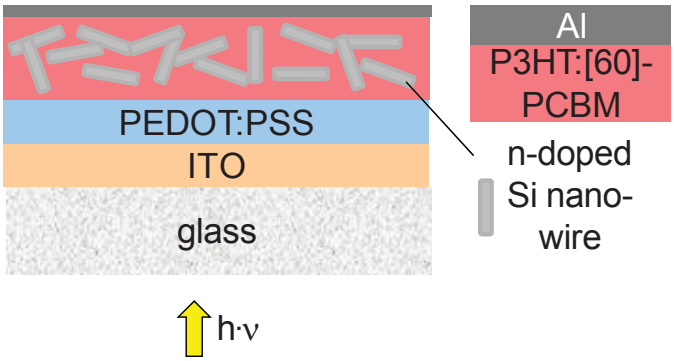

Fig.2 Device architecture of polymer solar cells blended with SiNW

Presently, the devices with SiNW reached a relative efficiency improvement of about 10 % compared with the reference cell, which is attributed to a reduced series resistance and an increase in the short circuit current (Tab.1, Tab.2, Fig.3).

Tab.1 Device properties of glass/ ITO/ PEDOT:PSS/ P3HT:PCBM (1:0.8 w/w):SiNW/ Al polymer solar cells blended with different amounts of heavily n-doped etched SiNW (length 3-5 µm)

sample	Isc [mA/cm²]	Voc [mV]	FF	$\eta_{AM1.5}$ [%]	R_s [Ωcm²]
reference cell (without SiNW)	9.79	641	0.60	3.77	5.78
60wt.-% photoactive solution + 40wt.-% SiNW suspension	9.98	639	0.64	4.08	3.17
50wt.-% photoactive solution + 50wt.-% SiNW suspension	10.45	638	0.62	4.13	3.17
30wt.-% photoactive solution + 70wt.-% SiNW suspension	10.25	637	0.63	4.11	2.81
with spin-coated SiNW (200 rpm)	9.33	635	0.66	3.91	2.46

The external quantum efficiency is slightly increased with SiNW, but up to now there is no spectral contribution of the silicon to the photocurrent realizable (Fig.4). The detailed contribution of the SiNW is not really clarified, we just can exclude an optical effect of light scattering for which the nanowire density is still too low. Scanning electron microscopy

images show the problem of a too low nanowire density with an inhomogeneous distribution in the P3HT:PCBM film (Fig.5).

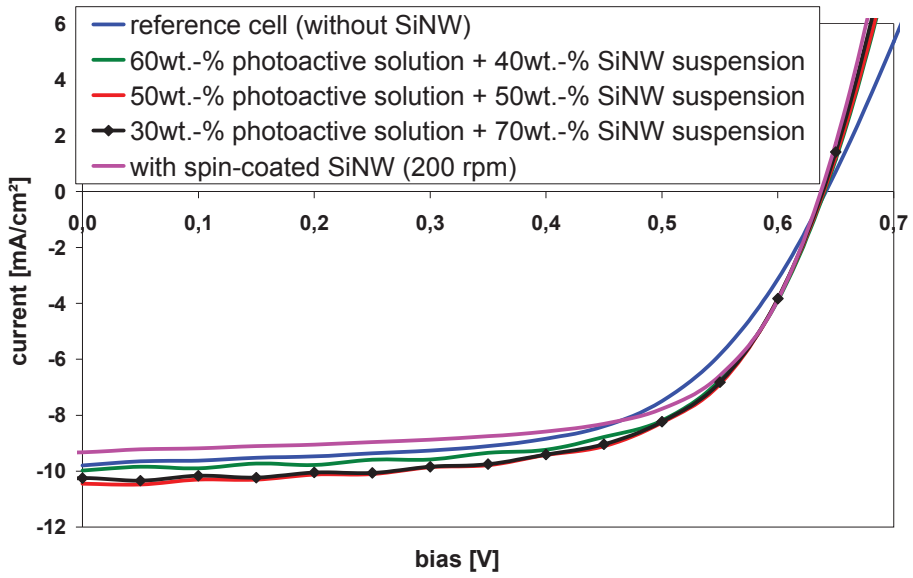

Fig.3 I-V characteristics of glass/ ITO/ PEDOT:PSS/ P3HT:PCBM (1:0.8 w/w):SiNW/ Al polymer solar cells blended with different amounts of heavily n-doped etched SiNW (length 3-5 µm)

Tab.2 Device properties of glass/ ITO/ PEDOT:PSS/ P3HT:PCBM (1:0.8 w/w):SiNW/ Al polymer solar cells blended with different amounts of moderately n-doped etched SiNW (length 3-5 µm)

sample	Isc [mA/cm²]	Voc [mV]	FF	$\eta_{AM1.5}$ [%]	R_s [Ωcm²]
reference cell (without SiNW)	9.77	626	0.65	3.98	2.96
50wt.-% photoactive solution + 50wt.-% SiNW suspension	10.08	634	0.65	4.15	2.70
30wt.-% photoactive solution + 70wt.-% SiNW suspension	10.13	622	0.63	3.97	2.75
with spin-coated SiNW (400 rpm)	10.31	621	0.65	4.16	3.12

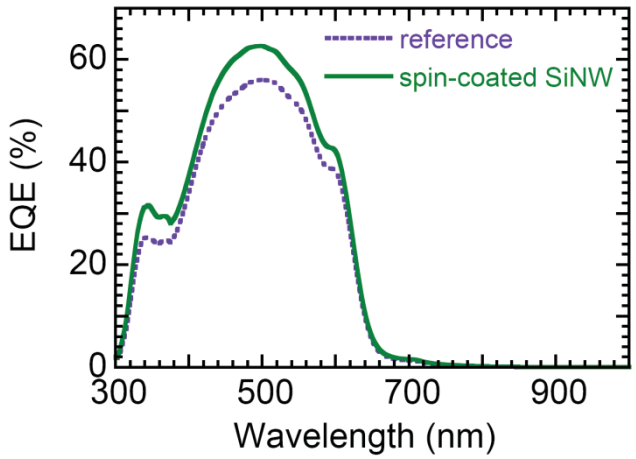

Fig.4 External quantum efficiency of a P3HT:PCBM solar cell with spincoated SiNW (moderately n-doped) on the PEDOT:PSS layer in comparison to the reference cell without SiNW (see Tab.2)

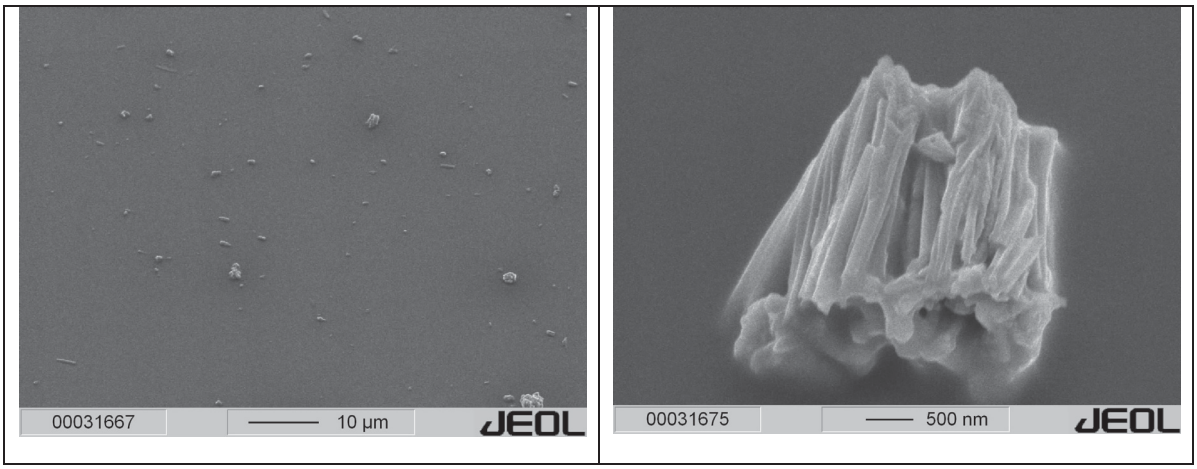

Fig.5 SEM images showing a still too low SiNW density in P3HT:PCBM films with an inhomogeneous distribution and formation of SiNW agglomerates

Further optimization is needed to reach a higher nanowire density in the photoactive layer with reduced NW agglomeration.

Initial XPS/UPS measurements were carried out to investigate the band alignment at the polymer/silicon interface. First inverted P3HT:[60]-PCBM cells were prepared on planar Si wafers using heavily n-doped silicon as bottom and PEDOT:PSS/ Au (7 nm) as transparent top electrode. The insert of an a-Si layer between the n+-Si and P3HT:[60]-PCBM film seems to reduce recombination and improves the Voc and fill factor of the cells. Without an a-Si interlayer both parameters are dropping down (Tab.3).

Tab.3 Device properties of inverted P3HT:[60]-PCBM cells using planar heavily n-doped silicon wafers as bottom and PEDOT:PSS/ Au (7 nm) as transparent top electrode with different types of amorphous silicon (a-Si) interlayers

sample	Isc [mA/cm²]	Voc [mV]	FF	$\eta_{AM1.5}$ [%]
n^+ c-Si	3.53	352	0.44	0.54
n^+ c-Si / n^+ a-Si:H (50nm) / i-a-Si:H (5nm)	3.05	617	0.69	1.30
n^+ c-Si / n^+ a-Si:H (50nm)	4.14	603	0.65	1.62
n^+ c-Si / n^+ a-Si:H (25nm)	4.39	604	0.66	1.75
n^+ c-Si / n^+ a-Si:H (30nm) / i-a-Si:H (5nm)	3.85	604	0.60	1.40
n^+ c-Si / n^+ a-Si:H (10nm) / i-a-Si:H (5nm)	4.54	613	0.65	1.81

The EQE of these non-optimized cells amounts to ~30% in the peak, but does not clearly show a contribution of the silicon to the photocurrent up to now. Of course, the aim of further efforts is to be able to use the advantages of silicon (SiNW) and semiconducting polymers.

Acknowledgement

Financial support from the Federal Ministry of Education and Research (BMBF project No. 03SF0333C) is gratefully acknowledged.

BIOGRAPHIC DATA OF DR STEFFI SENSFUSS

Steffi Sensfuss received the diploma in Organic Chemistry in 1983 and a doctorate degree in 1987 in Polymer Chemistry under the mentorship of Dr. Elisabeth Klemm in the group of Prof. Hörhold at the University of Jena. During this time the main research activities had been in the development of optical adhesives and dental materials based on thiol/ene polyaddition, epoxy and acrylate polymers. Since 1998 she is working at the Thuringian Institute for Textile and Plastics Research in Rudolstadt in the group of Prof. Roth and Prof. Heinemann, respectively. The main research activities are actually in the field of applied research of conducting polymers. Presently she heads the activities of TITK group for polymer solar cells, hybrid solar cells, polymer gel electrolytes and textile-based dye-sensitized solar cells.

PRINTED ELECTRONICS BASED ON SOLUTION PROCESSABLE NANOWIRES

M. SHKUNOV*, C. OPOKU
Advanced Technology Institute, University of Surrey, Guildford GU2 7XH, UK

Solution-based assembly of thin-film field-effect transistors (FETs) using semiconducting inks at low temperatures on large areas, and on optically transparent substrates are finding potential applications in many areas including: sensors, RFID tags[1], memory elements[2], and flexible display applications.[3] Conventional hydrogenated silicon[4] (a-Si:H) and polycrystalline silicon (poly-Si) TFTs have limitations due to a trade-off between process temperatures and performance on transparent/flexible substrates.[5, 6] Organic field-effect transistors (OFETs) are gaining popularity as excellent material candidates, but are limited by their low carrier mobility, sensitive to semiconductor morphology and process conditions.[7] Single-crystalline semiconducting nanowires (NW) are offering potential breakthrough in the area of high performance, low cost device assembly due to their proven high charge carrier mobility and compatibility with solution based assembly techniques.[8] Small size of nanowires, typically tens of nanometres in diameter and 10 to 40 micron length allow these nanomaterials to be dispersed in solvents and processed as inks at room temperature to 'bridge' typical device electrodes. Significant advances in NW synthesis can now offer large quantities of high purity NW.

Most reports of high performance NW FETs have in the past dealt with inorganic dielectrics that are incompatible with solution assembly techniques.[8] Recently, organic based dielectrics such as poly(methyl methacrylate) (PMMA)[10], polyimide[11], and self assembly nanodielectrics (SAND)[12, 13] have been identified as alternative insulators for NW-based FETs that can be processed at low temperatures. These devices are hybrid where organic and inorganic components are integrated in a single FET system.[12]

In this report we investigate solution processable silicon nanowire based FETs with both polymer dielectric and a typical SiO_2 dielectric.

Si NWs used in this study were synthesised via the supercritical fluid-liquid solid method (SFLS)[9]. FETs have been fabricated as follows: several bottom gate (BG) devices were constructed on n^{++}-Si substrates with a 230nm thermally grown SiO_2. Hybrid top gate (TG) FETs with organic dielectrics were fabricated on glass substrates.

As a first device fabrication step anisole suspended Si nanowires were deposited onto cleaned substrates by solution coating. Then metal source and drain (*s/d*) contacts (Au/Cr

(100nm/2nm) were patterned on top NWs by the standard lift-off photolithography. After metallisation, substrates were annealed at ~170°C for 30 minutes. This step completed the BG FETs preparation. Extra steps were required to define organic gate insulator and gate electrode in the hybrid devices, and this was achieved by spin coating ~1µm thick dielectric followed by shadow mask evaporation of gate electrode (Au, 60nm). Electrical transport measurements were carried out using Keithley 4200 characterisation system.

Transfer (I_D-V_G) and output (I_D-V_D) characteristics for a representative BG Si NW-array FET with SiO_2 dielectrics are shown in Fig. 1a-b. For this device, the on/off ratio is ~10^7. Notably, influence of high contacts resistance can be seen in the output scans in Fig. 1b. This can be explained by the presence of surface layers on Si NWs[9], or energetic barriers resulting from unoptimised *s/d* contacts.

The clear increase in I_{on} with V_G is indicative of good gate-channel modulation. The turn-on voltage (V_O), subthreshold swing (s-s), and transconductance (*gm*) at V_D = -6V are extracted as ~7.7V, 1.4V/dec, and 0.2µS respectively.

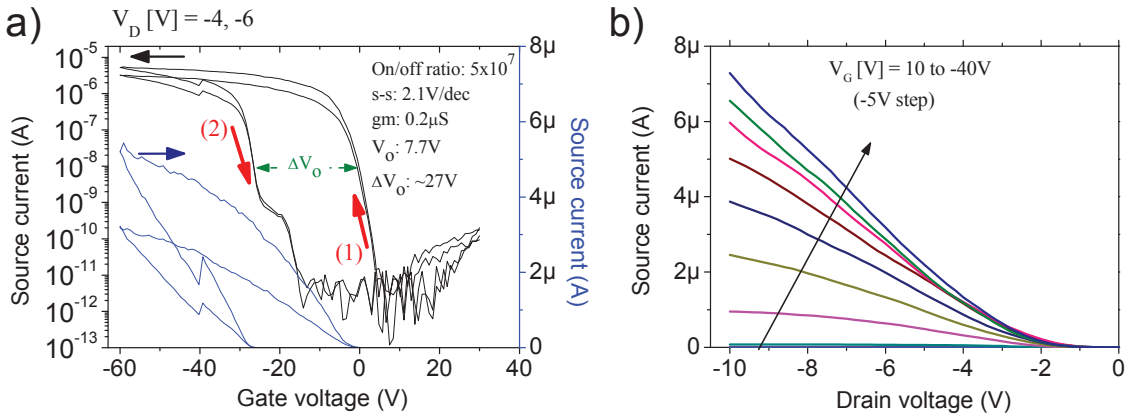

Figure 1 Transfer (I_D-V_G) characteristics at V_D = -5V and -10V b) Output (I_S-V_D) scans for the same device at V_G from 10V to -40V.

A significant shift in V_O (ΔV_O or hysteresis) is observed upon forward (denoted as 1) and reverse sweep (denoted as 2) of the gate voltage. The shift also appears to be independent to the value of V_D. Adsorption of polar species such as water molecules on SiO_2 is known to cause hysteresis effects in carbon nanotubes FET and also in NW FETs.[14] Since our BG transistors have been measured in a dry N_2 atmosphere one would expect the influence of moisture to be minimal. On the other hand, trap states at the interface between NW and SiO_2 cannot be easily eliminated. Wang *et al*[15] have shown that interface state in ultra high density Si NWs constructed as FETs can be reduced by forming (5% H_2 in N_2) gas anneal at

470^{O}C. However, such high temperature processes are impractical in low temperature solution assembly approaches described here. Dielectrics with low trap states are therefore highly attractive for the realisation of high performance NW-based FETs that can be processed at relatively low temperatures.

Due to the cylindrical nature of NWs, extraction of the gate capacitance requires special treatment to account for the electrostatic fringing between individual NWs that constitute the active channel. The capacitance is obtained using Eq. 1 which describes the capacitance for individual NWs according to cylinder on infinite plate model[16]

$$C_{NW} = \frac{2\pi\varepsilon_o\varepsilon_i L}{cosh^{-1}\left(\frac{r+d}{r}\right)} \qquad (1)$$

where ε_o, ε represent the permittivity of free space and the dielectric constant (~3.9) of the gate dielectric (SiO_2 in this case); r (= 5nm) is the average radius of individual NWs, d is the dielectric thickness (230nm) and L (= 10μm) is the channel length. Accordingly, the total capacitance (C_T = N x C_{NW}) is then obtained by multiplying the number of NWs (N) in the FET channel. Using Eq. 1 and the parameters of the BG device structure, C_{NW} is approximated as 0.62fF, and the total channel capacitance (C_T) for the 5NWs in the representative BG is estimated to be ~3.1fF.

With the estimated channel capacitance C_T, the field effect mobility can be calculated for the representative BG device using the Eq. 2 in the linear regime

$$g_m = \frac{\mu C_T}{L^2} V_D \qquad (2)$$

where g_m (~0.2μS at V_D = -6V) is the transconductance, defined as $\partial I_S/\partial V_G$, μ is carrier mobility (holes in the present case) and V_D of the drain voltage bias. Using Eq. 2 and the measured parameters for the device we estimate the field effect hole mobility to be ~11cm^2/V-s which is noticeably higher than that of typical organic FETs.

The transfer and output scans for a representative hybrid TG Si NW FET with organic gate insulator are shown in Fig. 2. Despite much thicker dielectric layer devices demonstrate excellent transistor characteristics and also offer significantly reduced hysteresis. From the transfer scans (Fig. 2a) for this device, we extract the current *on/off* ratio, *s-s*, and *gm* as ~10^6, 1.6V/dec, 0.2μS respectively. High on/off ratio exhibited by the device suggests that the gate

can effectively modulate the NW conductance even with a 1µm thick organic dielectric. The peak currents at V_D = -10Vand -15V are 1.9µA and 2.3µA.

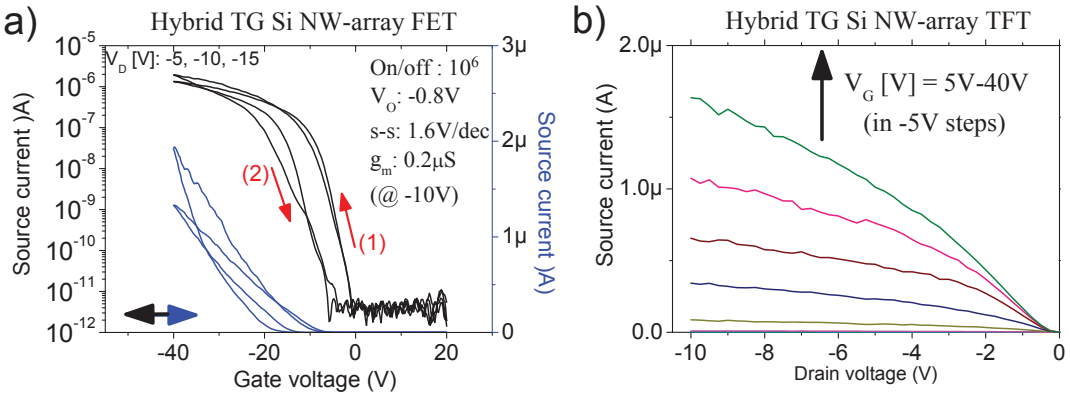

Figure 2 Transistor characteristics for a representative hybrid TG Si NW-array FET a) Transfer characteristics for V_D = -10V and -15V. b) Output scans for the same device measured from V_G = 5V to -40V in -5V steps.

Hole mobility is extracted as follows: the TG channel length and NW density (N) are 10µm and 3NWs respectively. Thus C_{NW} based on the cylinder on infinite plate model for a 1µm thick organic film with low dielectric constant is estimated to be ~0.24fF. So for the channel capacitance of the representative hybrid TG device containing just 3 NWs is ~0.72fF. Using the extracted g_m at V_D = -10V, µ is calculated to be ~28cm^2/V-s, which is substantially higher than that attained in the BG FET with SiO_2 dielectric.

From Fig. 2a the subthreshold slope is estimated as ~1.6V/dec, which suggests low density of interface traps at nanowire/organic dielectric interface during consecutive gate sweeps. Of particular relevance is the hysteresis loop (ΔV_O ~9V) in the transfer scans which is considerably smaller than that of the BG device in Fig. 1a. The relatively small hysteresis may be attributed to the low density of localised states at the semiconductor-dielectric interface.

The output scans (Fig. 2b) also show excellent gate modulation. The device exhibits some contact resistance (at V_D < 2V) which can be explained by the non ohmic contact formation.

In summary we have demonstrated hybrid top-gate nanowire field-effect transistors where the active channel is composed of Si nanowires. The device deposition methods are compatible with solution based fabrication techniques envisioned for printed plastic

electronics. The devices with organic dielectric show excellent transistor characteristics with on/off ratio for10^6, low hysteresis, field effect mobility ~28cm^2/V-s.
The high mobility, and the small hysteresis exhibited by the hybrid TG Si NW-array FETs make solution processable nanomaterials very attractive candidates for printed electronics.

Acknowledgements
The authors thank EPSRC UK for the provided support CASE/CNA/07/79 and grant EP/I017569/1.

References:

BIOGRAPHIC DATA OF DR MAXIM SHKUNOV

Maxim Shkunov studied physics and applied mathematics at Moscow Institute of Physics and Technology and trained at Russian Academy of Sciences (Moscow) prior to receiving his PhD in condensed matter physics from the University of Utah, USA, where he conducted research in ultrafast spectroscopy and laser action in conjugated polymers, microcavities and photonic crystals. He has since developed and evolved his research to encompass charge transport phenomena in organic semiconductors, plastic field-effect transistors, self-assembly at organic/inorganic interfaces, self-organisation with pi-conjugated liquid crystals and polymers, semiconducting nanowires, solution processable nanowire electronics and organic-inorganic hybrid devices. He has 20 years of experience in the field and worked at Cavendish Laboratory (U. Cambridge) and Merck Chemicals (UK). Maxim (co)-authored more than 90 publications, including articles in peer reviewed journals, book chapter and patents. He is now a Lecturer in Nanoelectronics at the Advanced Technology Institute, University of Surrey (UK) with a range of research, teaching, and administrative duties.

ORGANIC AND HYBRID ORGANIC HETEROJUNCTIONS IN ORGANIC ELECTRONICS AND SPINTRONICS APPLICATIONS

S. Braun,[1] L.M. Andersson,[1] P. Sehati,[1] Y.Q. Zhan,[1,2,] M.P. de Jong,[3] M. Fahlman[1*]
[1]*Department of Physics, Chemistry and Biology, Linköping University, Sweden.*
[2]*Microelectronics Department, IT School, Fudan University Shanghai, China*
[3]*MESA+ Institute for Nanotechnology, University of Twente, Enschede, the Netherlands*
E-mail: mafah@ifm.liu.se

Organic electronic and spintronic devices such as solar cells and spin valves are multi-layered devices where their ultimate performance is to a large extent dominated by the electronic processes at interfaces. The relative position of energy levels across a stack of thin organic layers is important for charge/spin injection and exciton separation, and hence for device engineering and optimization. Here we will present some recent results on P3HT and PCBM where we explore the effects of inter- and intra-molecular order at the interface on the $E_{ICT+,-}$ and how these parameters affect exciton dissociation and charge transport [1]. In the latter case P3HT, both in a well ordered state and with temperature induced disorder, is characterized and analyzed in terms of the ICT model, the Gaussian disorder model and a simple polaronic approach consistent with Marcus theory. In a separate set of experiments we explore so-called spinterfaces, where the energy level alignment and spin-polarization of the molecular orbitals of π-conjugated molecules are studied for the Alq_3/Fe and C_{60}/Fe systems. We demonstrate hybridization and exchange coupling between a π-conjugated orbital in Alq_3 molecules adsorbed on the Fe surface. The hybridization results in an Ohmic-like contact and efficient charge injection. Furthermore, the exchange coupling induces spin-polarization of a π-conjugated orbital in Alq_3, which enable the efficient spin injection [2]. For the C_{60}/Fe system, hybridization between the frontier orbitals of C_{60} and continuum states of Fe leads to a significant magnetic polarization of C_{60} π^*-derived orbitals [3].

[1] Harri Aarnio, et al, Adv. Energy Mater, **1**, 792 (2011).
[2] Yiqiang Zhan, et al, Adv. Mater., **22**, 1626 (2010).
[3] T.L.A. Tran, et al, Appl. Phys. Lett., **98,** 222505 (2011).

BIOGRAPHIC DATA OF PROFESSOR MATS FAHLMANN

Personal data:
Date of birth - 22 of June, 1967

Academic preparation:
Undergraduate degree- 1991, Master of Applied Physics and Electrical Engineering (Civ. Ing. Y-linjen)
PhD degree- 1995, Surface Physics and Chemistry
Post-Doc- 1996 - 1998, Department of Physics, The Ohio State University, USA.
Docent- Linköping University, 2000.

Current position:
Professor in Surface Physics and Chemistry at the Department of Physics, Chemistry and Biology (IFM), 2008 - present.

Former positions:
- Professor in Experimental Physics at the Department of Science and Technology, Campus Norrköping, Linköping University, 2005 – 2008.
- Associated professor at the Department of Science and Technology, Campus Norrköping Linköping University, 1999 – 2005.
- Assistant professor at the Department of Physics, Chemistry and Biology, Linköping University 1998-1999.

Current and previous appointments:
- Director of the Division of Surface Physics and Chemistry at IFM, Linköping University, 2008 – present.
- Principal investigator in SUNFLOWER (EU FP7), 2011-2015.
- Principal investigator in HINTS (EU FP7), 2011-2014.
- Principal investigator in MOLESOL (EU FP7), 2010 -2013.
- Principal investigator in ONE-P (EU FP7), 2009-2011.
- Principal investigator in MINOTOR (EU FP7), 2009-2012.
- Director of the division of Physics and Electronics, Department of Science and Technology, Campus Norrköping, Linköping University, 2001- 2005. 2006 (Dec.) – 2007 (July).
- Principal investigator in OFSPIN, (EU FP6), 2007 – 2009.
- Deputy director of the Electronics Engineering, Physics and Mathematical programs at Linköping University, 2007 – 2008.
- Director of the Master of Engineering Programs at the Norrköping Campus, Linköping University, 2003-2006.
- Principal Investigator in LAMINATE (EU FP5), 2003-2005.
- Principal Investigator in COE (Organic Electronics center funded by Swedish Foundation for Strategic Research), 2003-2008.
- Dean of Physics and Electronics Education at Campus Norrköping, Linköping University, 2001-2002.
- Coordinator of Industrial Research in the Center for Advanced Molecular Materials (center funded by Swedish Foundation for Strategic Research), 2000 – 2008.

Commissions of trusts:

- Chairman of the FASM (the Association for Synchrotron Radiation Users at MAX-lab) board, 2004-2006.
- Member of the Board of Directors, National Synchrotron Radiation Laboratory MAX-Lab, Lund, Sweden, 2001 – 2010
- Opponent and committee member on Ph.D. defences; referee in numerous journals, organizer of symposia, spring/summer schools, etc.

Bibliometrics

Field-normalized crown indicator (2003-2010): 1.98

Bibliography data (Career, ISI Web of Knowledge, 2012-03-26):

- 128 items
- h-index: 31
- average citation: 26.2
- Total citations: 3354

See http://www.researcherid.com/rid/A-1524-2009 for complete list.

Part VI: Solar cells / OPV 1

NARROW BANDGAP COPOLYMER DERIVATIVES BASED ON 4*H*-CYCLOPENTA(2,1-B;3,4-B´)DITHIOPHENE UNITS: SYNTHESIS AND PHOTOVOLTAIC PERFORMANCE

D. J. M. VANDERZANDE[1,2], S. VAN MIERLO[1], L. MARIN[1], P. VERSTAPPEN[1], A. HADIPOUR[5], M.J. SPIJKMAN[4], N. VAN DEN BRANDE[3], B. RUTTENS[1], J. KESTERS[1], J. D'HAEN[1], G. VAN ASSCHE[3], D. M. DE LEEUW[4], T. AERNOUTS[5], J. MANCA[1], L. LUTSEN[2], W. MAES[1]

[1] University of Hasselt, Institute for Materials Research (IMO), Agoralaan Bld D, B-3590 Diepenbeek, Belgium

[2] IMEC/ IMOMEC, Wetenschapspark 1, B-3590 Diepenbeek, Belgium

[3] Vrije Universiteit Brussel (VUB), Pleinlaan 2, B-1050 Brussel, Belgium.

[4] Philips Research Laboratories, High Tech Campus 4, 5656 AE Eindhoven, The Netherlands

[5] IMEC, Kapeldreef 75, B-3001 Leuven, Belgium

Organic or polymer solar cells (OSC's) offer a real potential toward their application as a new renewable energy source, as they combine unique features such as potential low cost by large-area fabrication (printing), light weight, solution processability, (semi)transparency and be produced on a flexible substrate.[1] Bulk heterojunction (BHJ) OSC's based on regioregular poly(3-hexyl-thiophene) (P3HT) and [6,6]-phenyl-C_{61} butyric acid methyl ester ($PC_{61}BM$) as active layer donor and acceptor materials, respectively, have achieved reproducible power conversion efficiencies (PCE's) of 4–5%.[1,2] However, one of the main problems associated with the P3HT:$PC_{61}BM$ combination is the mismatch between the OSC absorption window and the terrestrial solar emission spectrum due to the relatively large band gap of the polythiophene donor polymer and the limited absorption width of the material blend. The most popular approach to obtain low bandgap structures is based on alternating copolymerization of (heteroaromatic) donor and acceptor moieties.[1] Incorporating electron rich and electron deficient subunits within one polymer structure produces in this way a significant decrease in the bandgap due to intramolecular charge transfer.

4*H*-cyclopenta[2,1-*b*:3,4-*b'*]dithiophene (CPDT) has emerged as an attractive heterocyclic system for organic photovoltaics (OPV) with good electron-donating properties, a rigid coplanar structure favoring π-π intermolecular interactions, and the possibility of side-chain manipulation to influence solubility (and processability).[3] On the other hand, electron deficient systems such as 2,1,3-benzothiadiazoles (BT),[1,3] thiazolo[5,4-*d*]thiazoles (TzTz),[4] and quinoxalines (Qx)[5] have been introduced as interesting building blocks for integration in OPV devices due to their strong electron-withdrawing properties, high oxidative stability and straightforward synthesis. In our research group, CPDT units have been combined with these electron poor systems in donor-acceptor alternating copolymers. Furthermore blends of the

resulting donor polymers with $PC_{71}BM$ as acceptor have been investigated as active layers in bulk heterojunction OSC's.

High-performance CPDT-based low bandgap copolymers are typically synthesized from symmetrically dialkylated (either branched or linear) CPDT building blocks.[3] Nowadays it is generally accepted that the shape and size of the solubilizing alkyl side chains have a crucial effect on the photovoltaic performances of blends of polymers with fullerenes - affecting stacking properties, the phase separation process and as such the nano-morphology of the blend. To enable a larger variability of solution characteristics of CPDT derivatives a novel synthetic protocol was developed allowing a versatile introduction of different types of side chains (Scheme 1).

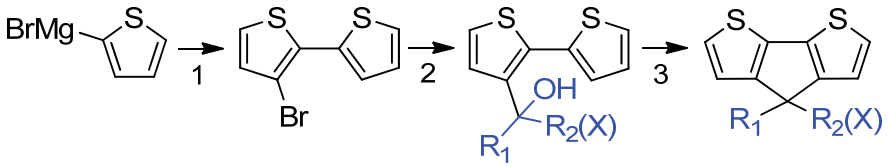

1. 2,3-dibromothiophene, $Pd(dppf)Cl_2$; 2. *n*-BuLi, ketone; 3. H_2SO_4

Scheme 1. Three-step synthetic protocol toward asymmetrically substituted 4*H*-cyclopenta[2,1-*b*:3,4-*b'*]dithiophenes.

A convenient and efficient three-step route toward both symmetrically and non-symmetrically functionalized CPDT's has been developed within our group.[6] Using this method a broad collection of functionalized bridged bithiophenes can smoothly be accessed. Starting from 3-bromo-2,2'-bithiophene, prepared by Kumada coupling of 2-thienylmagnesium bromide with 2,3-dibromothiophene under $Pd(dppf)Cl_2$ catalysis, lithiation and subsequent reaction with dialkyl ketones afforded (non-)symmetrically dialkylated tertiary alcohol derivatives. By means of a Friedel-Crafts type dehydration and cyclization in sulfuric acid medium diluted with octane, these derivatives were converted to the 4,4-dialkyl-CPDT's in satisfactory yield.

A first series of materials were synthesized using one particular CPDT derivative with a branched and a linear alkyl side chain, *in casu* the 4-(2-ethylhexyl)-4-octyl-CPDT. As the most performant CPDT-based copolymer to date is composed of alternating 4,4-bis(2-ethylhexyl)-CPDT and 2,1,3-benzothiadiazole units, affording 5.5% PCE,[3b] we first synthesized the analogous **PCPDT-BT** material. The dibrominated CPDT precursor was combined in a Suzuki polymerization reaction with the BT-bis(boronate) ($Pd(PPh_3)_4$, K_2CO_3, Aliquat, toluene, 80 °C for 3 days), affording a **PCPDT-BT** polymer in 80% yield after successive Soxhlet extractions and precipitation from MeOH (Figure 1).

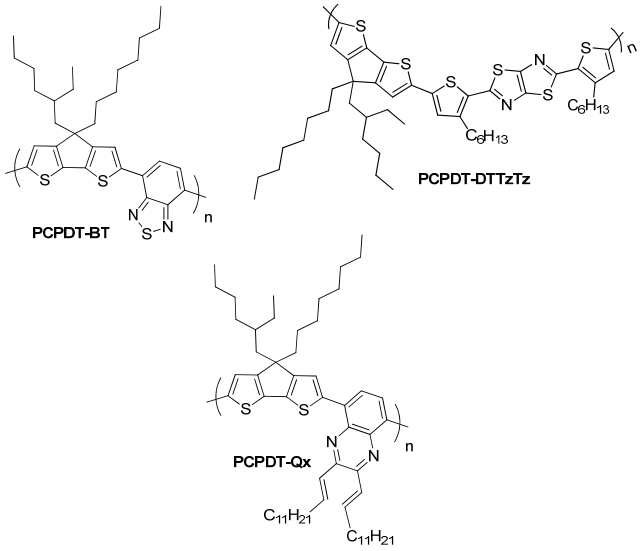

Figure 1. Overview of the synthesized polymers: **PCPDT-BT**, **PCPDT-DTTzTz** and **PCPDT-Qx**.

Toward the synthesis of the second polymer, the CPDT-bis(boronate) was prepared and combined with a dibrominated dithienyl-TzTz precursor[7] under similar Suzuki polycondensation conditions, affording a **PCPDT-DTTzTz** material in 64% yield after a similar work-up (Figure 1). For the electron deficient quinoxaline building block, a monomer with an extended absorption window was prepared by expanding the conjugated system in the vertical direction. Toward the desired **PCPDT-Qx** copolymer (Figure 1), the dibrominated quinoxaline was combined with the bis(trimethylstannyl)-CPDT analogue in a Stille polycondensation reaction. The donor polymers so obtained were blended with $PC_{71}BM$ as an electron acceptor, BHJ OSC's were fabricated and the photovoltaic properties of the devices were investigated. Preliminary non-optimized device results are presented in Table 1.

Table 1. PCE's for the PCPDT-X Copolymers.

Polymer	M_n	PDI	V_{oc}	J_{sc}	FF	PCE (%)
PCPDT-BT	1.3 x 10^4	3.3	0.64	7.44	0.38	1.81
PCPDT-DTTzTz[a]	1.7 x 10^4	2.9	0.58	9.0	0.47	2.43
PCPDT-DTTzTz[b]	1.4 x 10^4	2.4	0.67	11.13	0.54	4.03

[a] *Unpurified polymer.* [b] *Polymer purified by recycling preparative SEC.*

When the **PCPDT-BT** polymer, as obtained after Soxhlet extraction and precipitation (M_n 1.3 x 10^4, PDI 3.3), was blended with $PC_{71}BM$ in a 1:3 w/w ratio and the active layer was spin coated from *o*-dichlorobenzene (with the addition of 1,8-octanedithiol), the resulting solar cell device (ITO/PEDOT:PSS/active layer/Yb/Ag) showed a rather moderate performance with an open circuit voltage (V_{oc}) of 0.64 V, a fill factor (FF) of 0.38, a short-circuit current density (J_{sc}) of 7.44 mA/cm^2, and a resulting PCE of 1.81% under air mass 1.5 global illumination conditions (AM 1.5G; 100 mW/cm^2) (Table 1). Compared to the top **PCPDT-BT**

performance,[3b] the J_{sc} and FF are not at the required level. The **PCPDT-DTTzTz** copolymer, as obtained after Soxhlet extraction and precipitation (M_n 1.7 x 10^4, PDI 2.9), was also blended with $PC_{71}BM$ in a 1:3 w/w ratio. The active layer was spin coated from chlorobenzene (without any additive) and the resulting solar cell (ITO:PEDOT/PSS:active layer:Ca-Ag) showed a slightly better performance with a V_{oc} of 0.58 V, a FF of 0.47, a J_{sc} of 9.0 mA/cm^2, and a resulting PCE of 2.43% (Table 1). As polymer molecular weight and purity are essential parameters influencing the opto-electronic properties and the final solar cell outcome, purification and fractionation of the **PCPDT-DTTzTz** copolymer were pursued by recycling preparative SEC. The solar cell device, prepared in an identical way, obtained from a purified batch of the polymer (M_n 1.4 x 10^4, PDI 2.4) showed a significant increase in PCE till 4.03% by noticeable improvement of all three parameters (V_{oc} 0.67 V, FF 0.54, J_{sc} 11.13 mA/cm^2; Table 1). The thin-film transistor field-effect mobility, calculated in the linear regime, was found to be 1.0 x 10^{-3} cm^2/Vs, one order of magnitude higher than reported values in literature for different TzTz-based copolymers,[4a] and hence in good agreement with the photovoltaic properties. The **PCPDT-DTTzTz** polymer showed semi-crystalline behavior, as evidenced by DSC and XRD experiments[8].

In conclusion a series of novel low bandgap copolymers with asymmetrical alkyl substitution on the cyclopentadithiophene building block **PCPDT-X** (X = 2,1,3-benzothiadiazole, thiazolo[5,4-*d*]thiazole or quinoxaline**)**, have been successfully synthesized, by Suzuki and Stille polycondensation protocols. Preliminary investigations of these materials in organic solar cells have afforded a power conversion efficiency of 4.03% for the **PCPDT-DTTzTz**:$PC_{71}BM$ combination, without extensive optimization work. A noticeable increase in efficiency was obtained upon purification of the polymer by recycling SEC.

Acknowledgement. The authors gratefully acknowledge the IWT for their financial support via the SBO-project 060843 ”PolySpec”. We also acknowledge the ONE-P project for the financial support from the European grant agreement n° 212311 related to the Hasselt-Eindhoven collaboration.

(1) (a) Bundgaard, E.; Krebs, F. C. *Sol. Energy Mater. Sol. Cells* **2007**, *91*, 954. (b) Thompson, B. C.; Fréchet, J. M. J. *Angew. Chem. Int. Ed.* **2008**, *47*, 58. (c) Boudreault, P. T.; Najari, A.; Leclerc, M. *Chem. Mater.* **2011**, *23*, 456.

(2) Dang, M. T.; Hirsch, L.; Wantz, G. *Adv. Mater.* **2011**, *23*, 3597.

(3) (a) Mühlbacher, D.; Scharber, M.; Morana, M.; Zhu, Z.; Waller, D.; Gaudiana, R.; Brabec, C. *Adv. Mater.* **2006**, *18*, 2884. (b) Peet, J.; Kim, J. Y.; Coates, N. E.; Ma, W. L.; Moses, D.; Heeger, A. J.; Bazan, G. C. *Nat. Mater.* **2007**, *6*, 497. (c) Bijleveld, J. C.; Shahid, M.; Gilot, J.; Wienk, M. M.; Janssen, R. A. J. *Adv. Funct. Mater.* **2009**, *19*, 3262. (d) Coffin, R.

C.; Peet, J.; Rogers, J.; Bazan, G. C. *Nat. Chem.* **2009**, *1*, 657. (e) Tsao, H. N.; Cho, D. M.; Park, I.; Hansen, M. R.; Mavrinskiy, A.; Yoon, D. Y.; Graf, R.; Pisula, W.; Spies, H. W.; Müllen, K. *J. Am. Chem. Soc.* **2011**, *133*, 2605. (f) Manceau, M.; Bundgaard, E.; Carlé, J. E.; Hagemann, O.; Helgesen, M.; Søndergaard, R.; Jørgensen, M.; Krebs, F. C. *J. Mater. Chem.* **2011**, *21*, 4132.

(4) (a) Jung, I. H.; Yu, J.; Jeong, E.; Kim, J.; Kwon, S.; Kong, H.; Lee, K.; Woo, H. Y.; Shim, H.-K. *Chem. Eur. J.* **2010**, *16*, 3743. (b) Lee, S. K.; Cho, J. M.; Goo, Y.; Shin, W. S.; Lee, J.-C.; Lee, W.-H.; Kang, I.-N.; Shim, H.-K.; Moon, S.-J. *Chem. Commun.* **2011**, 1791. (c) Subramaniyan, S.; Xin, H.; Sunjoo Kim, F.; Shoaee, S.; Durrant, J. R.; Jenekhe, S. A. *Adv. Energy Mater.* **2011**, *1*, 854. (d) Zhang, M.; Sun, Y.; Guo, X.; Cui, C.; He, Y.; Li, Y. *Macromolecules* **2011**, *44*, 7625. (e) Helgesen, M.; Madsen, M. V.; Andreasen, B.; Tromholt, T.; Andreasen, J. W.; Krebs, F. C. *Polym. Chem.* **2011**, *2*, 2536.

(5) (a) Wang, E.; Hou, L.; Wang, Z.; Hellström, S.; Zhang, F.; Inganäs, O.; Andersson, M. R. *Adv. Mater.* **2010**, *22*, 5240. (b) Lee, S. K.; Lee, W.-H.; Cho, J. M.; Park, S. J.; Park, J.-U.; Shin, W. S.; Lee, J.-C.; Kang, I.-N.; Moon, S.-J. *Macromolecules* **2011**, *44*, 5994. (c) He, Z.; Zhang, C.; Xu, X.; Zhang, L.; Huang, L.; Chen, J.; Wu, H.; Cao, Y. *Adv. Mater.* **2011**, *23*, 3086. (d) Zhang, Y.; Zou, J.; Yip, H.-L.; Chen, K.-S.; Zeigler, D. F.; Sun, Y.; Jen, A. K.-Y. *Chem. Mater.* **2011**, *23*, 2289.

(6) Van Mierloo S.; Adriaensens, P.; Maes, W.; Lutsen, L.; Cleij, T. J.; Botek, E.; Champagne, B.; Vanderzande, D. J. *J. Org. Chem.* **2010**, *75*, 7202.

(7) Van Mierloo, S.; Chambon, S.; Boyukbayram, A. E.; Adriaensens, P.; Lutsen, L.; Cleij, T. J.; Vanderzande, D. *Magn. Reson. Chem.* **2010**, *48*, 362.

(8) Van Mierloo S., Hadipour A., Spijkman M. J, Van den Brande N., Ruttens B., Kesters J., D'Haen J., Van Assche G., de Leeuw D. M., Tom Aernouts T., Manca J., Lutsen L., Vanderzande D. J. and Maes W. *Chem. Mat.* **2012**, *24*, 587−593

BIOGRAPHIC DATA OF PROFESSOR DIRK VANDERZANDE

Name: Dirk Vanderzande
Address: University of Hasselt, Institute of Material Research (IMO), Agoralaan, Building D, B-3590 Diepenbeek, Belgium
Tel.:+32 1126.83.21, Fax: +321126.83.01,
E-mail: dirk.vanderzande@uhasselt.be
Born: 12-6-1957, Genk, Belgium.

Master in Chemistry at KULeuven in 1979;
PhD at KULeuven in 1986 in Organic synthesis and studies of mechanisms of thermal induced rearrangement reactions of ortho-quinodimethane systems.

Permanent position as senior post-doc researcher since January 1987 at the University of Hasselt (Belgium) joining the research group "Organic and Polymeric Chemistry". Expert domains: Organic Synthesis, Polymer Synthesis, Advanced Organic and Polymeric Materials for Optical and Electronic applications.
1988: Start up of his research in the field of conjugated polymers. Two topics were started. The first topic relates to low band gap conjugated polymers, their synthesis, structural characterization and the underlying polymerization mechanisms. The second topic relates to the polymerization behavior of p-quinodimethane systems towards the synthesis of precursors for conjugated polymers.
1992: Appointed as assistant professor at U Hasselt.
1992: A new route was developed and optimized at the level of synthetic routes towards the monomer, the polymerization conditions and conditions of conversion of the precursor polymer.
1995: appointed as associated professor at U Hasselt.
1997 Concerning latter topic important breakthroughs were achieved and the so developed methodologies extended towards other systems. Start of material development specific towards polymer LEDs in collaboration with Philips and Covion.
1999: Appointed as "hoogleraar" at U Hasselt.
2000: Extending the efforts of material development towards applications of conjugated polymers in thin film FET transistors and organic solar cells. Start of studies related to defect structures in conjugated polymers.
2001: Start of association of the group as a division IMOMEC in IMEC vzw.
2003: Appointed as full professor (gewoon hoogleraar) at U Hasselt.
2003: New route was discovered towards Poly(Thienylene Vinylene) via the so called dithiocarbamate route which is under further investigation;
Since 1th of October 2010 Director of the institute imo-imomec at UHasselt.
Full partner in many EC research projects in collaboration with industry over the last 10 years.
More than 226 refereed papers in international journals.
16 original patents in the field of synthetic routes towards conjugated polymers.

The abstract of the lecture Dr. Hoppe

entitled

“Imaging methods for quality control and degradation analysis of organic solar cells”

was not available to the editorial deadline.

The abstract of the lecture Dr. Troshin

entitled

“Novel methods for controlling the quality and evaluation of the degradation profiles of conjugated polymers designed for photovoltaic applications”

was not released for publication.

HIGHLY EFFICIENT FLEXIBLE PLASTIC SOLAR CELLS MADE BY A REEL-TO-REEL COATING PROCESS

M. Schrödner, L. Blankenburg, K. Schultheis, H. Schache, S. Sensfuss

TITK Rudolstadt, Dept. Functional Polymer Systems and Physical Research
Breitscheidstr. 97, 07407 Rudolstadt, Germany
e-mail: schroedner@titk.de

Summary

We could demonstrate the feasibility of flexible polymer thin film bulk-heterojunction solar cells with photo-conversion efficiencies (PCE) of more than 3 % using a reel-to-reel slot-die coating process for the preparation of the hole transport and the photoactive layer. The photoactive material was a blend of poly(3-hexylthiophene) (P3HT) as donor and indene-C60 bisadduct (ICBA) as acceptor, which enables more than 6 % PCE on glass. Using flexible PET foils with ITO as substrate we achieved a maximum PCE of 4.55 % by spin coating and 3.2 % by reel-to-reel coating, which are with respect to substrate and coating technique among the highest reported PCE values in the literature so far.

1. Introduction

Organic thin film solar cells have made much progress during the last years. Since the discovery of the ultrafast charge transfer in p-conducting polymer/fullerene composites by Sariciftci and Heeger in 1992 [1] the power conversion efficiency (PCE) of bulk hetero-junction solar cells was increased up to 10 % [2]. These efficiencies together with the possibility to use low cost materials and low cost reel-to-reel coating or printing techniques enable costs of production of 0.63 €/Wp and below [3] making polymer solar cells competitive to other organic or inorganic solar cell devices. But there is still a lack in efficiency between best laboratory cells and flexible solar cells which had been made in a reel-to-reel (R2R) process. Best flexible organic solar cells on foils made by spin coating have an efficiency of 3.66 % [4]. Using R2R-processing techniques the maximum efficiency reported so far is 2.33 % only [5]. So, it is a challenge to improve R2R-processed flexible solar cells markedly to close the gap to the best laboratory cells on glass.

Several continuously working printing and coating techniques like gravure and flexographic printing [6, 7], slot-die and knife coating [8-11] were examined with respect to polymer solar cell production.

In this work we demonstrate flexible polymer solar cells with a PCE of more than 3 % made by two reel-to-reel coating steps. The photoactive system is poly(3-hexylthiophene) (P3HT) as donor and bisindene fullerene (ICBA) as acceptor, which was shown to enable more than 6% PCE on glass [12-14].

2. Materials

Ready to use P3HT/ICBA solution PV2000 and regioregular P3HT (Plexcore OS 2100) were obtained from Plextronics. ICBA was also synthesized by ourselves via a [4+2]-cycloaddition reaction of fullerene and bisindene. PEDOT:PSS (poly(3,4-ethylenedioxy-thiophene):polystyrene-sulfonate) was obtained from H. C. Starck (Clevios PH and Clevios 4083). Alternately to PEDOT:PSS also an hole-transport material from Plextronic (Plexcore PV 2000 HTL ink) was tested. All solutions were filtered before use.

ITO coated PET foil (125 µm thick) was purchased from Southwall. The ITO thickness was about 100 nm and the surface resistance 45 Ω_{sq}. ITO glasses were obtained from Merck (13 Ω_{sq}).

I-V curves were recorded with a Keithley SMU 2400 Source Meter by illuminating the cells from the ITO side with 100 mW/cm² white light from a Steuernagel solar simulator to realise AM 1.5 conditions. The illuminating light was calibrated using a silicon reference cell from ISE (Freiburg). All cells were measured in a glove box.

3. Results

3.1 Solar cells made by spin coating

For optimisation of the layer setup solar cells were first processed on ITO coated glass. The photoactive layer was made from the Plexcore PV 2000 ink containing regioregular poly(3-hexylthiophene) (P3HT) and the fullerene derivative ICBA as electron acceptor. Compared with the mostly used fullerene acceptor [6,6]-phenyl-C61-butyric acid methyl ester (PCBM) the ICBA has a 0.17 eV higher LUMO level resulting in a higher open circuit voltage V_{OC} > 0.8 V. The optimum thickness of the photoactive layer was about 200 nm. Annealing up to 170 °C leads to an improved PCE.

The hole transport layer (HTL) between ITO anode and photoactive layer was made from PEDOT:PSS (Clevios 4083) or from the Plexcore PV 2000 HTL ink, which were annealed after spin-coating at 120 °C and 150 °C respectively. The cathode was made by thermal evaporation of Ca (15 nm) and Al (50 nm). The complete layer sequence is ITO/HTL/P3HT:ICBA/Ca/Al.

The resulting solar cells reach PCE values up to 5.8 % (I_{SC} = 10.3 mA/cm², V_{OC} = 0.823 V; FF = 0.68), Fig. 1. Besides the high open circuit voltage also high fill factors up to 0.71 were observed.

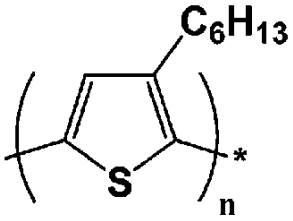

P3HT

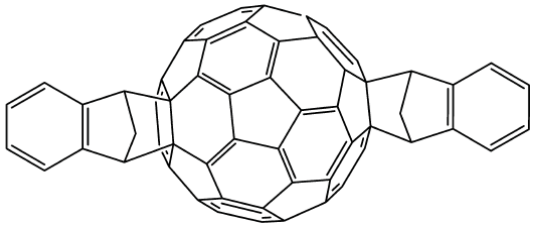

indene C_{60} bisadduct (ICBA)

Flexible solar cells on ITO/PET foils were processed analogous to glass cells with the exception that Clevios PH was used instead of Clevios 4083 as HTL. As expected the PCE is lower compared to cells on glass, which is mainly attributed to a lower current. The maximum PCE was 4.55 % (I_{SC} = 8.56 mA/cm², V_{OC} = 0.804 V; FF = 0.66), Fig. 1.

The choice of the HTL material (PEDOT:PSS *vs*. Plexcore PV2000 HTL ink) had nearly no effect on the device performance.

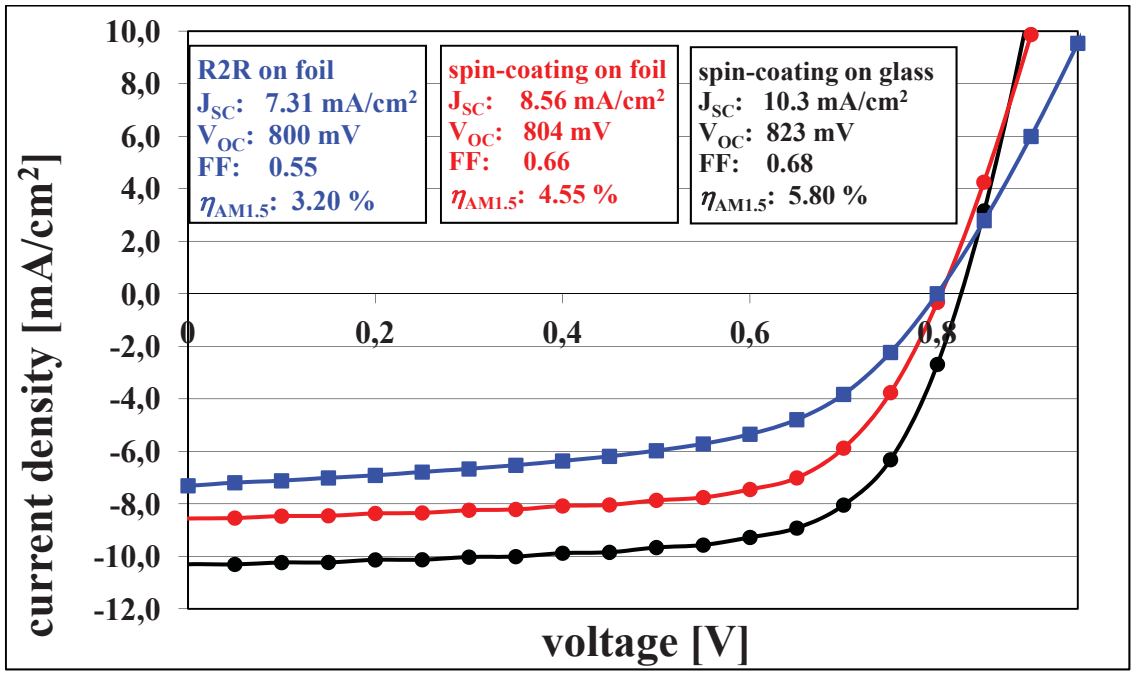

Fig. 1: J-V-characteristics of P3HT:ICBA solar cells made on glass and foil by spin coating (circles) and reel-to-reel coating (squares)

3.2 Solar cells made by reel to reel coating

Taking advance of the results from the spin coating experiments R2R-coating of the photoactive layer and the hole-transport layer was investigated. The reel to reel coater LBA 200 used for these experiments has a maximum web width of 200 mm and can be equipped with several slot-die casters for application of the coating fluid (Fig. 2). By this coating technique the fluid is forced through a slot which allows an accurate adjustment of the wet film thickness by flow rate and web speed. The lips of the die are placed some ten micrometers above the web surface so that a stable meniscus is formed. The stability of the meniscus is determined by the coating window which depends on ink properties (viscosity, surface tension) and process parameters (web speed, lip design).

PEDOT:PSS was coated from a Clevios PH dispersion diluted 1:1 by isopropyl alcohol at a web speed of 2 m/min and fluid feed rates of 1.2 ml/min for 40 mm coating width and 2.1 ml/min for 7 cm coating width. Drying was done by infrared radiation followed by a hot air dryer (90°C). The thickness of the resulting layer was 98 nm.

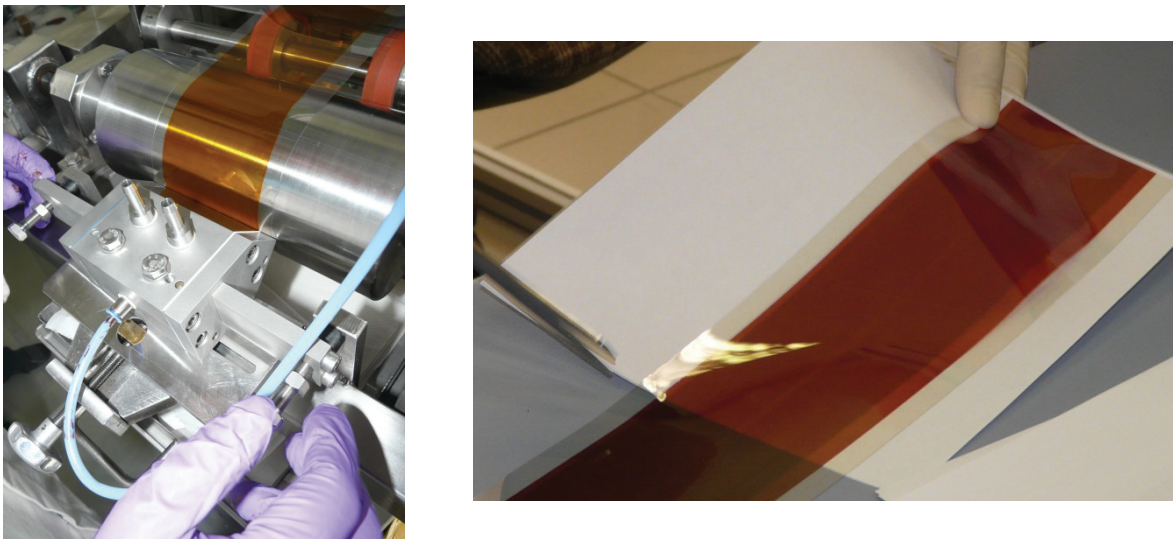

Fig. 2: Application of the photoactive ink with the slot-die coater and cutting samples from the coated foil for preparation of solar cells

The photoactive layer was coated from a 3 wt.% solution of P3HT (Plexcore OS 2100) and ICBA (ratio 1:0.8). The solvent was a mixture of o-dichlorobenzene and chloroform which allows a fast drying before the web is deflected from the horizontal to a perpendicular direction for the first time. The layers were only dried by mild heating at 30°C. The web speed (1 m/min) together with feed rates of 0.3 ml/min at 40 mm width and 0.55 ml/min at 70 mm width gives resulting layer thicknesses of between 220 nm and 250 nm. After drying

pieces (5 x 5 cm²) were cut from the coated foil (Fig. 2) and annealed at temperatures up to 170°C.

Thereafter Ca and Al were evaporated as cathode and the cells were measured as described above. The maximum PCE obtained for these reel-to-reel processed cells was 3.2 % (Fig. 1) which is the highest reported yet.

4. Discussion

As can be seen in Fig. 1 there is a loss of efficiency of P3HT/ICBA solar cells when the substrate is changed from ITO/glass to ITO/foil and again when the spin coating technique is replaced by reel-to-reel coating. The first drop is known from former experiments and from the literature [11, 15] and can be ascribed to the lower surface conductivity of ITO on foil compared to ITO on glass resulting in a higher series resistance.

Changing layer processing from spin to reel-to-reel coating the losses are linked equally with a decrease of the short circuit current and the fill factor whereas the values of the open circuit voltage remain nearly unaffected. This is an indication that the morphology of the photoactive layer is quite different from those made by spin coating. The reason for this is not clear yet, but may be connected with different properties of the photoactive materials used (commercial Plexcore PV 2000 for spin coating vs. self-made P3HT/ICBA solutions for reel-to-reel coating). Moreover, addition of chloroform to the coating solution could also be counterproductive for the development of an optimised morphology because of a faster drying kinetics.

So there is still some space and need for further improvements to overcome the 4 % hurdle also with reel-to-reel coated solar cells on plastic foils. In combination with alternative solution processable materials for the electrodes together with new cell concepts (inverse, ITO free) a complete reel-to-reel processing with high through-puts up to some thousand m²/h should enable low production costs and make polymer solar cells competitive.

5. Conclusions

We could demonstrate the feasibility of flexible polymer thin film bulk-heterojunction solar cells with efficiencies of more than 3 % using a reel-to-reel die-coating process for the preparation of the HTL and the photoactive layer. The maximum PCE achieved so far is more than half the value obtained with the same materials on glass by spin coating and it is about 70 % the value obtained by spin coating on the same plastic substrate. Nonetheless both the PCE values of polymer solar cells on plastic foil made by spin-coating (4.55 %) and reel-to-reel coating (3.2 %) are the highest reported in the literature up to now.

Further improvement of the PCE of large area flexible polymer solar cells is a challenging task for future technology development as well as increasing the through-put up to some thousands of square meters per hour and replacing all steps which are not compatible to reel-to-reel processing.

Acknowledgement

Financial support from the Thuringian Ministry TMWAI (2004 WI0282), from the German Federal Ministries BMBF (project "SonnTex", 03X3518A) and BMWi (IW061016; 1136/03, VF071005, IW082026, VF090063 and KA0406302DA7) is gratefully acknowledged.

References

[1] N. S. Sariciftci, L. Smilowitz, A. J. Heeger, F. Wudl, Science 258 (1992) 1474

[2] M. A. Green, K. Emery, Y. Hishikawa, W. Warta and E. D. Dunlop, Prog. Photovolt. Res. Appl. 2012, 20, 12

[3] N. Espinosa, M. Hösel, D. Angmo and F. C. Krebs, Energy Environ. Sci. 2012, 5, 5117

[4] K.-H. Tsai, J.-S. Huang, M.Y. Liu, C.-H. Chao, C.-Y. Lee, S.-C. Hung, C.-F. Lin, J. Electrochem. Soc. 156(10) (2009) B1188-B1191

[5] F.C. Krebs, S. A. Gevorgyan, J. Alstrup, J. Mater Chem. 2009, 19, 5442-5451

[6] M.M. Voigt, R.C.I. Mackenzie, C.P. Yau, P. Atienzar, J. Dane, P.E. Keivanidis, D.D.C. Bradley, J. Nelson, Sol. Energy Mater. Sol. Cells 95 (2011) 731-734.

[7] P. Kopola, T. Aernouts, S. Guillerez, H. Jin, M. Tuomikoski, A. Maaninen, J. Hast, Sol. Energy Mater. Sol. Cells 94 (2010) 1673-1680

[8] L. Blankenburg, K. Schultheis, H. Schache, S. Sensfuss, M. Schrödner, Sol. Energy Mater. Sol. Cells 93 (2009) 476-483.

[9] F.C. Krebs, Sol Energy Mater Sol Cells (2009) **93**, 465.

[10] Wengeler, L., et al., Chem Eng Process (2011) **50**, 478.

[11] Y. Galagan, I.G. de Vries, A.P. Langen, R. Andriessen, W.J.H. Verhees, S.C. Veenstra, J.M. Kroon, Chem. Eng. Process.: Process Intensification 50(5-6) (2011) 454-461

[12] Y. He, H.-Y. Chen, J. Hou, Y. Li, J. Am. Chem. Soc. 132 (2010) 1377-1382

[13] G. Zhao, Y. He and Y. Li, Adv. Mater. 2010, 22, 4355-58

[14] Y. Sun , C. Cui, H. Wang and Y. Li, Adv. Energy Mater. 2011, 1, 1058

[15] M. Al-Ibrahim, H.-K. Roth, U. Zhokhavets, G. Gobsch, S. Sensfuss, Solar Energy Mater. & Solar Cells 85 (2005) 13-20

BIOGRAPHIC DATA OF DR MARIO SCHRÖDNER

born: 1958 in Burgstaedt (Saxonia, Germany)

studies: Physics at the Leipzig University, 1979-1984, diploma degree

PhD 1989 at Leipzig University

ESR spectroscopy on radiation induced radicals

1988-1995 **scientific assistant at the Technical University of Leipzig**

- intrinsically conducting polymers;
- laser processing of polymers for applications in micro system technologies

1995- now **Thuringian Institute of Textile and Plastics Research (TITK) in Rudolstadt**

- polymer electronics, photovoltaics and actuators
- laser micro machining of polymers

Part VII: Materials and technologies 3

INTERFACE ENGINEERING AND ELECTRONIC FUNCTIONALITY VIA MOLECULAR SELF-ASSEMBLY

M. HALIK

University Erlangen-Nürnberg, Organic Materials & Devices – OMD, Department of Materials Science, Martensstrasse 07, D-91058 Erlangen, Germany

Functionalized molecules that organize to self-assembled monolayers (SAMs) are gaining importance in organic electronic devices. They are fully compatible with flexible substrates, are amenable to low-cost processing, and show reliable film-forming behavior [1]. Starting from auxiliary layers, which improve and modify surfaces and interfaces in traditional thin-film devices, the applications of SAMs develop towards molecular scale electronics. Hybrid dielectrics composed of tiny oxide layers and self-assembled molecules provide low-voltage device operation and control the molecular orientation of subsequently deposited organic semiconductors [2,3]. By adjusting the molecular dipole of such SAM molecules, the threshold voltage in organic transistors can be tuned [4]. With multifunctional molecules, in which several layer functions of a device are implemented, self-assembled monolayer field effect transistors (SAMFETs) can be realized with p- and n-type transport [5]. Detailed studies on the impact of SAM morphology to the device performance indicate that a balance between dense surface packaging, optimized ππ-interaction and reduced leakage current can be realized by mixed SAMs and the stoichiometric control of the composition of different SAM-forming molecules [6]. A theoretical approach to describe the transport in SAMFET devices will be presented. Finally, an example of SAMs in organic solar cells will document the general potential of the self-assembly approach [7].

[1] M. Halik and A. Hirsch, Adv. Mater. 23 (2011), 2689-2695.

[2] H. Klauk, et al., *Nature* 445 (2007) 745 – 748.

[3] M. Novak, et al., Appl- Phys. Lett. 98 (2011), 093302.

[4] A. Y. Amin, et al., Langmuir 27 (2011), 15340-15344.

[5] M. Novak, et al., Nano Letters 11 (2011), 156-159.

[6] A. Rumpel, et al., Langmuir 27 (2011), 15016-15023.

[7] T. Stubhan, et al., Advanced Energy Materials (2012), DOI: 10.1002/aenm.201100668

BIOGRAPHIC DATA OF PROFESSOR MARCUS HALIK

Marcus Halik
Prof. Dr. rer. nat., Dipl.-Chem.

geboren am: 13.01.1971 in Heiligenstadt

Email: Marcus.Halik@ww.uni-erlangen.de
Web: http://www.omd.uni-erlangen.de

Education

09/1990 – 07/1995	Study of Chemistry at the Technischen Hochschule Leuna-Merseburg and Martin Luther University Halle-Wittenberg
09/1995 – 10/1998	Dissertation: "*2,2-Difluor-1,3,2-(2H)-dioxaborine als Bausteine zur Darstellung von langwellig absorbierenden Methin-farbstoffen*" at the Martin-Luther-University Halle-Wittenberg

Scientific Career

03/1999 – 03/2000	Post-Doc with Prof. Dr. S.R. Marder, University of Arizona (USA),
04/2000 – 08/2005	Engineer - Infineon Technologies AG
09/2005 -	W2-Professur für Polymerwerkstoffe (Organic Materials & Devices – OMD) at the Institute of Polymer Materials at the Friedrich-Alexander University Erlangen-Nürnberg

FUNCTIONAL OLIGOTHIENYLENEVINYLENE-BASED MATERIALS FOR OPTOELECTRONICS

F. LANGA*; R. CABALLERO; A. ALJARILLA, L. LOPEZ-ARROYO; M. URBANI; B. PELADO; P. DE LA CRUZ

Instituto de Nanociencia, Nanotecnología y Materiales Moleculares. Universidad de Castilla-La Mancha. Campus de la Fábrica de Armas, 45071-Toledo (Spain)

Linear π-conjugated oligomers with well-defined chemical structures have been used as molecular wires in molecular electronics or nanoscopic systems; among the different π-conjugated oligomers, oligothienylenevinylene oligomers (nTVs) are excellent wires besides good electron donors. Here, we will report on the synthesis and properties of some new derivatives (Figure 1) were nTVs behave as wires or electron donors in donor-bridge-acceptor linking porphyrins and fullerenes, were the phophysical events were studied, or used as dyes in dye sensitized solar cells, acceptor-bridge-acceptor or donor-bridge-donor systems, studying the mixed valence systems.

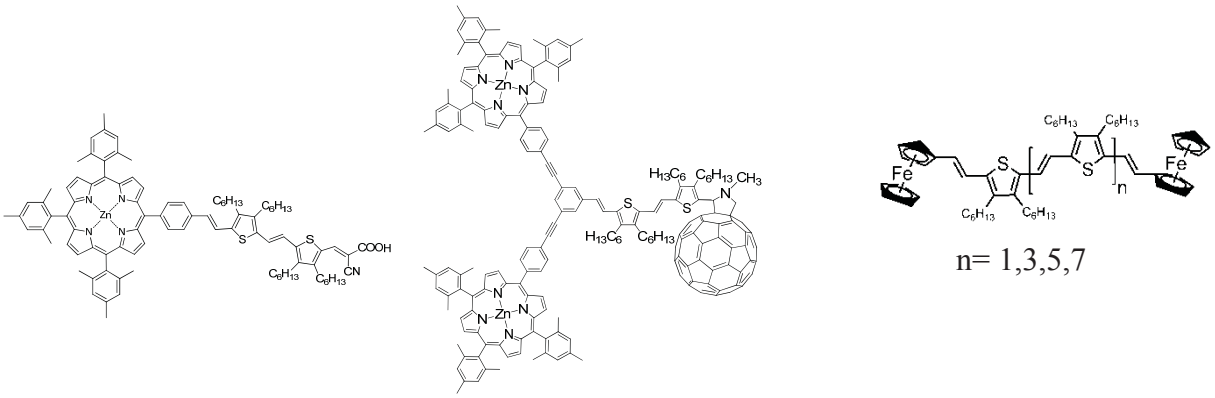

Figure 1

References:

E. Mª Barea, R. Caballero, F. Fabregat-Santiago, P. de la Cruz, F. Langa, J. Bisquert. *ChemPhysChem* 2010, 11, 245.

M. Urbani, B. Pelado, P. de la Cruz, K. Yamanaka, O. Ito, F. Langa, *Chem. Eur. J.* 2011, 17, 5432.

S. Rodríguez, R. González, M. C. Ruiz Delgado, R. Caballero, P. De la Cruz, F. Langa, J. T. López-Navarrete, J. Casado. *J. Am. Chem. Soc*. 2012 (in press).

Maxence Urbani, Kei Ohkubo, Shafiqul D. M. Islam, Shunichi Fukuzumi, Fernando Langa. *Chem. Eur. J.* 2012 (in press).

BIOGRAPHIC DATA OF PROFESSOR FERNANDO LANGA

Prof. Fernando Langa is Professor or Organic Chemistry at Univ. de Castilla-La Mancha (Spain) since 2002. Graduate of the University Complutense of Madrid (UCM), he worked as a postdoctoral fellow at University of Dundee (Scotland). After joining (1990) the Organic Chemistry Department at the University of Castilla-La Mancha (Campus of Toledo) as Assistant Professor, he has been Visiting Professor at the University of Paris-Sud (France) and later, in 1997, at the Institute for Polymers and Organic Solids (IPOS) at the University of California, Santa Barbara (UCSB). He is actually Director of the Institute for Nanoscience, Nanotechnology and Molecular Materials of UCLM at Toledo.

His research interests span a range of targets with emphasis on the chemistry of carbon nanostructures such as fullerenes, carbon nanotubes, graphene, π-conjugated systems as molecular wires, and electroactive molecules, in the context of electron-transfer processes, photovoltaic applications, and nanoscience.

He is editor of the book “Fullerenes: Principles and Applications” (Royal Society of Chemistry) as well as author of several book chapters and more than 130 publications in international journals.

INORGANIC AND ORGANOMETALLIC LOW COST DOPANTS FOR TRANSPORT LAYERS IN ORGANIC ELECTRONIC DEVICES

GUENTER SCHMID[1], JAN HAUKE WEMKEN[1], ANNA MALTENBERGER[1], MARINA A. PETRUKHINA[2], THOMAS DOBBERTIN[3], ARNDT JAEGER[3]

[1]Siemens AG, Guenther-Scharowsky-Strasse 1, 91058 Erlangen

[2]Department of Chemistry, State University of New York University, Albany, NY 12222

[3]Osram Opto Semiconductor, Wernerwerks-Strasse 2, 93049 Regensburg

Highly conductive transport layers are one of the technical prerequisites to manufacture organic light emitting diodes (OLEDs) with high luminous efficacies above 50 lm/W. The conductivity is usually enhanced by doping of the organic hole or electron conductor host material. In the class of inorganic and organometallic compounds, the electron withdrawing or donating properties can be varied in a very large range.

In the presentation, we show a structure-property relationship within a series of p-dopants based on organometallic Lewis-acids. The conductivity enhancement of the hole conductor was balanced to other important OLED requirements, such as cost, transparency and off-state-appearance. The fundamental properties of the doped layers were characterized by current-voltage measurements, impedance, UV/Vis and photoluminescence spectroscopy. The maximum conductivity was found to be in the range of 10^{-4} to 10^{-3} Scm^{-1} without a significant additional absorption owing to a charge transfer band or the radical cation of the host material.

The selected dopant was incorporated into a white OLED stack. Luminous efficacy and lifetime data will be presented.

The synthetic depth of the preparation of the dopants determines its cost and thus, its contribution to an OLED product. The compounds were prepared in large quantities from readily available basic chemicals in only two steps. The compounds were characterized by standard chemical analytics and X-ray crystallography. Molecular modeling supported the course of Lewis acidity within the series of compounds.

BIOGRAPHIC DATA OF DR GÜNTER SCHMID

Principal Research Scientist

Global Technology Field Organic Electronics

Dr. Günter Schmid is a Principal Research Scientist at Corporate Technology of Siemens AG in the global technology field “Organic Electronics”. His current focus is the material development of organic light emitting diodes for lighting applications. He earned his PhD degree from the University of Ulm (Germany) in 1993 and joined 1994 the Laboratory for Molecular Structure and Bonding at the Texas A&M University for a postdoctoral position. From 1996 to 1999 he developed organic dielectrics for the application in silicon based semiconductors. Since 1999 organic electronics became his main field of interest, first as project manager for ultra low cost electronics at Infineon Technologies AG until 2005 and second at his current position.

Hydrogen-bonded Indigoids and Acridones: Highly Ordered Semiconductors for High Performance Organic Electronics

Mihai Irimia-Vladu[1,*], Eric Glowacki[1], Gundula Voss[1], Lucia Leonat[2], Uwe Monkowius[1], Günther Schwabegger[1], Zeynep Bozkurt[3], Helmut Sitter[1], Siegfried Bauer[1] and Niyazi Serdar Sariciftci[1]

[1]*Johannes Kepler University Linz, Austria*

[2]*Polytechnica Bucharest, Romania*

[3]*Sabanci University, Turkey*

[*]Corresponding author: Mihai.Irimia-Vladu@jku.at

The burgeoning field of organic electronics is driven by the notion of mass-producing cheap and sustainable electronic devices. Future large-scale application of organic electronics should also focus on sustainability in order to address the current problem of electronic waste. In our recent activity we considered investigating natural and nature inspired materials for organic electronics applications[1-4]. We have demonstrated that nature is an immense reservoir of inexpensive materials that are suitable for the fabrication of organic electronic devices operating at state-of-the-art level[1-4].

Our investigation of naturally occurring pigments revealed interesting properties of those materials, such as strong dipolar interaction, *i.e.* hydrogen bonding. This type of chemical bond is a stronger dipolar force than typical van der Waals interaction featured by synthetic π–conjugated chromophores currently employed in organic electronics. H-bonding is ubiquitous in natural systems, being responsible for the unique properties of water and the forces holding together DNA and RNA strands, three of the systems that allows the existence of life on Earth. The consequence of H-bonding is the presence of highly ordered organic films that have a high dielectric constant. This long range intermolecular interaction tremendously influences the dynamics of photogenerated excited states in such molecules. Indigo and its synthetic derivatives represent an interesting class of organic semiconducting materials. Indigo for example is among the very few known blue-colored chromophores of truly natural-origin. Indigo (extracted from plants) and 6,6'-dibromoindigo (Tyrian purple, extracted from sea shells) have been exploited for thousands of years as valuable dyestuffs. We recently found that vacuum-evaporated indigo and Tyrian purple films show high ordering with a crystalline texture featuring a single preferential orientation and have high dielectric constants (in the range of 4–6). These properties are responsible for those materials displaying high carrier mobilities. We measured for example, high and well-balanced field effect mobility of ~ 0.4 cm^2/Vs for both electrons and holes for

OFET devices with Tyrian purple channel. Tyrian purple was also remarkable for its air-stable transport of both electrons and holes, a consequence of its deep LUMO level of ~ -4.0 eV.

With the knowledge that the exciton binding energy is inversely proportional to ε^2, we sought to create nonexcitonic single-material solar cells. We achieved interesting results with the dye quinacridone, also known as pigment violet 19, used extensively in paints and cosmetics. Quinacridone features intermolecular hydrogen bonding similar to indigo, and can be perceived as an H-bonded pentacene analogue. Different than indigo, it does not have characteristic a fast internal conversion. In effect quinacridone is highly fluorescent and has a long excited state lifetime, two facts that make quinacridone an interesting candidate for the development of a "single layer" organic solar cell. Single-layer metal-quinacridone-metal structures produced short-circuit photocurrents in the milliamp per square centimeter range and external quantum efficiencies of 10% at the absorption peak of the dye. Moreover, temperature dependence of photocurrent experiment showed excitation binding energies below 100meV. As a comparison to the above values, single-layer polymer cells featuring poly(thiophene) or poly(phenylene vinylene), showed short circuit currents in the microamperes range and quantum efficiencies of less than 1%. Our finding demonstrates that highly ordered organic materials that have strong intermolecular interactions could be efficiently used to produce high efficiency nonexcitonic organic solar cells.

Our investigation of natural and nature-inspired materials proved that those materials can be employed in the fabrication of organic devices operating at state-of-the-art performance. Better understanding of the strong intermolecular interactions in these materials and making use of those interactions is the focus of our present and future research activity. We are aiming to synthesize better absorbers to make viable single-layer solar cells as well as to control and optimize film growth conditions in order to maximize mobilities and semiconductor performance in transistor-based devices.

References

1. E.D. Głowacki, L. Leonat, G. Voss, M. Bodea, Z. Bozkurt, M. Irimia-Vladu, S. Bauer, N.S. Sariciftci, *Natural and nature-inspired semiconductors for organic electronics*, Proc. SPIE 8118, 81180M (2011).
2. M. Irimia-Vladu, E.D. Głowacki, P. Troshin, G. Schwabegger, L. Leonat, D. Susarova, O. Krystal, M. Ullah, Y. Kanbur, M.A. Bodea, V.F. Razumov, H. Sitter, S. Bauer, N.S. Sariciftci, *Indigo—a natural pigment for high-performance ambipolar organic field effect transistors and circuits*, Adv. Mater. 24(3), 375-380 (2012).
3. E.D. Głowacki, L. Leonat, G. Voss, M.A. Bodea, Z. Bozkurt, A. Montaigne Ramil, M. Irimia-Vladu, S. Bauer, N.S. Sariciftci, *Ambipolar organic field effect transistors and inverters with the natural material Tyrian Purple*, AIP Adv. 1, 042132–042137 (2011).
4. M. Irimia-Vladu, P.A. Troshin, M. Reisinger, L. Shmygleva, Y. Kanbur, G. Schwabegger, M. Bodea, R. Schwödiauer, A. Mumyatov, J. Fergus, V.F. Razumov, H. Sitter, N.S. Sariciftci, S. Bauer, *Biocompatible and biodegradable materials for organic field-effect transistors*, Adv. Funct. Mater. 20(23), 4069–4076 (2010).

The abstract of the lecture Mr. Kolbusch
entitled
“Production technologies for large area printed flexible electronics”
was not available to the editorial deadline.

Part VIII: Solar cells / OPV 2

STRUCTURAL CORRELATIONS IN THE GENERATION OF POLARON PAIRS IN COPOLYMERS FOR PHOTOVOLTAICS

Enrico Da Como[1], Raphael Tautz[1], Jochen Feldmann[1], Ullrich Scherf[2] and Elizabeth von Hauff[3]

[1]*Photonics and Optoelectronics Group, Ludwig-Maximilians-Universität München, 80799, Munich, Germany*
enrico.dacomo@lmu.de
[2]*Department of Chemistry and Institute of Polymer Chemistry, Wuppertal University, 42097 Wuppertal, Germany*
[3]*Fraunhofer Institute for Solar Energy Systems, Freiburg, Germany*

The most recent advances in the power conversion efficiency of organic solar cells considered the design of low-bangap copolymers with an extended absorption in the near infrared. These materials, based on the donor-acceptor concept have attracted a considerable interest. The low bandgap offers optimal light-harvesting characteristics and has inspired much work towards the achievement of record power-conversion efficiencies in solar cells. It remains an open question what are the fundamental photoexcitations in these macromolecular semiconductors. In conjugated *homopolymers* an exciton is formed upon light absorption. This can later dissociate forming a polaron pair because of the energetic disorder in the polymer solid system. Donor-acceptor *copolymers* show an intrinsic alternation of units with different electron affinities, which may favour the formation of polaron pairs.
Here, we report on how the chemical structure of donor and acceptor moieties controls one of the primary steps in light absorption and photocarrier generation, i.e. the yield of polaron pairs. We analyze several copolymers in which the acceptor part is modified according to different electron affinities and the distance between the center of mass between the donor and acceptor moiety is varied. The experimental technique for such measurements is based on a femtosecond pump-probe setup with a near infrared pump resonant with the first absorption peak of the polymers and a probe in the middle infrared (MIR) monitoring the polaron absorption bands. This allows us for a reliable and accurate estimation of the polaron generation yield upon photoexcitation. We focussed our attention on four different copolymers having the same 4,4-bis-(2-ethylhexyl)-4H-cyclopenta[2,1-b;3,4-b`]-dithiophene donor moiety indicated as **CPDT** and different acceptors; benzo-[1,2-*c*;4,5-*c'*]bis[1,2,5]thiadiazole] (**BDT**), (2,1,3-benzothiadiazole) (**BT**) di(thien-2-yl)-2,3-diphenylthieno[3,4-*b*]pyrazine (**2TTP**) and di(thien-2-yl)- (2,1,3-benzothiadiazole) (**2TBT**). The chemical structures for such systematic series of compounds are reported as insets in Figure 1 together with the absorption spectra in the main figure frame.

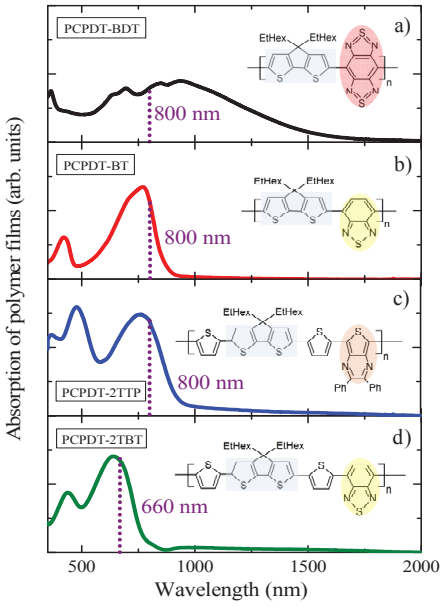

Figure 1 Absorption spectra of the polymers: a) PCPDT-BDT, b) PCPDT-BT, c) PCPDT-2TBT, d) PCPDT-2TTP.

We make the important observation that copolymers with donors and acceptors spatially adjacent along the polymer backbone (PCPDT-BDT and PCPDT-BT), show a more efficient formation of polaron pairs (> 24% of the initial photoexcitations). On the other hand, we do not observe any clear correlation between the acceptor strength, i.e. the electron affinity of the acceptor moiety, and the yield. Interestingly, also the dynamics of the recombination process differ and can be correlated to the structure. The results provide useful input into the understanding of how structure-property relationships determine the initial ultrafast branching of photoexcitations in low-bandgap polymers for photovoltaics.

BIOGRAPHIC DATA OF DR ENRICO DA COMO

E-Mail: edc25@bath.ac.uk
Website: **http://www.phog.physik.uni-muenchen.de/**

Educational Background

- 01/03 to 03/06 **Ph.D. in Chemical Physics,** University of Bologna (Italy)

- 09/97 to 10/02 **Laurea in Chemical Physics (equivalent to 5 years M.Sc.)**, 110/110 *cum laude*. University of Modena (Italy)

Appointments

- Since 05/12: **Reader in Physics** at the Department of Physics, University of Bath (United Kingdom)

- 01/08 to 04/12: **University Assistant (W1 level), in Experimental Physics** at the Photonics and Optoelectronics group, Department of Physics, Ludwig-Maximilians-University Munich (Germany)

- 08/08 and 08/09 (1 month per visit): **visiting scientist** at the Department of Physics, University of Utah, UT (U.S.A.) (Group Prof. J. Lupton)

- 04/06 to 12/07: **Postdoc** at the Photonics and Optoelectronics group, Department of Physics, Ludwig-Maximilians-University Munich (Germany) (Chair of Prof. J. Feldmann)

- 01/06 to 03/06: **Research Assistant** at the at the Istituto per lo Studio dei Materiali Nanostrutturati, National Research Council (C.N.R.), Bologna (Italy)

Current Fields of Interest

- Optical spectroscopy of excitons and polarons in organic semiconductors and conductors.
- Single molecule and ultrafast spectroscopy of semiconductor nanocrystals, graphene and plasmonic nanoparticles.
- Morphological studies on nanostructured materials by optical, scanning-probe and electron microscopy (both transmission and scanning).

ORIGIN OF SUB-BANDGAP ABSORPTION IN P3HT: PCBM SOLAR CELLS

Martin Presselt, Felix Herrmann, Erich Runge, Sviatoslav Shokhovets, Harald Hoppe, Gerhard Gobsch

To explain the origin of sub-bandgap (SBG) absorption contributing to the photocurrent in bulk-heterojunctions (BHJ) made of poly(3-hexylthiophene-2,5-diyl) (P3HT) and [6,6]-phenylC61-butyric acid methyl ester (PCBM) at least four different models are discussed in the literature. In an earlier work we have shown that an exponential in addition to a Gaussian function is needed to reproduce SBG external quantum efficiency (EQE) spectra. There, the exponential function was assigned to a disorder related absorption tail, while the SBG EQE Gaussian was not assigned unambiguously. In the present work, the SBG EQE Gaussian is assigned to a hole-polaron transition at P3HT rather than to a direct charge transfer transition from the P3HT HOMO to the PCBM LUMO or absorption of molecularly dispersed PCBM as concluded from temperature dependent EQE measurements.

POLYMER SOLAR CELLS – VISUALIZING VERTICAL PHASE SEPARATION IN SOLUTION-PROCESSED FILMS OF POLYMER FULLERENE BLENDS

Ana Sofia Anselmo,[1] Andrzej Dzwilewski,[1] Jakub Rysz,[2] Andrzej Budkowski[2], Krister Svensson[1], Jan van Stam[3], Ellen Moons[1]

1 Department of Physics and Electrical Engineering, Karlstad University, SE-65188 Karlstad, Sweden

2 Institute of Physics, Jagiellonian University, Kraków, Poland

3 Department of Chemistry and Biomedical Sciences, Karlstad University, SE-65188 Karlstad, Sweden

ellen.moons@kau.se

Recently power conversion efficiencies for polymer solar cells of over 8% have been reported.[1] Morphology control has been one major key to the improvements in energy conversion efficiency of polymer-based photovoltaic devices. Polymer bulk heterojunction solar cells consist of solution-cast thin films of electron donor and electron acceptor molecules mixed with one another, a so-called *bulk heterojunction*. This molecular distribution has a strong effect on the charge generation processes in the solar cell, such as the separation of excitons into mobile charges at the donor/acceptor interface and the transport of these mobile charges to the electrodes.

When a thin film is prepared by spincoating a blend of a conjugated polymer and the fullerene-based acceptor material, PCBM, demixing determines the nanostructure in the film, which is influenced by the polymer-fullerene-solvent interactions, the molecules' tendency to self-organise, and the kinetics of the film formation. During spincoating, characterized by rapid solvent evaporation, the kinetics of crystallization and of liquid-liquid phase separation compete.[2] The formation of lamellar phases and vertical concentration gradients has been reported for several blend systems, among which APFO3:PCBM[3] and P3HT:PCBM.[4-5]

Characterization of the composition at these interfaces requires techniques that exhibit both the chemical contrast and the lateral or depth resolution required to unveil the nanostructure of these bulk heterojunctions. A combination of surface techniques with depth profiling methods is necessary to obtain a full picture of the film.

Depth profiling methods such as dynamic secondary ion mass spectrometry (dSIMS),[3,6,7] electron tomography,[8-10] neutron reflectivity[11-12] and variable-angle spectroscopic ellipsometry (VASE)[13-14] have been used successfully to demonstrate the spontaneous vertical phase separation in thin films of most polymer:fullerene systems studied for OPVs.

Near-edge X-ray absorption fine structure (NEXAFS) spectroscopy has proven to be a powerful technique to study compositions at the surface and near the substrate of films of blends of P3HT (poly(3-hexylthiophene)) with PCBM.[15-17]

Here we have used a combination of dynamic Secondary Ion Mass Spectrometry (d-SIMS), and Near-Edge Absorption Fine Structure (NEXAFS) spectroscopy to probe the surface and bulk composition of blend films of APFO3 (poly[(9,9-dioctylfluorenyl-2,7-diyl)-co-5,5-(4',7'-di-2-thienyl-2',1',3'-benzothiadiazole]) and PCBM ([6,6]-phenyl-C61-butyric acid methyl ester) with 1:1 and 1:4 (w/w) blend ratios.

The different depth ranges of two NEXAFS detection modes, partial (PEY) and total electron yield (TEY), provide a tool to access compositional gradients in the surface region of APFO3:PCBM blend films. The PEY-NEXAFS spectra of APFO3, PCBM and a 1:4 blend of APFO3 and PCBM are shown in Figure 1. Because the characteristic X-ray absorption resonances of APFO3 and PCBM were easily resolved, the composition ratio of the blend films could quantified by fitting the blend NEXAFS spectrum with a linear combination of the pure component spectra. Results, shown in Table 1, show strong polymer enrichment of the top surface, both in blend films spin-coated from chlorobenzene (CB) and from chloroform (CF) solutions. Differences in composition between surface, sub-surface, and bulk are observed and form clear evidence for vertical phase separation.

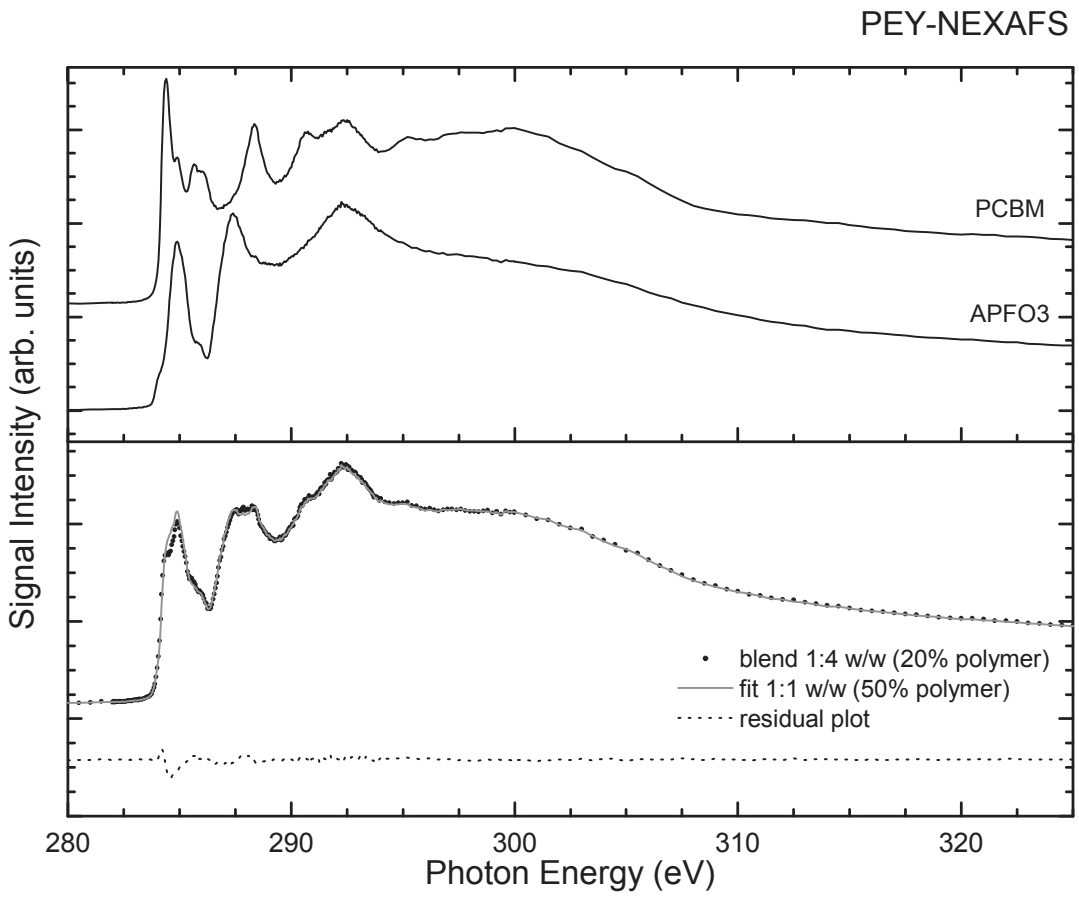

Figure 1. C1s-edge NEXAFS spectra measured at the magic angle in partial electron yield (PEY) of (top) the blend components and (bottom) the 1:4 w/w blend of APFO3 and PCBM prepared from chloroform. In the bottom graph the best linear combination fit is also shown.

Table 1. Weight blend ratios calculated from the best linear combination fit of the experimental blend NEXAFS spectra.

		APFO3:PCBM	
		50:50	**20:80**
CB	**PEY-NEXAFS**	63:37	48:52
	TEY-NEXAFS	44:56	23:77
CF	**PEY-NEXAFS**	67:33	54:46
	TEY-NEXAFS	45:55	28:72

References

1. Green, M. A.; Emery, K.; Hishikawa, Y.; Warta, W. *Progress in photovoltaics: research and applications* 2011, *19*, 84-92.
2. Nilsson, S. et al, Macromolecules **2007**, *40,* 8291.
3. C.M. Björström, A. Bernasik, J. Rysz, A. Budkowski, S. Nilsson, M. Svensson, M. R. Andersson, K. O. Magnusson, E. Moons, *J. Phys.: Condens. Matter* **2005**, *17*, L529.
4. D. S. Germack, C. K. Chan, B. H. Hamadani, L. J. Richter, D. A. Fischer, D. J. Gundlach, D. M. DeLongchamp *Appl. Phys. Lett.* **2009***, 94*, 233303.
5. B. Xue, B. Vaughan, C.-H. Poh, K. B. Burke, L. Thomsen, A. Stapleton, X. Zhou, G.W. Bryant, W. Belcher, P. C. Dastoor *J. Phys. Chem.* **2010***, 114*, 1.
6. Björström, C. M.; Nilsson, S.; Bernasik, A.; Budkowski, A.; Andersson, M.; Magnusson, K.; Moons, E. *Applied Surface Science* **2007**, *253*, 3906-3912.
7. A. S. Anselmo, L. Lindgren, J. Rysz, A. Bernasik, A. Budkowski, M. R. Andersson, K. Svensson, J. van Stam, E. Moons *Chem. Mater.* **2011***, 23*, 2295.
8. Yang, X.; Loos, J. *Macromolecules* **2007**, *40*, 1353-1362.
9. Bavel, S. van; Sourty, E.; With, G. de; Loos, J. *Nano letters* **2009**, *9*, 507-513.
10. Andersson, B. V.; Herland, A.; Masich, S.; Inganäs, O. *Nano letters* **2009**, *9*, 853-855.
11. Kiel, J. W.; Kirby, B. J.; Majkrzak, C. F.; Maranville, B. B.; Mackay, M. E. *Soft Matter* **2010**, *6*, 641-646.
12. Parnell, A. J.; Dunbar, A. D. F.; Pearson, A. J.; Staniec, P. A.; Dennison, A. J. C.; Hamamatsu, H.; Skoda, M. W. A.; Lidzey, D. G.; Jones, R. A. L. *Advanced materials* **2010**, *22*, 2444-2447.
13. Campoy-Quiles, M.; Ferenczi, T.; Agostinelli, T.; Etchegoin, P. G.; Kim, Y.; Anthopoulos, T. D.; Stavrinou, P. N.; Bradley, D. D. C.; Nelson, J. *Nature materials* **2008**, *7*, 158-164.
14. Müller, C.; Bergqvist, J.; Vandewal, K.; Tvingstedt, K.; Anselmo, A. S.; Magnusson, R.; Alonso, M. I.; Moons, E.; Arwin, H.; Campoy-quiles, M.; Inganäs, O. *Journal of Materials Chemistry* **2011**, advance article (DOI: 10.1039/c1jm11239b).
15. Germack, D. S.; Chan, C. K.; Hamadani, B. H.; Richter, L. J.; Fischer, D. A.; Gundlach, D. J.; DeLongchamp, D. M. *Applied Physics Letters* **2009**, *94*, 233303.
16. Germack, D. S.; Chan, C. K.; Kline, R. J.; Fischer, D. a; Gundlach, D. J.; Toney, M. F.; Richter, L. J.; DeLongchamp, D. M. *Macromolecules* **2010**, *43*, 3828-3836.
17. Xue, B.; Vaughan, B.; Poh, C.-how; Burke, K. B.; Thomsen, L.; Stapleton, A.; Zhou, X.; Bryant, G. W.; Belcher, W.; Dastoor, P. C. *Solar Cells* **2010**, 15797-15805.

BIOGRAPHIC DATA OF PROFESSOR ELLEN MOONS

Ellen Moons is professor in materials physics at Karlstad University in Sweden. Her present research focus is the morphology control in solution-deposited films of conjugated polymers and fullerenes for the optimization of the performance of polymer solar cells. By synchrotron-based electron spectroscopy and depth profiling techniques she visualizes the development of vertical phase separation in molecular films.

photo: Andreas Reichenberg

Ellen Moons received her Ph.D. from the Weizmann Institute (Israel) in 1995. After postdoctoral research on dye-sensitized solar cells at the University of Technology in Delft, The Netherlands and at EPFL in Lausanne, Switzerland, she moved in 1998 to the Cavendish Laboratory in Cambridge, UK, and to the spin-off company Cambridge Display Technology, where she studied the effect of morphology in thin films of conjugated polymer blends on the performance of polymer light-emitting diodes. In 2000 she moved on to Karlstad University in Sweden. In 2011 she received the Göran Gustafsson prize in physics of the Royal Swedish Academy of Sciences.

Part IX: Materials and technologies 4

LOW TEMPERATURE SINTERING OF INKJET PRINTED SILVER TRACKS

J. Perelaer,[1,*] Ulrich S. Schubert[1,*]

[1] Laboratory of Organic and Macromolecular Chemistry (IOMC) and Jena Center for Soft Matter (JCSM), Friedrich-Schiller-University Jena, Humboldtstraße 10, 07743 Jena, Germany.
E-mail: jolke.perelaer@uni-jena.de and ulrich.schubert@uni-jena.de

Inkjet printing is an interesting technique for the production of microelectronic structures. The main advantage of printing lies in its flexibility, low cost, ease of processing and its potential for mass production. During the last years, there has been a growing interest in printing silver inks.[1-4]

After printing the silver nanoparticles are usually sintered in an unselective manner by heating them to 220 °C for 60 minutes, but we have developed a novel method to sinter nanoparticles in a fast and selective way by using microwave radiation.[2] Hereby, not only the sintering times are reduced to 3 minutes only, but also low Tg polymer foils can be used, like PET. The resistivity of the conductive features was similar to those sintered conventionally at 220 °C for 60 minutes. Moreover, when applying conductive antennae structures that absorb the electromagnetic waves in a more efficient manner, the sintering times were even improved down to a single second – a process now referred to as *flash sintering*.[6,7]

These conductive features may be used in many plastic electronic applications, such as radio frequency identification (RFID) tags, lighting & signage, electrodes in sensors, etc.

References

[1] J. Perelaer, P. J. Smith, D. Mager, D. Soltman, S. K. Volkman, V. Subramanian, J. G. Korvink, U. S. Schubert, *J. Mater. Chem.* **2010**, *20*, 8446.

[2] J. Perelaer, B.-J. de Gans, U. S. Schubert, *Adv. Mater.* **2006**, *18*, 2101.

[3] T. H. J. van Osch, J. Perelaer, A. W. M. de Laat, U. S. Schubert, *Adv. Mater.* **2008**, *20*, 343.

[4] C. E. Hendriks, P. J. Smith, J. Perelaer, A. M. J. van den Berg, U. S. Schubert, *Adv. Funct. Mater.* **2008**, *18*, 1031.

[5] I. Reinhold, C. E. Hendriks, R. Eckardt, J. M. Kranenburg, J. Perelaer, R. R. Baumann, U. S. Schubert, *J. Mater. Chem.* **2009**, *19*, 3384 (including Back Cover).

[6] J. Perelaer, M. Klokkenburg, C.E. Hendriks, U.S. Schubert, *Adv. Mater.* **2009**, *21*, 4830.

[7] J. Perelaer, R. Abbel, S. Wünscher, R. Jani, T. van Lammeren, U. S. Schubert, *Adv. Mater.* **2012**, DOI: 10.1002/adma.201104417.

BIOGRAPHIC DATA OF DR JOLKE PERELAER

Jolke Perelaer obtained his masters in chemistry at the University of Utrecht in 2004. In 2009 he finished his PhD within the group of Prof. Schubert (Eindhoven University of Technology, the Netherlands) with the research title "microstructures prepared via inkjet printing and embossing techniques." He continued his work with Prof. Schubert as project manager of the inkjet group at the Friedrich-Schiller-University in Jena (Germany). The topics include printed electronics (photovoltaic, OLED, RFID), combinatorial materials screening and printed bio-materials.

IMPROVING THE PHOTOVOLTAIC PERFORMANCE OF POLYMER BASED SOLAR CELLS WITH MOLECULAR DOPING

Antonietta De Sio[1], Ali Veysel Tunc[1], Enrico Da Como[2], Jürgen Parisi[1], Elizabeth von Hauff[3]

[1]*Energy and Semiconductor Laboratory, Institute of Physics, Carl von Ossietzky University of Oldenburg*

[2]*Photonics and Optoelectronics Group, Department of Physics and CeNS Ludwig-Maximilians-University, Munich, Germany*

[3]*Department of Physics, University of Freiburg and Fraunhofer ISE, Freiburg (Germany)*

Abstract

The power conversion efficiency of polymer:fullerene solar cells is limited by the low hole mobility in the polymer phase, and recombination effects at the donor-acceptor interface [1]. In this contribution, we demonstrate a novel strategy to improve the power conversion efficiency of polymer based solar cells. The electronic properties of the low bandgap polymer poly[2,6-(4,4-bis-(2-ethylhexyl)-4H-cyclopenta[2,1-b;3,4-b']dithiophene)-alt-4,7-(2,1,3-benzothiadiazole)] (PCPDTBT) are modified by doping with 2,3,5,6-Tetrafluoro-7,7,8,8-tetracyanoquinodimethane (F4TCNQ) molecules via co-solution. We show that at low doping concentrations the hole conductivity and mobility increases. Transient and steady state photophysical investigations demonstrate an increase in the efficiency of charge separation [2] leading to higher polaron densities in the blend. We discuss the increase in performance in terms of trap filling with increased carrier density, and reduced recombination correlated to the improvement in mobility. The results demonstrate a new approach to tune the charge separation and transport efficiency to achieve optimised solar cell performance [3].

References:

[1]M. Hallermann, E. Da Como, J. Feldmann, M. Izquierdo, S. Filippone, N. Martin, S. Juchter E. von Hauff, Appl. Phys. Lett. **97**, 023301 (2010).

[2]F. Deschler, E. Da Como, R. Tautz, E. Von Hauff, U. Scherf J. Feldmann, Phys. Rev. Lett. **107** 127402 (2011)

[3] A. De Sio, A. V. Tunc, E. Da Como, J. Parisi, E. von Hauff, submitted (2011)

BIOGRAPHIC DATA OF PROFESSORIN ELIZABETH VON HAUFF

Elizabeth von Hauff studied Physics at the University of Alberta, in Edmonton, Canada. From 2002-2005 she did her PhD work under the supervision of Prof. Dr. V. Dyakonov at the University of Oldenburg in Germany. From 2006-2011 she was an assistant professor in the group of Prof. J. Parisi in Physics, at the University of Oldenbug. Since July 2011 she is an associate professor in Physics at the University of Freiburg, Germany, and works in close cooperation with the Fraunhofer Institute for Solar Energy Systems (ISE). Her research focuses fundamental processes in organic semiconductors and the development of novel devices based on organic materials.

SILICON/ORGANIC HYBRID HETERO–JUNCTION INFRARED PHOTODETECTOR OPERATING IN THE TELECOM REGIME

Gebhard. J . Matt∗ , Mateusz Bednorz∗∗ , Eric Daniel Glowacki∗∗∗ , Christoph J. Brabec∗ , Markus Scharber∗∗∗∗ , Thomas Fromherz∗∗

∗Lehrstuhl für Werkstoffe der Elektronik- und Energietechnik, Friedrich-Alexander-Universität Erlangen-Nürnberg, Martensstraße 7, 91058 Erlangen (Germany); E-mail: gebhard.matt@ww.uni-erlangen.de
∗∗ Institute for Semiconductor and Solid State Physics, Johannes Kepler University, Altenbergerstrae 69, 4040 Linz (Austria)
∗∗∗ Linz Institute for Organic Solar Cells (LIOS), Johannes Kepler University, Altenbergerstrasse 69, 4040 Linz (Austria)
∗∗∗∗ Konarka Austria, Altenbergerstrasse 69, 4040 Linz (Austria)

The authors report on the fabrication of a Silicon/organic heterojunction based IR photodetector. It is demonstrated that an Al/p-Si/perylene-derivative/Al heterostructure exhibits a photovoltaic effect up to 2.3 µm. Although the devices are not optimized, at room temperature a rise time of 300 ns, a responsivity of ∼0.2 mA/W with a specific detectivity of $D^* \sim 7 \cdot 107$ Jones at 1.55µm is found [1]. The achieved responsivity is two orders of magnitude higher compared to our previous efforts [2]. It will be outlined that the photocurrent originates from an absorption mechanism at the organic/inorganic interface. The non-invasive deposition of the organic interlayer onto the Si results in compatibility with the CMOS process, making the presented approach a potential alternative to all inorganic device concepts.

[1] Mateusz Bednorz, Gebhard J. Matt, Eric Daniel Glowacki, Christoph J. Brabec, Markus C. Scharber, Helmut Sitter, and Thomas Fromherz. Silicon/organic hybrid hetero–junction infrared photodetector operating in the telecom regime. submitted, 2012.

[2] Gebhard J. Matt, Thomas Fromherz, Mateusz Bednorz, Saeid Zamiri, Guillaume Goncalves, Christoph Lungenschmied, Dieter Meissner, Helmut Sitter, Niyazi Serdar Sariciftci, Christoph J Brabec, and Günther Bauer. Fullerene sensitized silicon for near- to mid-infrared light detection. Advanced materials (Deerfield Beach, Fla.), 22(5):647–50, February 2010. Available from: http://onlinelibrary.wiley.com/doi/10.1002/adma.200901383/abstract,

IMPACT OF TRAP-ASSISTED RECOMBINATION ON THE PERFORMANCE OF POLYMER-FULLERENE BULK HETEROJUNCTION SOLAR CELLS

C. DEIBEL, A. FÖRTIG, J. LORRMANN, J. GORENFLOT, A. WAGENPFAHL, D. RAUH, J. RAUH, AND V. DYAKONOV

[1]Experimental Physics VI, Faculty of Physics and Astronomy, Julius-Maximilians University of Würzburg, Am Hubland, 97074 Würzburg, Germany

Recombination of photogenerated charges in organic photovoltaic devices limits the power conversion efficiency. Understanding its detailed nature is therefore an important prerequisite for a directed performance optimisation. We investigated devices made from P3HT and PTB7, as well as their blends with fullerene derivatives by temperature dependent transient absorption and charge extraction measurements. These experimental methods allow us to explore the important role the trapping of charge carriers plays in the charge transport and nongeminate recombination. Whereas the recombination in neat P3HT polymer is mainly determined by a recombination order of two, as expected for the recombination of free electrons and holes, we observe in the P3HT:PCBM blends a trap-limited process with recombination orders clearly exceeding two. For the latter, the current-voltage characteristics

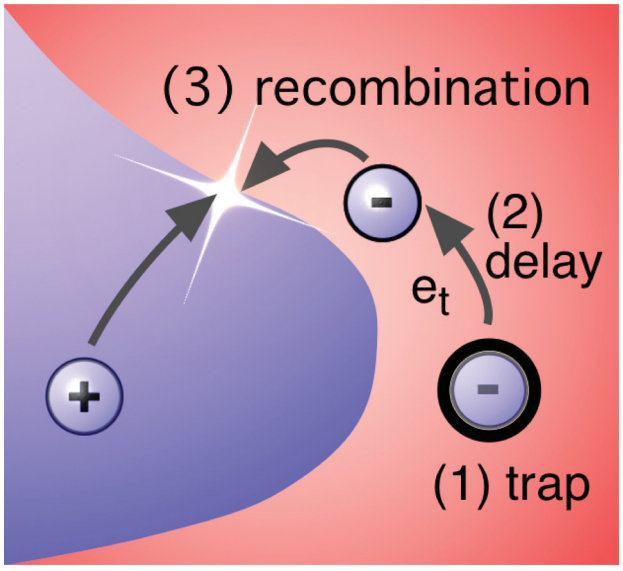

Figure 1: Slow nongeminate recombination of a free and a formerly trapped charge carrier at at donor-acceptor heterointerface within a polymer-fullerene solar cell. In this case, the emission rate from the trap determines the recombination rate.

can be completely reconstructed by considering nongeminate recombination with the experimentally determined, carrier concentration dependent recombination rate and the carrier concentration at a range of different voltage bias values. However, in order to explain these results in view of the nature of nongeminate recombination, we present a multiple-trapping-and-release model, optimised for describing charge recombination in organic solar cells based on coupled continuity equations with continuous trap distributions. With this approach, we can describe the experimentally determined charge carrier dynamics quantitatively. We find that a trap-induced delay of the bimolecular recombination leads to the higher apparent recombination orders. This effect is amplified if the donor-acceptor phase separation is considered: charge carriers trapped within one of the material phases can only recombine with a mobile charge (before extraction from the device) if and when they are re-emitted from the trap. We discuss our findings in terms of the impact of trapping on the recombination rate and the solar cell performance.

[1] D. Rauh, C. Deibel, V. Dyakonov, *Charge density dependent nongeminate recombination in organic bulk heterojunction solar cells*, accepted for publication by Adv. Funct. Mater. (2012) [arXiv:1203.6105]

BIOGRAPHIC DATA OF DR CARSTEN DEIBEL

Dr. Carsten Deibel is junior researcher and group leader at Prof. Vladimir Dyakonovâ™s Chair of Experimental Physics VI, University of Würzburg, Germany. He obtained his Master of Philosophy (Physics) in 2000 from University of Sussex, Brighton. His PhD research was done ain the group of Prof. Jürgen Parisi at the University of Oldenburg, Germany; it concerned the characterisation of defects in inorganic thin film solar cells made of Cu(In,Ga)(S,Se)2 in cooperation with Shell Solar (now Avancis). He obtained his PhD in natural sciences (Physics) in 2002. From 2003-2005, he had a postdoctoral position at the Interuniversity Microelectronics Center, Leuven, Belgium, in the Polymer and Molecular Electronics Group of Prof. Paul Heremans, working on polymer solar cells and discotic liquid crystalline devices. Since 2005, he holds the position in Würzburg, where he is responsible for the fundamental research of charge generation and transport in organic semiconductors and optoelectronic devices, which bears direct relevance to organic and hybrid photovoltaics. In 2010, he was selected to join the Förderkolleg of the Bavarian Academy of Sciences and Humanities.

Part X: Posters

CHARGE SEPARATION DYNAMICS AT ZNPC: C_{60} BULK HETERO-JUNCTIONS USING TIME-RESOLVED TERAHERTZ SPECTROSCOPY

Andreas F. Bartelt, Christian Strothkämper, Rainer Eichberger*

Helmholtz Center Berlin for Materials and Energy, Hahn-Meitner-Platz 1, D-14109 Berlin, Germany

Andreas.Bartelt@helmholtz-berlin.de

In organic donor-acceptor material compositions, photoexcitation results in the formation of excitons which can be separated at the donor-acceptor interface. However, for the generation of free charges the Coulomb attraction of the electron and hole across the interface needs to be overcome. In many cases these bound polaron pairs, or charge-transfer states, can result in enhanced geminate recombination of charges, which is detrimental for the photovoltaic performance. In this contribution, the influence of the donor-acceptor morphology on the ability to separate interfacially bound charges is analyzed for the model system ZnPc:C_{60}. The morphologies of ZnPc:C_{60} blend film can be optimized by controlling the growth temperature during deposition, inducing phase segregation and crystallinity. Here, the influence of growth temperature induced structural changes on the generation of free charges in ZnPc:C_{60} blend films is investigated using optical-pump terahertz-probe spectroscopy (OPTP)[1]. The growth temperature was varied between 25°C and 120°C. The all-optical OPTP method allows determining the photoconductivity of thin films with sub-picosecond time resolution and without contacts.

Excitation at 800 nm results in the creation of ZnPc-excitons and charge-transfer states. No C_{60} excitation occurs at this wavelength. The photo-generated ZnPc-excitons lead to the formation of vibrationally hot charge-transfer states at the interface with C_{60}. Taking advantage of the excess energy, some free charges are generated within 1 ps. The generation of a photoconductivity is detected within the time resolution of the experiment. In competition to the charge separation is the relaxation to the charge transfer ground state of Coulombically attracted charges, which usually occurs within picoseconds. An increased time-dependent photoconductivity is observed for improved C_{60} crystallinity and domain size in films with higher growth temperature. While for amorphous blends the interfacial charge-transfer state hampers the generation of free charges, growing crystalline C_{60} nanodomains help reaching the charge-separated state by separation of the relaxed interfacial charge transfer state. In this case, a sequential charge separation process is observed, which entails both vibrationally hot and relaxed charge transfer states, on time scales between <100 fs and ~100 ps. The separation from relaxed charge transfer states is in competition with geminate recombination, which can take place within hundreds of picoseconds to nanoseconds. The increase of photoconductivity with film growth temperature correlates with formerly observed solar cell photocurrent improvements.

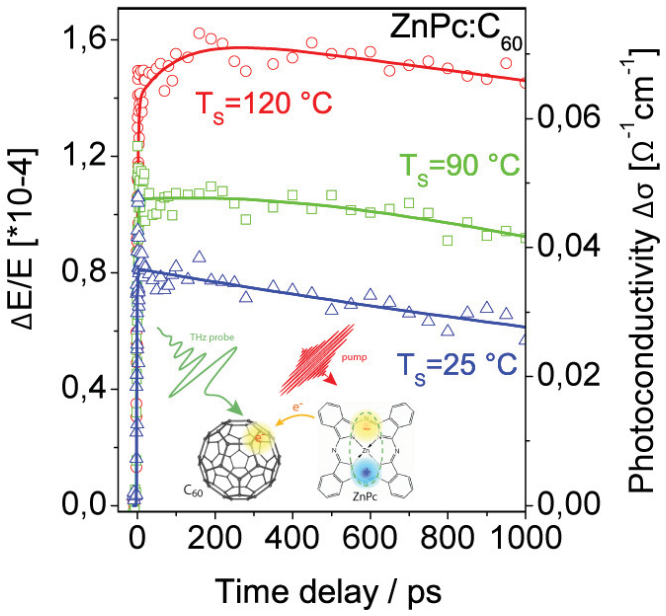

***Fig.1**: Photoconductivity transients following optical excitation of ZnPc:C_{60} blend layers grown on substrates with temperatures T_S=25°C, 90°C and 120°C. With increasing T_S, the instantaneous photoconductivity increases while a second and slower rise appears.*

High local mobilities of minimal μ~0.3 cm^2/Vs are obtained from the measured photoconductivities, which increase with higher growth temperatures. According to the Onsager-Braun theory, higher mobilities foster the probability for charge separation. Furthermore, when crystalline C_{60} domains are formed, the electrons become gradually more mobile and can relax to more delocalized states. The increased geminate charge distance lowers their binding energy and favors charge separation. Additionally, the dissociation yield improves as the average C_{60} domain size approaches the Onsager capture radius r_c ~ 15 nm which corresponds to the average C_{60} domain sizes in our T_S=120°C samples. We will also discuss the possibilities of an unfavorable interfacial band bending which might be reduced with increasing growth temperatures.

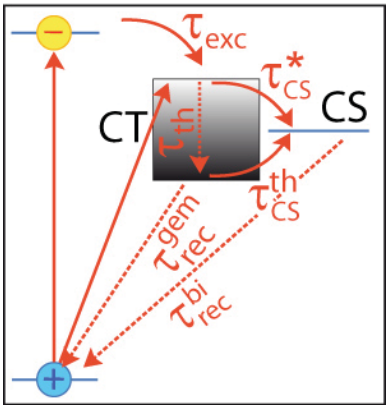

***Fig 2**: The separation of vibrationally hot charge–transfer states is in competition with thermal relaxation of charge-transfer states. Separation from thermalized charge-transfer states can result in the formation of the charge-separated state, and is in competition with geminate recombination.*

[1] Andreas F. Bartelt, Christian Strothkämper, Wolfram Schindler, Konstantinos Fostiropoulos, und Rainer Eichberger, Appl. Phys. Lett. **99**, 143304 (2011).

Curriculum vitae

Dr. Andreas F. Bartelt

Dr. Andreas F. Bartelt

Helmholtz-Zentrum Berlin für Materialien und Energie

Institut für Solare Brennstoffe und Speichermaterialien, E-I6

Hahn-Meitner-Platz 1

14109 Berlin

Career

Since 09/2007	Helmholtz-Center Berlin for Materials and Energy
2004 - 2007	Lawrence Berkeley National Laboratory (USA)
2002 - 2004	Princeton University (USA)
1997 - 2002	Free University Berlin (Germany)
1996 - 1997	Max-Planck-Institut für Strömungsforschung Göttingen (Germany)

University

1997 – 2002	Dissertation at the Free University Berlin, physics department
	Degree: Dr. rer. nat. (2002)
1993 – 1997	Graduate school in physics (Hauptstudium) at the Georg-August-University Göttingen (Germany)
	Degree: Diploma in physics (1997)
1992 – 1993	ERASMUS-scholarship for a one-year university exchange programm with the University of Lisbon (Portugal), department of physics
1989 – 1992	Undergraduate school in physics at the Georg-August-University Göttingen (Germany)

IN SITU REFLECTANCE IMAGING OF ORGANIC THIN FILM FORMATION FROM SOLUTION

J. BERGQVIST[1*]; H. ARWIN[2]; O. INGANÄS[1]

[1]Biomolecular and Organic Electronics, IFM, and Center of Organic Electronics, Linköping University, SE-581 83 Linköping, Sweden
E-mail: jonbe@ifm.liu.se

[2]Laboratory of Applied Optics, IFM, Linköping University, SE-581 83 Linköping, Sweden

The rapid progress of organic photovoltaic devices during the last decade, with power conversion efficiencies now exceeding 8%[1], has brought the technology close to an industrial breakthrough. Organic photovoltaic devices (OPV) based on polymer:fullerene blends has the benefit of being solution processable, thereby roll to roll printing is desired to gain the production advantage. The formation of the photoactive material from solutions needs to be controlled and optimized. Therefore a suitable method to monitor the deposition process is needed as deviations of drying times[1] and drying rates[2] during the coating process have proven to generate morphology variations causing variations in photocurrent generation.

In this work we demonstrate how reflectance imaging can be used as a non-invasive tool for areal surveillance of the drying process, both for spin coating and blade coating deposition. A blue LED with a narrow bandwidth is used as light source to generate specular reflections imaged by a CMOS camera. The thinning of the wet film can then be observed by thin film interference. Each pixel display a sine shaped reflectance with increasing amplitude versus time due to the alternating fulfillment of the conditions for constructive and destructive interference, as the thickness of the wet film decrease. This enables an estimation of the solvent evaporation rate for each pixel during the later stage of coating, as the evaporation rate is proportional to the frequency of the reflectance curve. By averaging the frequency for each pixel and subsequently map this over the substrate, variations in evaporation rate can be illustrated. For spin coating the evaporation rate is shown to increase with the distance from the rotation center, whereas the air flow is the determining parameter during blade coating. By mapping the times when interference ceases, lateral variations in drying time are visualized.

For blade coating a mixed solvent of toluene and orthodichlorobenzene (oDCB) is used, as OPV efficiency is superior from oDCB but toluene is preferred as being less hazardous to the environment. An initial fast evaporation is observed from a high frequency of the reflectance

oscillations as the toluene evaporate, while the final stage of the drying is dominated by a slower evaporating oDCB phase. Moreover lateral thickness variations of the dry film can be visualized by scanning ellipsometry. The possibility to monitor the thin film formation as well as lateral variations in thickness *in-situ* by a non-invasive method, is an important step for future large scale applications where stable high performing generating morphologies have to be formed over large areas.

References:

[1]Service, R.F. Outlook brightens for plastic solar cells (2011) *Science*, 332 (6027), 293.

[2]Schmidt-Hansberg, B.; Sanyal, M.; Klein, M.F.G.; Pfaff, M.; Schnabel, N.; Jaiser, S.; Vorobiev, A.; Müller, E.; Colsmann, A.; Scharfer, P.; Gerthsen, D.; Lemmer, U.; Barrena, E.; and Schabel, W., *ACS Nano 5 ,* 2011, 8579-8590

[3] Hou, L.; Wang, E.; Bergqvist, J.; Andersson, V.B.; Wang, Z.; Müller, C.; Campoy-Quiles, M.; Andersson, M.R.; Zhang, F.; Inganäs, O., *Adv. Func. Mat. 21 ,* 2011, 3169–3175

BIOGRAPHIC DATA OF JONAS BERGQVIST

Jonas Bergqvist

jonbe@ifm.liu.se

2010	Master of Science in Applied Physics, Linköping University, Sweden
2011	Started Ph.D. on the topic of Optical methods to study material and components for polymer solar cells, Biomolecular and Organic electronics, IFM, Linköping University

MULTI-FREQUENCY TRANSCONDUCTANCE TECHNIQUE ON OFET'S

I. Hörselmann[1]; S. Scheinert[1]

[1] Ilmenau University of Technology, Department of solid state electronics, P.O. Box 100565, D-98684, Ilmenau, Germany

The characterization of the interface properties is import to improve the performance of organic field effect transistors (OFET's). In [1] the application of the multi-frequency transconductance (MFT) technique, developed for silicon based MOSFET's [2,3], on OFET's was described to estimate the surface trap state density. Motivation of our contribution is to check the applicability of the MFT-technique on OFET's with two dimensional numerical simulation methods.

The simulated bottom contact thin film transistor is similar to paper [1], with 100nm gate oxide (C''_{ox}=34.5nFcm^{-2}). Only the channel length was reduced from 50 to 2µm and the mobility of the semiconductor increased, to ensure the channel transit time is small against trap time constant. Fig. 1 shows the cross section of simulated transistor. The semiconductor material is a 35nm thin P3HT layer with following properties: mobility µ=1cm^{2}V^{-1}s^{-1}, affinity χ =3.0eV, gap E_g=2.0eV, doping level N_A=5×10^{16} cm^{-3}, density of states in the valence and conduction band N_V=N_C=10^{21}cm^{-3} and thermal velocity v_{th}=10cms^{-1}. Source and drain contacts are ohmic, the gate work function was chosen to 4.17eV. The drain-source voltage for all following simulation results is V_{DS}=-0.2V. The interface trap density was set to N''_{it}=1.5×10^{12}cm^{-2}. Fig. 2 illustrates the influence of different trap levels on the transfer characteristic compared with the trap free case. The diagram 3 shows the difference between high- (g_m^{HF}) and low- (g_m^{LF}) frequency transconductance (g_m) with donor-like interface traps. At high frequencies the trap states are not able to follow the ac-signal, consequently g_m increases at frequencies higher then trap time constant. The publication [1] suggest to calculate the trap density per unit energy from the difference of g_m^{HF} and g_m^{LF} with the following equation:

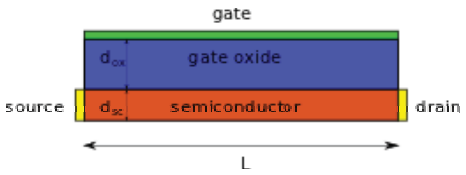

Fig.1: Simulated device structure.

$$D''_{it} = \frac{I_D C''_{ox}}{k_B T}\left[\frac{1}{\mathrm{Re}\{g_m^{LF}\}} - \frac{1}{\mathrm{Re}\{g_m^{HF}\}}\right] \qquad (1).$$

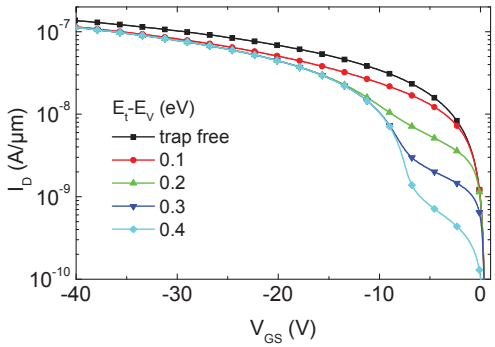

Fig. 2: Transfer characteristic for donor-like interface trap states in comparison to trap free case.

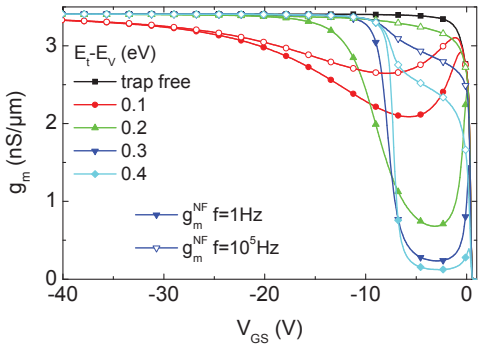

Fig. 3: Transconductance in case of donor like interface trap states simulated for 1 and 1×10^5 Hz.

The results are shown in Fig. 4. However, this approximation is valid for weak inversion [3], but not for the accumulation or depletion, were the OFET operates. As a result the calculated trap densities are too high and the MFT-method is not applicable to OFET's without a modification. We modified the MFT-technique starting with eq. 2 and 3, for $V_{DS}<V_{GS}$:

$$I_D = \frac{w}{L}\mu Q_p^{"}\frac{d\varphi_{Fp}}{dx} \approx \frac{w}{L}\mu V_{DS}(Q_{sc}^{"}+Q_{it}^{"}) \qquad (2)$$

$$g_m = \frac{\partial I_D}{\partial V_{GS}} = \frac{w}{L}\mu V_{DS}\frac{\partial\varphi_S}{\partial V_S}\frac{(Q_{sc}^{"}+Q_{it}^{"})}{\partial\varphi_S} \qquad (3).$$

At high frequencies there is no contribution from $Q"_{it}$ to g_m because the trap states can't follow the ac signal, together with the voltage balance on the MOS-structure, and the approximation $C_{sc}^{NF}=C_{sc}^{HF}$ we obtain eq. 4:

$$D_{it}^{"} = \frac{C_{ox}^{"}}{e}\left[\frac{g_m^{LF}}{KV_{DS}+g_m^{LF}} - \frac{g_m^{HF}}{KV_{DS}+g_m^{HF}}\right] \quad \text{with} \quad K=\frac{w}{L}\mu C_{ox}^{"} \qquad (4).$$

Fig. 5 contains the $D"_{it}$ calculated by the modified MFT-method (eq. 4). As expected, using eq. 4 the calculated trap densities per unit energy multiplied by the energetic distribution of $2*k_BT$ are not higher than the implemented interface density $N"_{it}$.

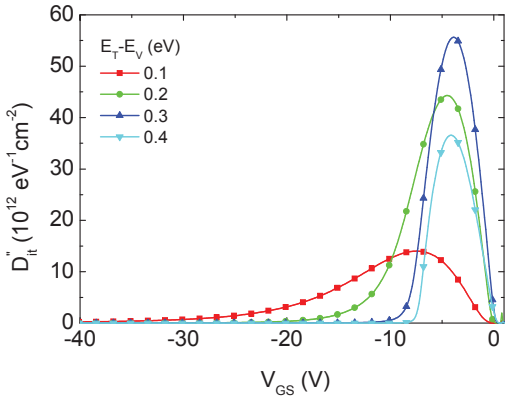

Fig. 4: D”it calculated by MFT-method eq. 1

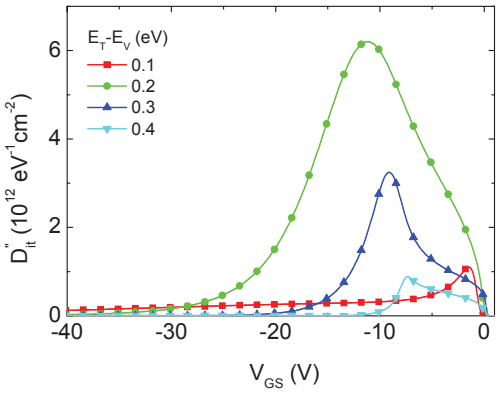

Fig. 5: D”it calculated by modified MFT-method eq. 4

The value of interface trap density N''_{it} itself can easily be determined by integration the difference of g_m^{HF} and g_m^{LF} over the gate voltage with eq. 5. The results of eq. 5 are listed in tab. 1.

$$N''_{it} = -\frac{L}{ew\mu V_{DS}} \int_{V_{GSstart}}^{V_{GSstop}} \left(g_m^{HF} - g_m^{LF} \right) dV_{GS} \qquad (5)$$

The calculated interface trap densities are lower than $1.5\times10^{12}cm^{-2}$, because trap states close to the valence band are able to follow the ac-signal even in HF-case and deeper trap states don’t change the occupation during the gate sweep.

Tab.1: Calculated trap densities, using eq. 5

E_T-E_V (eV)	0.1	0.2	0.3	0.4
N''_{it} (cm^{-2})	0.45×10^{12}	1.38×10^{12}	1.26×10^{12}	1.01×10^{12}

With the modified MFT-technique it is possible to calculate the trap density per unit energy D''_{it} and the interface trap density N''_{it} on OFET’s.

References

[1] P. Srinivas et al. A simple and direct method for interface characterization of OFETs. In *Proceedings of 14th IPFA 2007, Bangalore, India*, pages 306–309, 2007.

[2] Sheng S. Li P.C. Yang, H.S. Chen. Measurements of interface state density in partially- and fully-depleted silicon-on-insulator MOSFETs by a high-low-frequency transconductance method. *Solid-State Electronics*, 35(8):1031–1035, 1992

[3] Hisram Haddara and Gérard Ghibaudo. Analytical modeling of transfer admittance in small mosfets and application to interface state characterization. *solid state electronics*, 31(6):1077–1082, 1987.

BIOGRAPHIC DATA OF INGO HÖRSELMANN

Name:	Ingo Hörselmann
Telephone:	+49 3677 693406
E-mail:	ingo.hoerselmann@tu-ilmenau.de
Organization:	TU Ilmenau, Institute of micro- and nanoelectronics
Adress:	Gustav-Kirchhoff-Straße 7 98693 Ilmenau Germany

Ingo Hörselmann has received his diploma in electrical engineering at the University Ilmenau in 2003. In this year he joined the working group polymer electronics at the department of solid state electronics, under the leadership of PD Dr. S. Scheinert. Main research is numeric simulation and dynamic behavior of organic field effect transistors.

DIFFERENT APPROACHES FOR IMPROVING ORGANIC SOLAR CELLS

M. SCHIEK[1,2,*], N. TRAUTWEIN[3], A. OSADNIK[2], J. JENSEN[1], L. BEVERINA[4], A. LÜTZEN[2], H. BORCHERT[3], J. PARISI[3], F. BALZER[1]

[1] NanoSYD, Mads Clausen Institute, University of Southern Denmark, Alsion 2, DK-6400 Sønderborg, Denmark

[2] Kekulé-Institute of Organic Chemistry and Biochemistry, Rheinische Friedrich-Whilhelms-University of Bonn, Gerhard-Domagk-Strasse 1, D-53121 Bonn, Germany

[3] Energy and Semiconductor Research Laboratory, Department of Physics, University of Oldenburg, D-26111 Oldenburg, Germany

[4] Department of Materials Science, University of Milano-Bicocca, Via Cozzi 53, I-20125 Milano, Italy

Organic solar cells currently struggle to compete with their inorganic counterparts made from silicon, but there are a lot of possibilities to improve their performance. Four different approaches are presented here:

1) Lifetime and efficiency can be enhanced by employing new active materials such as squaraine dyes. These small molecule donor materials are readily available with a large variety of structural motifs, they are environmentally stable and show broad absorption within the visible-infrared in the solid state.

2) Controlling the device architecture and nanoscale morphology allows better charge-carrier separation and collection and hence increases efficiency. Thin films of the polymeric donor material P3HT are imprinted with a nanostructured silicon mold and subsequently covered with the PCBM acceptor to pave the way to an ideal, interdigitating heterojunction.

3) Light trapping additives such as silver nanoparticles help to exploit the incident sunlight more efficiently. Forward scattering of light lengthens the optical path in the active layer resulting in a higher degree of light absorption. Additionally, the silver nanoparticles' surface plasmon resonance leads to a local field enhancement increasing the number of excitons generated.

4) Novel transparent electrodes such as silver nanowire mesh electrodes avoid the rare material indium and allow the device fabrication on more flexible substrates. They are fully solution processed with high throughput, and the random mesh of interconnected, highly conductive nanowires is bendable and transparent over the visible-infrared range.

In all cases the key to improvement is to understand the complex structure-property-performance interplay. Due to the nature of charge generation and transport in solar cells occurring on the nanoscale it is crucial to correlate nanoscopic performance with bulk measurements. This can be realized by advanced AFM investigations, namely Kelvin Probe Force Microscopy (KPFM) and photoconductive AFM (pc-AFM).

PHOTOVOLTAIC PERFORMANCE OF PPV-PPE COPOLYMERS: EFFECT OF THE FULLERENE DERIVATIVE

Olga A. Mukhacheva[1], Pavel A. Troshin[1], Andrey E. Goryachev[1], N. Serdar Sariciftci[2], Daniel A. M. Egbe[2], and Vladimir F. Razumov[1],

[1]Institute for Problems of Chemical Physics of Russian Academy of Sciences, Semenov Prospect 1, Chernogolovka, Moscow region, 142432, Russia, Email: troshin2003@inbox.ru.
[2] Linz Institute for Organic Solar Cells (LIOS), Johannes Kepler University Linz, Altenbergerstrasse 69, A-4040 Linz, Austria

Several conjugated PPV-PPE copolymers were studied as electron donor materials in bulk heterojunction organic solar cells in combination with a library of electron acceptor fullerene derivatives. It was shown that molecular structure and solubility of the fullerene counterpart affect significantly photovoltaic performance of both polymers. Use of [60]PCBM as electron acceptor material yielded quite moderate power conversion efficiencies. The best results were achieved when some fullerene derivatives with better suiting molecular structures and solubilities were applied. In some cases the photovoltaic performance of the polymer/fullerene blends shows direct correlation with the molecular structures of the materials.

The obtained results suggest that every newly designed conjugated polymer should be evaluated in solar cells using a library of fullerene derivatives instead of just conventional PCBMs. We believe that only this combinatorial approach might bring the best performing donor/acceptor combinations for future generations of efficient organic solar cells.

ADVANCED CALORIMETRY FOR ANNEALING STUDIES OF ORGANIC PHOTOVOLTAICS

Niko Van den Brande[a], Fatma Demir[a], Sabine Bertho[b], Dirk Vanderzande[b], Bruno Van Mele[a], Guy Van Assche[a]

[a]Physical Chemistry and Polymer Science (FYSC), Vrije Universiteit Brussel (VUB), Pleinlaan 2, B-1050 Brussels, Belgium.

[b]Institute for Materials Research (IMO-IMOMEC), Hasselt University, Wetenschapspark 1, 3590 Diepenbeek.

Introduction

Bulk-heterojunction (BHJ) solar cells are composed of a nanoscale co-continuous composite of donor and acceptor phases, facilitating exciton dissociation. Conjugated, light-excitable polymers are most often used as an electron donor, while fullerene derivatives are the most widespread type of electron acceptor due to their high electron affinity and ability to transport charge [1]. An important advantage of such a system is that it can be cast from solvent, facilitating processing. Post-production annealing of such polymer:fullerene bulk heterojunction solar cells is vitally important, not only for fine-tuning the morphology and thus increasing the efficiency, but also for retaining the desired morphology during long-term operation [2-3]. However, knowing the optimal conditions for annealing temperatures and times requires knowledge about thermal transition temperatures and annealing kinetics of the blend systems. Using advanced fast-scanning thermal analysis techniques, the formation of nuclei and growth of crystals during heating or cooling can be reduced or avoided, allowing for the study of the crystallization processed during annealing. In this study, non-isothermal and isothermal crystallization kinetics of the P3HT:PCBM (poly(3-hexyl thiophene: [6,6] – phenyl C_{61} – butyric acid methyl ester) were studied by *Rapid Heating Cooling Calorimetry (RHC*) [4] and *Fast Scanning Differential Chip Calorimetry (FSDCC)* [5].

Methodology

P3HT (Merck, M_w=35 000 g mol^{-1}, M_w/M_n = 1.8; regioregularity greater than 98.5%) is mixed with PCBM (Solenne) in a 1:1 ratio and dissolved in chlorobenzene (CB) at a concentration of about 1-2.5 wt %, stirring overnight at 50 °C. The solutions were deposited by drop-casting on large glass plates in a glove box under a nitrogen atmosphere to form films with a thickness of 1 μm. After drying in nitrogen atmosphere at room temperature for 50 hours to remove the residual solvent, the remaining solid films were scratched off the glass substrates and collected as a powder for RHC and FSDCC measurements.

RHC experiments were performed on a prototype instrument made available by TA Instruments equipped with a liquid nitrogen cooling and specifically designed for operation at high scanning rates. Sample masses in the order of 250 - 300 µg were used in aluminium RHC crucibles. This allows for heating and cooling rates in the order of 2000 $K.min^{-1}$.

FSDCC was performed on a prototype Fast-Scanning Differential Chip Calorimeter (Rostock Univeristy, Germany) using Xensor Integration XI39399 chips, with an active area of 100 µm by 100 µm, having two on-chip heaters and 6 thermopiles for accurate temperature measurements. The whole chip calorimeter is submerged in a liquid nitrogen vessel, providing effective fast cooling. The highest rates achieved so far with this setup are in the order of 10^6 $K.s^{-1}$, for sensor chips with a heated area of about 10 µm by 10 µm. The rates used in this work are limited to 5000 $K.s^{-1}$. For both devices thermal annealing from the melt and from the glass were simulated by a temperature program as illustrated in figure 1, were the thermal transitions seen during the heating runs after isothermal treatment were used for analysis.

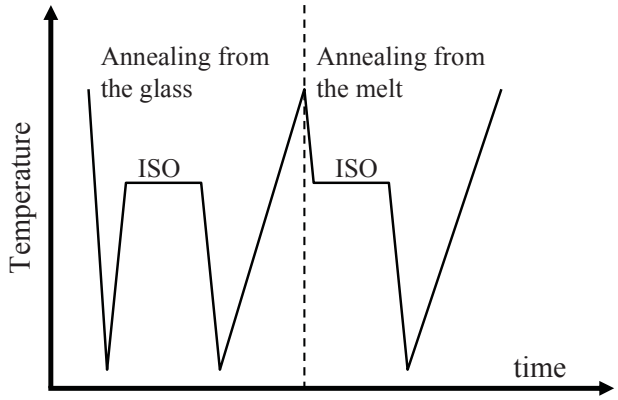

Figure 1: Temperature program used to simulate thermal annealing, both from the glass and from the melt. The heating runs after the isothermal segments were used for data analysis.

Results & Discussion

Controlled fast heating and cooling are imperative for an isothermal crystallization study of rapidly crystallising systems such as P3HT:PCBM.. The fast heating and cooling capacity of advanced fast-scanning thermal analysis techniques enables the reduction of nuclei formation and crystal growth during heating or cooling, by restricting the time available for the blend to crystallise by quickly passing through the crystallisation temperature window that extends from the melting temperature down to the glass transition temperature.

The thermal annealing process in P3HT:PCBM blends was studied first by performing RHC isothermal annealing experiments at 110 °C for a wide range of isothermal times. All measurements were performed with a heating rate of 500 $K.min^{-1}$ and ballistic cooling. Ballistic cooling reaches more than 1500 $K.min^{-1}$ at the beginning of the cooling, which drops down to 750 $K.min^{-1}$ around 60 °C.

Figure 2 shows the subsequent heating curves of the system for increasing annealing times. It is clear that the cold crystallization enthalpies are decreasing and melting enthalpies are increasing by longer annealing times. Besides, by longer annealing at the isothermal annealing temperature, the step in T_g is getting smaller since less amorphous fraction is remaining in the material, and the T_g shifts to higher temperatures. As discussed in previous work, the crystallization of P3HT (having a lower T_g) from the blend is enriching the fraction of PCBM (having a higher T_g) in the remaining amorphous phase, leading to a higher T_g in the subsequent heating. Of course, the T_g is further increased by the close presence of crystalline domains, as is the case for semi-crystalline homopolymers. Another important remark is the clear difference between isothermal crystallisation from the melt and from the glass (without or with cooling before annealing). The crystallization rate is clearly higher when annealing from the glass [6].

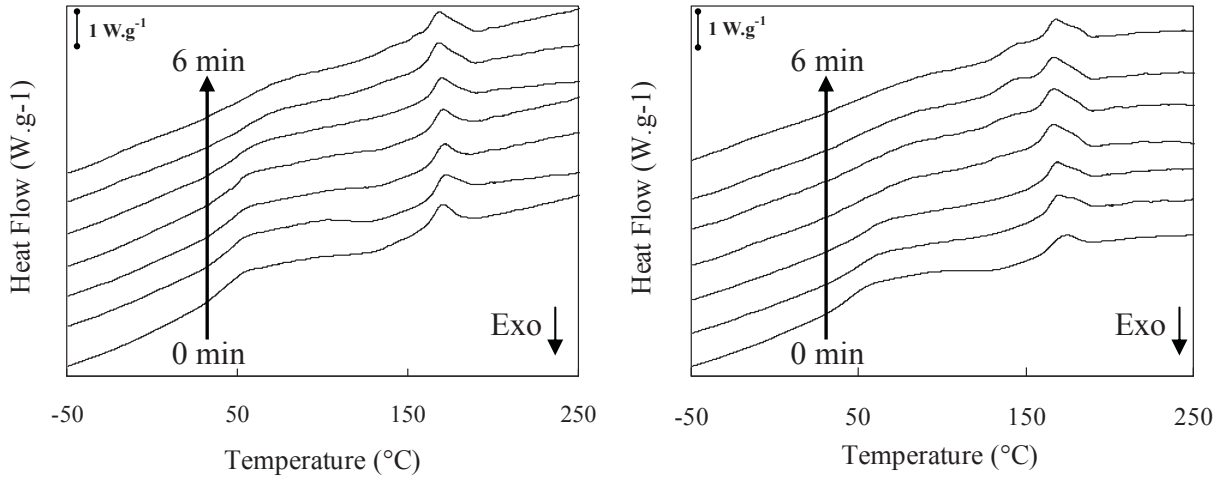

Figure 2: RHC heating cycles at 500 K.min^{-1} for a P3HT:PCBM 1:1 blend after isothermal annealing both from the melt (left) and from the glass (right)..

This difference between the two possible paths of thermal annealing can be explained by a significant difference between the two in the amount of crystal nuclei. This suggests that the rates available in RHC are not sufficient to avoid most of the nucleation.

When similar tests are conducted using FSDCC, using heating and cooling rates of 5000 K.s^{-1}, cold crystallization disappears (see figure 3). There is also no longer a significant difference between isothermal crystallization from the melt and from the glass. Based on these results, it can be concluded that nucleation is mostly avoided by using heating and cooling rates available in FSDCC, and the crystallinity seen results only from the isothermal treatment. This allows for a reliable investigation of the crystallization processes during isothermal annealing, both from the glass and from the melt.

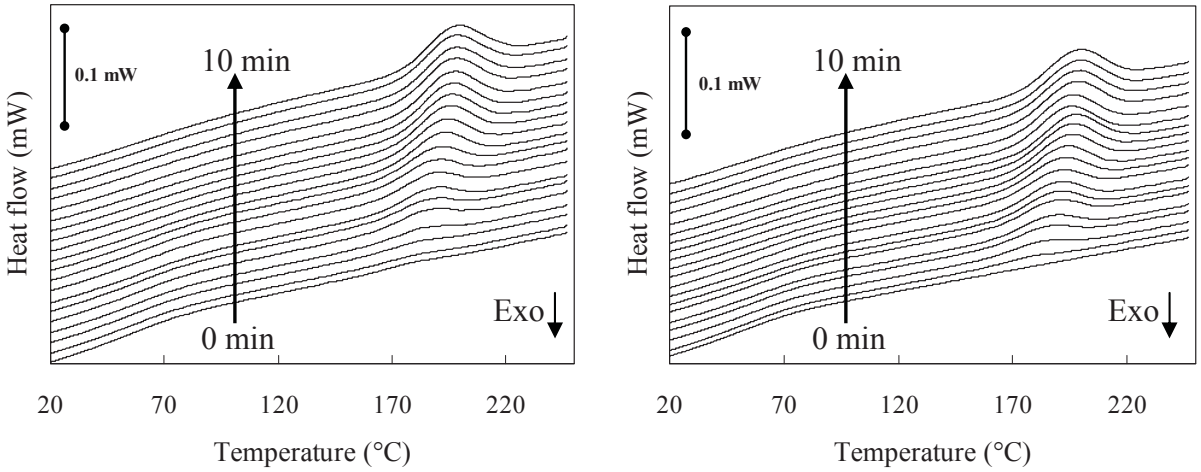

Figure 3: FSDCC heating cycles at 5000 $K.s^{-1}$ for a P3HT:PCBM 1:1 blend after isothermal annealing, both from the melt (left) and from the glass (right).

Conclusion

The isothermal crystallisation at the annealing temperature of 110 °C was investigated for 1:1 P3HT:PCBM using the advanced fast-scanning thermal analysis techniques RHC and FSDCC. RHC allowed for an in depth study of the isothermal crystallisation of these systems, but does not avoid most of the nucleation, leading to a difference in isothermal crystallisation rates for annealing treatments from either the glass or the melt. This difference, as well as cold crystallisation, disappears when FSDCC is used, owing to the much higher rates of heating and cooling. Because of this it is now possible to obtain only information about the isothermal crystallisation, without unwanted effect of the preceding thermal treatment.

References

1. Thompson B.C. and Frechet J.M.J., Angewandte Chemie-International Edition, 2008. **47**(1): p. 58.
2. Erb T., Zhokhavets U., Gobsch G., Raleva S., Stuhn B., Schilinsky P., Waldauf C., and Brabec C.J., Advanced Functional Materials, 2005. **15**(7): p. 1193.
3. Hoppe H. and Sariciftci N.S., Journal of Materials Chemistry, 2006. **16**(1): p. 45.
4. Danley R.L., Caulfield P.A., and Aubuchon S.R., American Laboratory, 2008. **40**(1): p. 9.
5. Minakov A.A., van Herwaarden A.W., Wien W., Wurm A., and Schick C., Thermochimica Acta, 2007. **461**(1-2): p. 96.
6. Demir F., Van den Brande N., Van Mele B., Bertho S., Vanderzande D., Manca J., and Van Assche G., Journal of Thermal Analysis and Calorimetry, 2011. **105**(3): p. 845.

A COMPARATIVE STUDY OF BISFUNCTIONALIZED [60]FULLERENE DERIVATIVES AS ELECTRON ACCEPTOR MATERIALS FOR ORGANIC SOLAR CELLS

D. K. Susarova, A. E. Goryachev, P. A. Troshin, and V. F. Razumov

Institute for Problems of Chemical Physics of Russian Academy of Sciences, Semenov Prospect 1, Chernogolovka, Moscow region, 142432, Russia. E-mail: *diana-susarova@yandex.ru*, *troshin@cat.icp.ac.ru*

One of the main trends in the ongoing research in the filed of organic photovoltaics is the development of fullerene-based electron acceptor materials with decreased electron affinity. Such compounds have higher lying LUMO energy levels compared to conventional PCBM (C_{60} or C_{70} versions) and therefore they yield higher open circuit voltages in organic solar cells.

We report the synthesis and investigation of eight different fullerene bis-adducts. All the compounds were characterized using several physicochemical methods that enabled them to establish the molecular and isomeric composition. All prepared fullerene derivatives were evaluated as electron acceptor materials in fullerene/polymer solar cells under identical conditions with the reference material bis-[60]PCBM. It is shown that the molecular compositions of the [60]fullerene bis-adducts affect strongly their photovoltaic performance. In particular, some of the designed fullerene-based materials outperform mono[60]PCBM and bis[60]PCBM in solar cells due to their optimized molecular structures.

INFLUENCE OF VARIOUS STRESS TYPES ON THE DEGRADATION OF POLYMER/FULLERENE FILMS

Vida Turkovic, Sebastian Engmann, Gerhard Gobsch, and Harald Hoppe

Institute of Physics, Ilmenau University of Technology, Weimarer Str. 32, 98693 Ilmenau, Germany

In search of eco-friendly, sustainable energy sources that could reduce and eventually make the fossil fuel and nuclear power redundant, the attention within the recent years has been directed towards polymer solar cells. Being low-cost, highly scalable, flexible, light-weight, and having a short energy payback time, makes this type of solar cells an interesting commercially applicable product.

Recently, record efficiencies over 10% PCE have been reported by Mitsubishi. Still, improving their long term stability remains a serious issue that has to be resolved in order to make them commercially widespread. Their organic nature makes them especially sensitive to chemical decay in contact with light, oxygen, heat, and water. As all of the mentioned factors are present in the normal working environment of the solar cells, it is important to investigate the degradation mechanisms and possibly find solutions how to overcome them.

An important shortcoming is their low charge carrier mobilities and short lifetimes, which gives special importance to obtaining and maintaining the optimal morphology within the device. To balance the charge carrier separation on one side, and charge transport on the other, a continuous path in form of interpenetrating network of polymer and fullerene is needed[1]. However, as the optimal morphology is not thermodynamically stable, the fullerene molecules in blends with polymeric donors tend to diffuse and recrystallize after deposition, which is especially pronounced with increase in temperature[2]. This process accelerates under thermal exposure, and eventually leads to a morphological destruction of the organic solar cell[3].

In order to investigate the chemical[4] and morphological[5] stability of the photoactive layer in thin film devices, we developed a simple set of experiments performed within ambient and inert atmosphere using various stress conditions with respect to photo-, thermal and oxidative

[1] Hoope H., Sariciftci N.S., "Morphology of polymer/fullerene solar cells", J. Mater. Chem. 16, p 45 (2006)

[2] Zhao J., Swinnen A., Van Assche G., Manca J., Vanderzande D., Van Mele B., „Phase diagram of P3HT/PCBM blends and its implication for the stability of morphology", J. Phys. Chem. B 113, p 1587 (2009)

[3] Bertho S., Janssen G., Cleij T.J., Conings B., Moons W., Gadisa A., D'Haen J., Goovaerts E., Lutsen L., Mancea J., Vanderzande D., "Effect of temperature on the morphological and photovoltaic stability of bulk heterojunction polymer:fullerene solar cells", Sol. Energy Mater. Sol. 92, p 753 (2008)

[4] Turkovic V., Engmann S., Gobsch G., Hoppe H., „The influence of typical degradative stresses on the photoactive layer of polymer:fullerene solar cells", in preparation

[5] Turkovic V., Engmann S., Gobsch G., Hoppe H., „Methods in determination of morphological degradation of polymer:fullerene solar cells", Synt. Met. 161, p 2532 (2012)

stability. The thin films were characterized with standard spectroscopic measurements, whereas devices – completed on degraded layer stacks – were probed by electrical measurements.

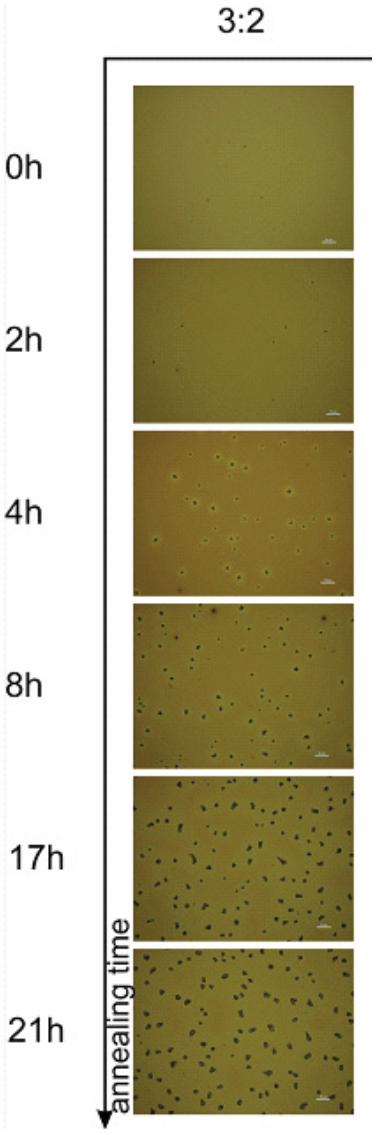

Figure 1. Optical microscopy images of the P3HT:[60]PCBM films exposed to elevated temperature (120°C) in absence of air (N_2 glovebox)

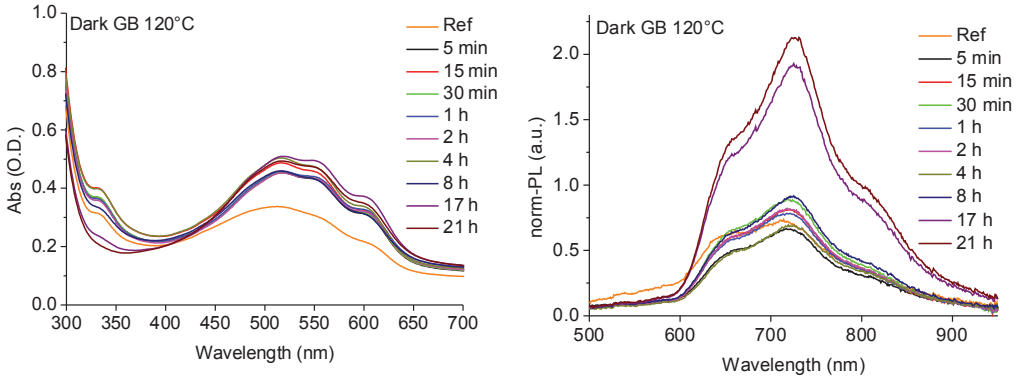

Figure 2. Absorbance and photoluminescence spectra of ITO/PEDOT:PSS/P3HT:[60]PCBM layer stacks exposed to elevated temperature (120°C) in absence of air

REVEALING BULK HETEROJUNCTION BLEND MORPHOLOGY BY SPECTROSCOPIC ELLIPSOMETRY

Authors:
S. Engmann, V. Turkovic, H. Hoppe, and G. Gobsch

Affiliation:
Institute of Physics, Ilmenau University of Technology, Weimarer Str. 32, 98693 Ilmenau, Germany

Abstract:
The nanoscale morphology of bulk heterojunction solar cells is very crucial for their performance[01]. Hence, a lot of effort has been invested to reveal and control it. In order to elucidate the nanoscale morphology, many different complex techniques have been applied. Recently, TEM-tomography has been used to portray the structure of the polymer-fullerene active layer in all three dimensions [02]. In this work we used another non-destructive method, in order to gain information about the predominant morphology and the donor-acceptor distribution within P3HT:PCBM blend films. We demonstrate that spectroscopic ellipsometry can be used to investigate the composition profile over the film thickness[03] and provides detailed information about the shape and extension of phase separation. Furthermore, the shape of nano-inclusions of the fullerene phase within the polymer matrix was determined[04]. The non-invasive character of the method allowed studying morphological aging and changes in the concentration profile, initiated by surface-directed spinodal decomposition[05] of the film, could be traced[06].

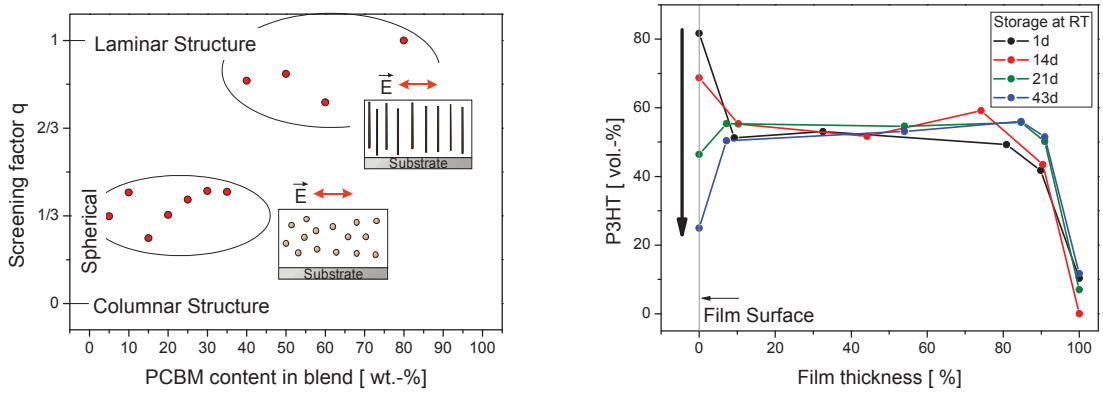

References:

[01] Hoppe, H. & Sariciftci, N. S.
Journal Of Materials Chemistry, **2006**, *16*, 45-61

[02] van Bavel, S.; Sourty, E.; de With, G.; Frolic, K. & Loos, J.
Macromolecules,, **2009**, *42*, 7396-7403

[03] Germack, D. S.; Chan, C. K.; Kline, R. J.; Fischer, D. A.; Gundlach, D. J.; Toney, M. F.; Richter, L. J. & DeLongchamp, D. M.
Macromolecules, **2010**, *43*, 3828-3836

[04] Engmann, S.; Turkovic, V.; Gobsch, G. & Hoppe, H.
Advanced Energy Materials, **2011**, *1*, 684-689

[05] Vaynzof, Y.; Kabra, D.; Zhao, L. H.; Chua, L. L.; Steiner, U. & Friend, R. H.
Acs Nano, **2011**, *5*, 329-336

[06] Engmann, S.; Turkovic, V.; Hoppe, H. & Gobsch, G.
Synthetic Metals, **2012**, *161*, 2540-2543

POLYMER SOLAR CELL LIFETIME: DEPENDENCE ON METAL BACK ELECTRODE AND ENCAPSULATION

Authors:
Roland Rösch, Kai-Rudi Eberhardt, Gerhard Gobsch and Harald Hoppe

Affiliation:
Institute of Physics, Ilmenau University of Technology, Weimarer Str. 32, 98693 Ilmenau, Germany

Presentation Type:
Poster

Abstract:
We investigated the degradation of sealed and unsealed polymer solar cells based on PCDTBT:PCBM photoactive layer with different metal back electrodes in classical device architecture [1]. Lifetimes were determined via automated IV-characterisation under illumination. A titaniumoxide interlayer was used to increase the lifetime compared to bare metal electrodes (compare with the figure below). Furthermore and to learn about the acting degradation mechanisms, lateral inhomogeneities like shunts or electrode oxidation, were studied by luminescence imaging and lock-in thermography.

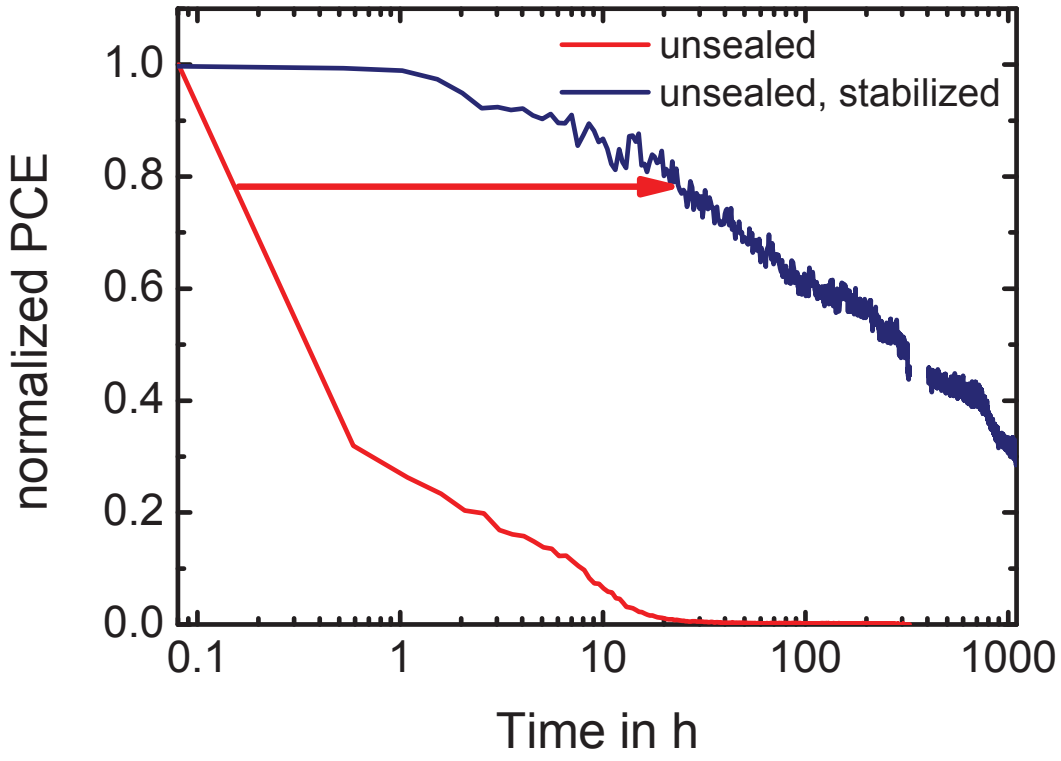

A lifetime increase for unsealed devices by a factor of ~100 was observed.

[1] Roland Rösch et al., in preparation (2012)

QUALITATIVE AND QUANTITATIVE CHARACTERIZATION OF POLYMER SOLAR CELLS BY LATERALLY RESOLVED DETECTION OF LUMINESCENCE

Marco Seeland, Roland Rösch, Gerhard Gobsch and Harald Hoppe

Institute of Physics, Ilmenau University of Technology, Weimarer Str. 32, 98693 Ilmenau, Germany

Imaging of luminescence patterns by laterally resolved detection of luminescence using appropriate cameras is a versatile characterization tool for polymer solar cells and modules [1]. The non-invasive nature of this characterization method allows applications ranging from quality control after processing of polymer solar modules [2] to advanced investigation of local device degradation [3]. We present results where the combined application of electro- and photoluminescence imaging was used to localize the degradation effects both laterally and in depth with respect to the affected layer [4]. Furthermore the application of electroluminescence imaging yields direct information concerning the local current flow trough the active layer, where a lateral gradient in the electroluminescence and thus the current distribution is observed. A quantitative interpretation of electroluminescence profiles is shown and the effect on the lateral photovoltaic response is discussed [5].

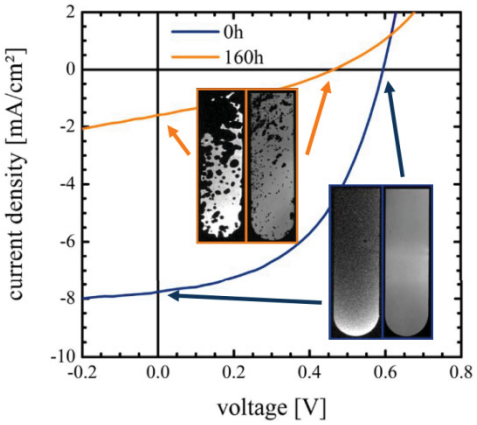

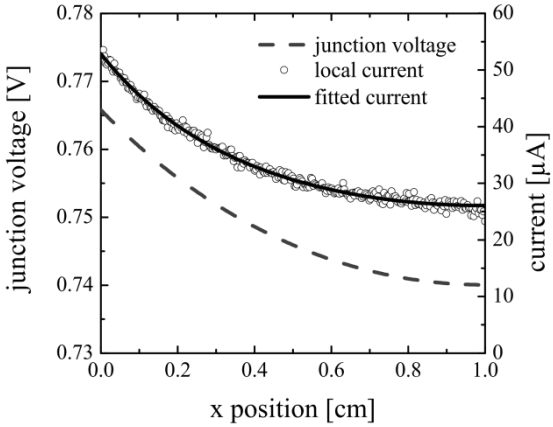

References:

[1] M. Seeland, R. Rösch and H. Hoppe, Imaging Techniques for Studying OPV Stability and Degradation, in *Stability and Degradation of Organic and Polymer Solar Cells*, edited by F. C. Krebs (John Wiley & Sons, 2012).

[2] M. Seeland, R. Rösch, B. Muhsin, *et al.*, Energy Procedia (Proceedings of Organic Photovoltaics: Science and Technology (E-MRS 2011, Symposium S)), acc. (2012).

[3] R. Rösch, D. M. Tanenbaum, M. Jorgensen, *et al.*, Energy Environ. Sci. (2012).

[4] M. Seeland, R. Rösch and H. Hoppe, J. Appl. Phys. **109** (6), 064513 (2011).

[5] M. Seeland, R. Rösch and H. Hoppe, J. Appl. Phys. **111** (2), 024505 (2012).

INFLUENCE OF ORGANIC ACIDS ON DEVICE PERFORMANCE OF P3HT : PCBM SOLAR CELLS

Authors:
B. Muhsin, F. Herrmann, C.-R. Singh, G. Gobsch, M. Presselt, and H. Hoppe

Affiliation:
Institute of Physics, Ilmenau University of Technology, Weimarer Str. 32, 98693 Ilmenau, Germany

Abstract:
We have investigated the effects of addition of organic acids to polymer solar cells based on poly(3-hexylthiophen):phenyl-C61-butyric-acid-methyl-ether (P3HT:PCBM) [1]. We have observed a significant increase of the device performance based on improved fill factors [2]. We correlate these results with dark and photogenerated concentrations of charge carriers evaluated from CELIV measurements as well as sub-bandgap absorption performed by photo-thermal-deflection (PDS) spectroscopy. The material class is rated in terms of processing agents.

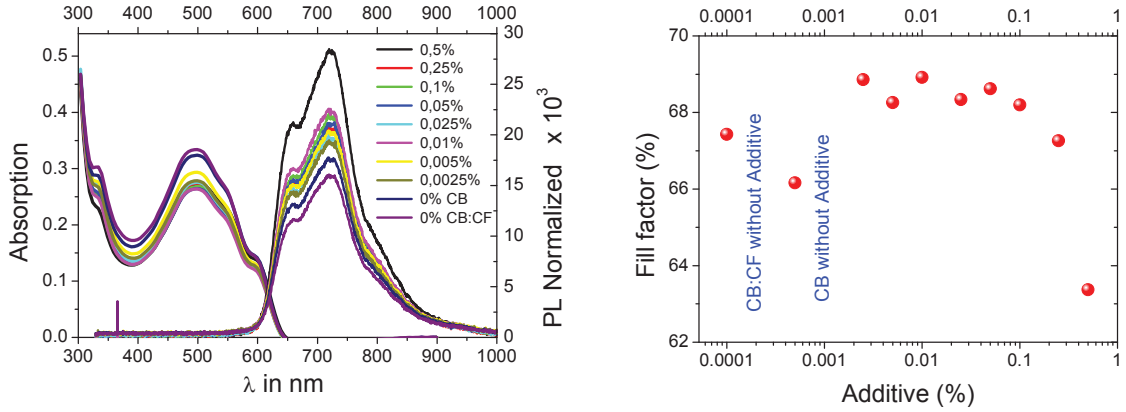

Absorption and photoluminescence of P3HT:PCBM films processed by different amounts of additives (left). Fill factors of solar cells in dependence of additive concentration (right).

[1] J. A. Renz, T. Keller, M. Schneider, S. Shokhovets, K. Jandt, G. Gobsch, and H. Hoppe, Sol. Energy Mater. Sol. Cells 93, 508 (2009).
[2] F. Herrmann, B. Muhsin, C.-R. Singh, G. Gobsch, M. Presselt, and H. Hoppe, *in preparation* (2012)

OPTIMIZATION OF ORGANIC SOLAR CELLS BASED ON BTD/DPP COPOLYMERS

Olesia Synooka[(a)], Florian Kretschmer [(b, c)], Martin D. Hager [(b, c, d)] , Ulrich S. Schubert [(b, c, d)], Gerhard Gobsch [(a)] and Harald Hoppe[(a)]

(a) Institute of Physics, Ilmenau University of Technology, Weimarer Str. 32, 98693 Ilmenau, Germany
(b) Laboratory of Organic and Macromolecular Chemistry (IOMC), Friedrich-Schiller-University Jena, Humboldtstr. 10, 07743 Jena, Germany.
(c) Jena Center for Soft Matter (JCSM), Friedrich-Schiller-University Jena, Humboldtstr. 10, 07743 Jena, Germany.
(d) Dutch Polymer Institute (DPI), John F. Kennedylaan 2, 5612 AB Eindhoven, The Netherlands

Conjugated polymers for organic solar cells offer a lot of advantages. To influence their light harvesting properties it is essential to tune the band gap and absorption of the polymers. Synthesis of a π-conjugated donor-acceptor polymer series based on thiophene, diketopyrrolopyrrole, benzothiadiazole and fluorene was accomplished by means of a *Suzuki* cross coupling reaction. The variation of the monomer contents strongly influences the light absorption of the polymers along with the HOMO and LUMO levels. In this case it is interesting to systematically vary the properties of the resulting materials for organic photovoltaics by combinatorial chemistry. Increasing amounts of diketopyrrolopyrrole lead to a lower band gap and enhanced absorption of red light caused by the stronger accepting properties of this moiety (compared to benzothiadiazole). We have optimized solar cell devices based on these materials and reveal difference between copolymer blends and these terpolymers [1]. Also different types of solvent additives were investigated to improve solar cells performance.

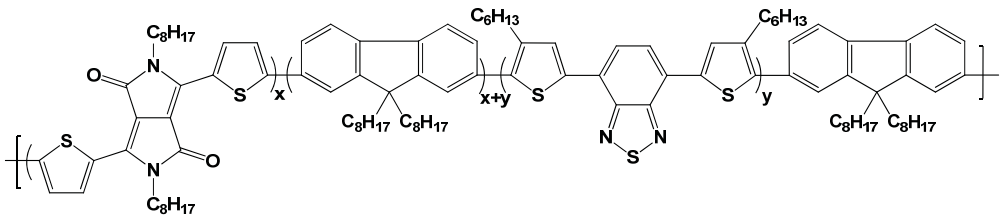

poly(BTD-*co*-F-*co*-DKPP)

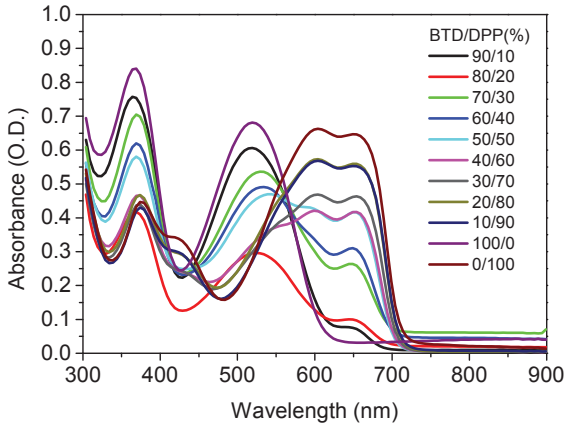

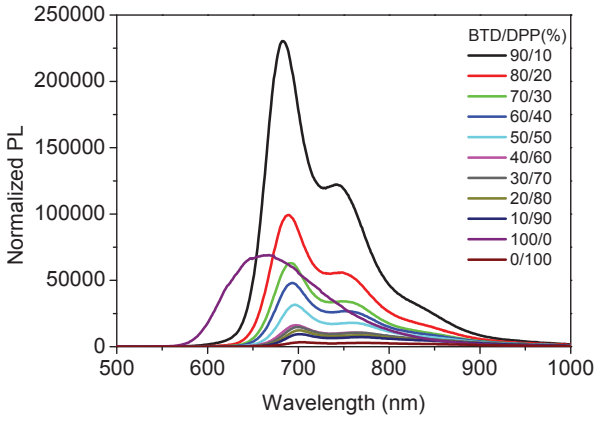

References:

[1] Florian Kretschmer, Martin D. Hager, Olesia Synooka, Harald Hoppe, Ulrich S. Schubert Donor-acceptor π-conjugated polymer libraries for polymer solar cells; submitted in 2012

List of Authors